APPLICATION AND COMPARISON OF MULTISTAGE TRIAXIAL COMPRESSION TEST PROCEDURES ON RECONSTITUTED ANKARA CLAY

A THESIS SUBMITTED TO
THE GRADUATE SCHOOL OF NATURAL AND APPLIED SCIENCES
OF
MIDDLE EAST TECHNICAL UNIVERSITY

BY

AMIRAHMAD VAKILINEZHAD

IN PARTIAL FULFILLMENT OF THE REQUIREMENTS
FOR
THE DEGREE OF MASTER OF SCIENCE
IN
CIVIL ENGINEERING

MAY 2022

Approval of the thesis:

APPLICATION AND COMPARISON OF MULTISTAGE TRIAXIAL COMPRESSION TEST PROCEDURES ON RECONSTITUTED ANKARA CLAY

submitted by **AMIRAHMAD VAKILINEZHAD** in partial fulfillment of the requirements for the degree of **Master of Science** i**n Civil Engineering, Middle East Technical University** by,

Prof. Dr. Halil Kalıpçılar
Dean, Graduate School of **Natural and Applied Sciences** _____

Prof. Dr. Erdem Canbay
Head of the Department, **Civil Engineering** _____

Assoc. Prof. Dr. Nabi Kartal Toker
Supervisor, **Civil Engineering, METU** _____

Examining Committee Members:

Prof. Dr. Erdal Cokca
Civil Engineering, METU _____

Assoc. Prof. Dr. Nabi Kartal Toker
Civil Engineering, METU _____

Assoc. Prof. Dr. Nejan Huvaj Sarihan
Civil Engineering, METU _____

Assoc. Prof. Dr. Onur Pekcan
Civil Engineering, METU _____

Prof. Dr. Yuksel Yilmaz
Civil Engineering, Gazi University _____

Date: 11.05.2022

I hereby declare that all information in this document has been obtained and presented in accordance with academic rules and ethical conduct. I also declare that, as required by these rules and conduct, I have fully cited and referenced all material and results that are not original to this work.

Name Last name :

Amirahmad Vakilinezhad

Signature :

ABSTRACT

APPLICATION AND COMPARISON OF MULTISTAGE TRIAXIAL COMPRESSION TEST PROCEDURES ON RECONSTITUTED ANKARA CLAY

Vakilinezhad, Amirahmad
Master of Science, Civil Engineering
Supervisor : Assoc. Prof. Dr. Nabi Kartal Toker

May 2022, 97 pages

The ability to conduct conventional triaxial compression tests on multiple identical specimens is restricted by available sample quantity, sample homogeneity, as well as testing duration. Multistage triaxial testing is an alternative method to tackle this issue by using a single specimen, sheared under different confining stresses to attain the strength parameters. Although there are widely accepted procedures to decide when to stop each shearing stage and proceed to the next stress level, the applicability of these procedures on different soil types is still a question. This study examines the applicability of three MST procedures (Rational Procedure, Minimum Slope and Maximum Curvature) under two different deviator stress conditions (Sustained or Cycled) during confining stress increase. The outcome is compared to conventional triaxial test results for both drained and undrained shearing of reconstituted specimens of high-plasticity Ankara Clay. Out of the six options, the rational procedure with cycled deviator and minimum slope with cycled deviator approaches are respectively found to give the most accurate strength parameters in reference to undrained single stage and drained single stage test results. The maximum applicable

number of the shearing-reconsolidation sequences before strength loss is also investigated for each MST procedure.

Keywords: Triaxial Compression Test, Multistage Test, Ankara Clay, Strength Parameters, High-Plasticity Clays

ÖZ

YENİDEN OLUŞTURULMUŞ ANKARA KİLİNDE ÜÇ EKSENLİ DAYANIM DENEYİ İÇİN KADEMELİ KESME PROSEDÜRLERİNİN UYGULANMASI VE KARŞILAŞTIRILMASI

Vakilinezhad, Amirahmad
Yüksek Lisans, İnşaat Mühendisliği
Tez Yöneticisi: Doç. Dr. Nabi Kartal Toker

Mayıs 2022, 97 sayfa

Özdeş numuneler üzerinde geleneksel üç eksenli kesme deneylerinin yapılabilirliği, mevcut numune miktarı, numune homojenliği ve test süresi ile sınırlıdır. Çok kademeli üç eksenli deneyi, kayma dayanımı parametrelerini elde etmek için tek bir numuneyi farklı çevre gerilmeleri altında keserek bu sorunları çözmeyi hedefleyen alternatif bir yöntemdir. Her bir kesme aşamasının ne zaman durdurulacağına ve bir sonraki gerilme seviyesine geçileceğine karar vermek için yaygın olarak kabul edilen prosedürler olmasına rağmen, bu prosedürlerin farklı zemin tipleri üzerinde uygulanabilirliği hala bir soru işaretidir. Bu çalışma, konsolidasyon gerilme artışı sırasında iki farklı deviatör gerilme koşulu (Sürekli veya Döngüsel) altında üç çok kademeli prosedürünün (Rasyonel Prosedür, Minimum Eğim ve Maksimum Eğrilik) uygulanabilirliğini incelemektedir. Yüksek plastisiteye sahip Ankara Kili'nin suya doygun örneklerinin hem drenajlı hem de drenajsız koşullarda, farklı prosedürler uygulanan çok kademeli deneylerinin sonuçları klasik üç eksenli kesme deneyleri ile karşılaştırılmıştır. Altı seçenekten, döngüsel deviatör gerilmeli rasyonel prosedürün drenajsız deneylerde, döngüsel deviatör gerilmeli minimum eğim yaklaşımının drenajlı deneylerde klasik üç eksenli kesme deneyleri sonuçları ile en iyi örtüşen doğru dayanım parametrelerini verdiği bulunmuştur. Dayanım kaybından önceki

maksimum uygulanabilir kesme - yeniden konsolidasyon aşamalarının sayısı da her çok kademeli prosedürü için incelenmiştir.

Anahtar Kelimeler: Üç eksenli deneyi, Çok kademeli kesme testi, Ankara kili, Kayma dayanimi parametreleri, Yüksek plastisiteli kil

I dedicate my thesis to my family.

My loving parents who never left my side,

And my sister who has always supported and guided me.

ACKNOWLEDGMENTS

First and foremost, I am extremely grateful to my advisor, Assoc. Prof. Dr. Nabi Kartal Toker for his invaluable pieces of advice, criticisms, guidance and endless support throughout the study. His immense knowledge encouraged me during my academic research and daily life. He is and always will be my idol and the source of inspiration and motivation for me.

I would like to express my gratitude to Assoc. Prof. Dr. Nejan Huvaj Sarihan for her kind support. Without her tremendous understanding and mentorship, it would be impossible for me to tolerate all the difficulties.

I appreciate all the support I received from my colleagues Melih, Emre, Berkan, Moutasem, Hossein, Elife, Mehmet, Bugrahan, Sefa, Alaa, Ahmad, Yilmaz Emre, Eray, Arda, Olgu, Tugce, Pinar and Burak. Their kind assistance and support formed a wonderful study and life for me in Turkey.

Last but not least, I am thankful to my professors, friends, and METU soil mechanics laboratory engineer Ulas Nacar and assistant Kamber Bilgen. They were always by my side and supported me throughout my study and life.

TABLE OF CONTENTS

LIST OF TABLES

TABLES

LIST OF FIGURES

FIGURES

CHAPTER 1

INTRODUCTION

1.1 Motivation

In almost all geotechnical projects (slope stability, foundation design, tunneling, etc.), the geosystem design and construction depend on soil strength. The conventional triaxial compression test is the most widely used and reliable laboratory test to attain the soil strength parameters, namely effective internal friction angle (ϕ') and apparent cohesion (c') (Budhu, 2015). In this regard, three or more soil specimens are consolidated under three different effective stresses (σ'_c) and axially loaded (σ'_a) to failure. For each test at different effective confining pressure, the deviator stress at failure will be different (higher the confining stress, higher the strength of the specimen). Therefore, after at least three tests, three stress-strain relations are available and are used to draw the failure envelope through three Mohr circles and investigate the soil's internal friction angle (slope of the failure envelope) and cohesion (the intercept) (Mitchel & Soga, 2005).

1.2 Limitation

In order to draw a realistic failure envelope for a specific soil sample, the specimens must be identical (dimensions, water content, stress state, temperature, etc.). However, it is almost impossible to have identical soil specimens in practice, which may lead to erroneous failure envelopes. In the case of undisturbed samples, even with extreme care, obtaining sufficient soil sample in one thin-walled tube to trim

three or more specimens is hard to achieve. Also, preparing identical homogenous specimens for reconstituted soil samples needs extreme attentiveness.

Another limitation of the conventional triaxial compression test is the long time it takes for the saturation of each specimen. A single set might take two weeks or more in case of fine soils. Hydraulic conductivity of clays is much lower than that of sands; therefore, the needed time for either consolidation or during the shearing phase (for a drained test) for clays is significantly longer than those for sands.

By taking all the above-mentioned arguments into consideration, engineers have established an alternative method to obtain the failure envelope using only one specimen. Using this method, it is possible to promptly yield a reliable failure envelope.

1.3 Research Question

In a multi-stage triaxial compression test, the soil specimen is tested under a consolidation pressure and sheared. The shearing phase is stopped right before the failure and the soil specimen is reconsolidated to higher effective stress. This process is repeated and shearing-reconsolidation are performed up to three or more sequences. One Mohr circle is drawn for each of them, and a failure envelope can be fitted to the circles to investigate the soil shear strength parameters.

The questions associated with the multi-stage triaxial compression test are:

1. When exactly to stop the shearing, since it needs to be at a point very close to failure without creating a failure plane in the specimen (Head, 1982).

2. Whether the deviator stress after shearing should be removed or sustained on the specimen during the following reconsolidation sequence (Ho & Fredlund, 1987).

3. What is the maximum reconsolidation-shearing cycles that the soil specimen can withstand before a significant reduction in strength is observed (Gräsle, 2011).

Note that the answers to these questions may differ with soil and test type and characteristics.

1.4 Scope

First, this study investigates the physical properties of Ankara clay with different experiments. Conventional isotropically consolidated triaxial compression tests (both drained and undrained) are conducted on reconstituted normally consolidated high plasticity Ankara clay specimens. The applicability of the multi-stage triaxial test procedures is investigated on reconstituted Ankara clay by comparing it to conventional triaxial test results. The research questions will be answered, and the best multi-stage triaxial approach will be calibrated for reconstituted Ankara clay and similar high-plasticity normally consolidated clays to be used in practice in a reliable and timely manner.

In chapter 2, a comprehensive literature review regarding the multi-stage triaxial tests is provided. Chapter 3 explains sample preparation, test setup, and test procedures. Chapter 4 includes the results of the experiments. Finally, in chapter 5 conclusion of this study and suggestions for future studies are presented.

CHAPTER 2

LITERATURE REVIEW

The history of the first triaxial test setup is not clear. In 1911 Theodore von Karman first used the triaxial cell to measure the strength of rocks (Deák et al., 2012). The device closer to the current triaxial cells was originated by Buisman in 1924. However, Casagrande introduced the evolved version in Vienna in early 1930 (Kayatürk et al., 2021).

2.1 Multi-stage Triaxial Testing

According to available literature, possibly De Beer (1950), for the first time, introduced the multi-stage triaxial test to obtain the strength parameters. Ten years later, (Kenny, 1960) asserted the sensitivity of the clay specimen is the critical factor for the applicability of the multi-stage triaxial test. According to their research, multi-stage gives acceptable results for undrained tests, whereas for the fully drained tests, it is applicable in the case of clays with low sensitivity. In undrained tests, the friction angle mobilization is relatively independent of sensitivity and the mineral composition of the soil. On the other hand, for the drained tests, the friction angle mobilization is highly dependent on the sensitivity of the soil and to a lower extent, on mineral composition. It is also concluded that three cycles of reconsolidation-shearing can be assumed for soft soils with low sensitivity.

Kim & Ko (1979) performed MST on three rock samples and compared the results to the conventional triaxial results in peak strength, residual strength, cohesion, and friction angle. It is suggested that this method is best applicable for brittle rocks which can withstand several cycles of reconsolidation-shearing.

Ho & Fredlund (1987) performed multi-stage on Hong Kong residual soil to investigate the effect of soil suction on strength. They argued the multi-stage test eliminates the effect of specimen variability from one test to another and gives reliable results. They introduced the "cyclic loading" and "sustained loading" procedures that are shown in Figure 2.1 and Figure 2.2. The former is applied when the deviator stress is removed from the specimen after the shearing stage and before starting the new consolidation stage, in other words, unloading-reloading cycle is applied. However, in the case of the latter one, the deviator stress is sustained on the specimen while the reconsolidation stage is going on. The "Sustained load" method leads to the accumulation of strain on specimen due to the creep and gives unrealistic results. For the "cyclic loading" method, rapid deviator stress removal is preferable to slow stress release due to a better strain recovery throughout the specimen. It is asserted that the Hong Kong residual soil can withstand up to three sequences of loading-reconsolidation, after which a drop in strength of soil specimen was observed. In this study, the term "cycled" is used when the deviatoric stress is removed from the specimen at each reconsolidation stage.

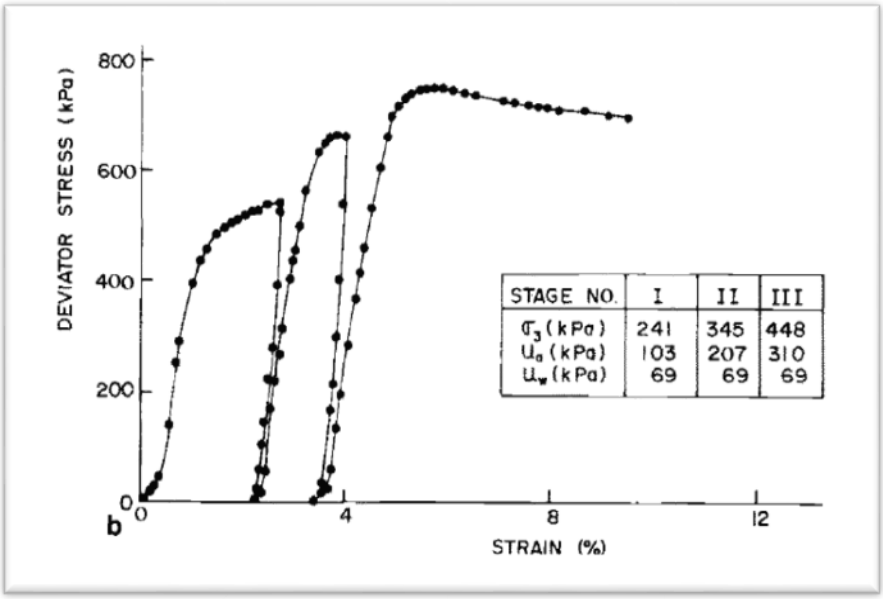

Figure 2.1. Representative multi-stage stress-strain curves for cycled loading

(Ho & Fredlund, 1987)

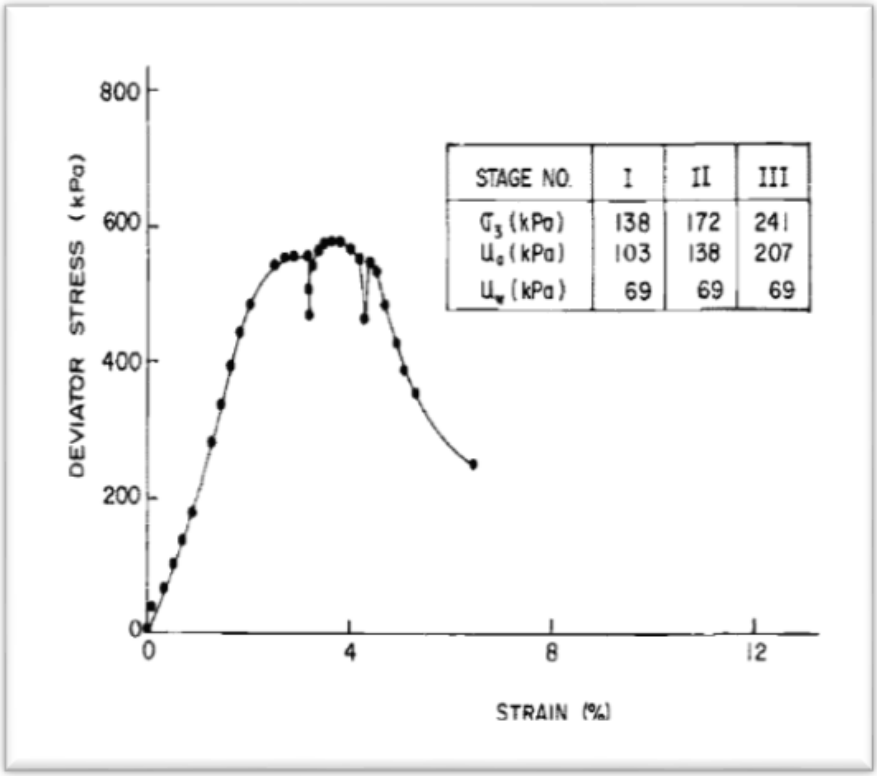

Figure 2.2. Representative multi-stage stress–axial strain curves for sustained loading (Ho & Fredlund, 1987)

One of the prominent works in the literature on the multi-stage triaxial test technique was done by Nambiar et al., (1985). They proposed the "rational procedure" employing the hyperbolic soil model suggested by Kondner (1963). Kondner hypothesized that the stress-strain relation of soils could be modeled by rectangular hyperbolae using Eq. 1 and Eq. 2, as are presented in Figure 2.3.

$$\varepsilon_a / (\sigma_1 - \sigma_3) = a + b\,\varepsilon_a \qquad \textit{Eq. 1}$$

$$\varepsilon_a / u = a_u + b_u\,\varepsilon_a \qquad \textit{Eq. 2}$$

Where $\boldsymbol{\varepsilon_a}$ is axial strain, $\boldsymbol{\sigma_1 - \sigma_3}$ is deviator stress, **u** is pore water pressure, **a**, **b,** $\mathbf{a_u}$ and $\mathbf{b_u}$ are constant numbers that can be determined experimentally. Figure 2.3

shows a plot of ε_a / (σ_1-σ_3) against ε_a, gives a line with a slope of **b** and intercept of **a**. by taking the limit of Eq. 1 and Eq. 2 for $\varepsilon_a \rightarrow \infty$ Eq. 3 and Eq. 4 are derived, where the $(\sigma_1-\sigma_3)_f$ and u_f are deviator stress and pore pressure at failure respectively. In Figure 2.3, ε_1 is axial strain as it was shown by ε_a in the text.

$$(\sigma_1-\sigma_3)_f = 1/b \qquad \textit{Eq. 3}$$

$$u_f = 1/b_u \qquad \textit{Eq. 4}$$

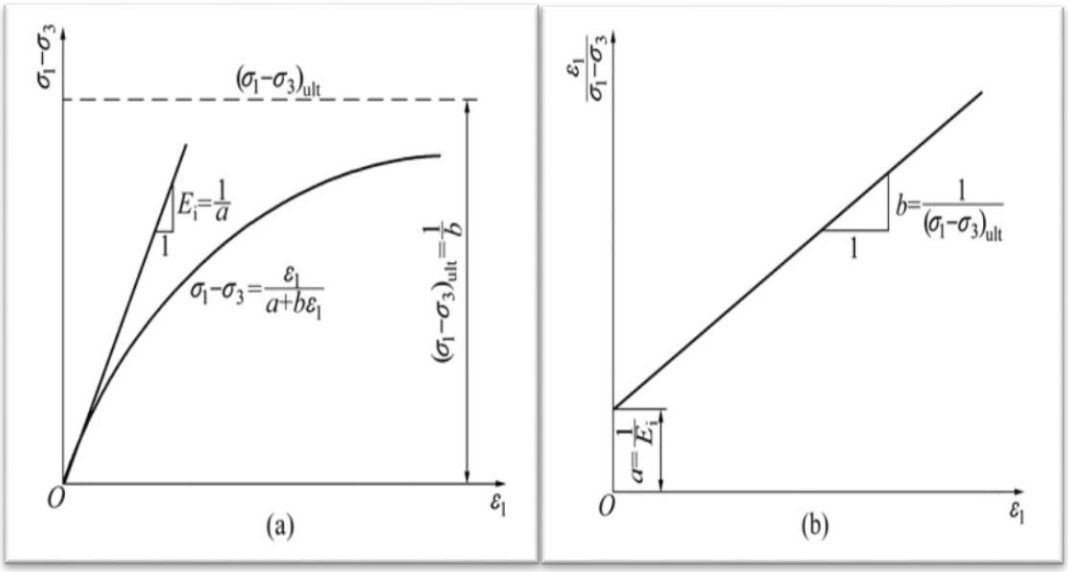

Figure 2.3. Hyperbolic representation of stress-strain curves a) Real b) Transformed (After Kondner, 1963)

Rational procedure suggests shearing the specimen in undrained test until 2 % - 4 % axial strain. Then stop the shearing and use Eq.3 and Eq.4 to find the stress and pore water pressure at failure numerically. The result is almost always in the form of a line with a slope of 1/**b** and intercept of **a,** as shown in Figure 2.4. Using this method, the minimum disturbance is applied to the specimen. Nambiar et al. (1985) also strongly recommend increasing the consolidation pressure at each stage at least twice the previous step. Therefore, the effect of shearing will be recovered under a higher consolidation pressure, and the results are more reliable.

Applying the infinite axial strain to obtain the stress and pore pressure at failure gives higher values than the actual values. In some cases, using Kondner's hypothesis, the axial strain of 10% or 12% represents the failure strain better than the asymptote value. Nambiar et al., (1985) tackled this issue by suggesting that one conventional triaxial is essential in rational procedure to find the axial strain at failure and extrapolate the data from 2%- 4% strain to that strain for each cycle. However, the estimated stress and pore water pressure at failure by using different axial strains give very close results and the difference is negligible. Therefore, in this study, the asymptote value is considered for the stress and pore water pressure calculations.

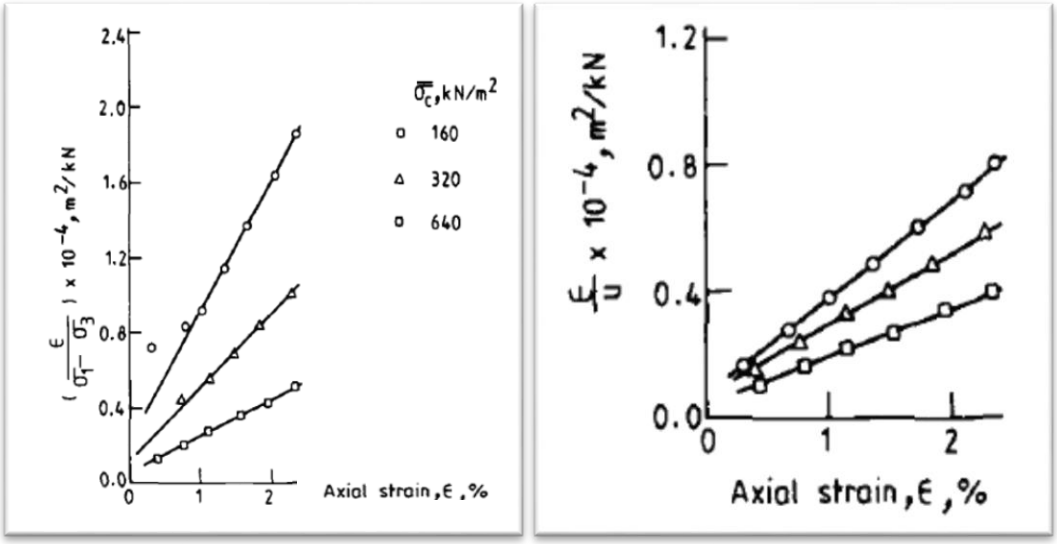

Figure 2.4. Transformed stress-strain and pore water pressure-strain relationships using the rational procedure (Nambiar et al. 1985)

Shahin & Cargeeg, (2011) addressed the issue associated with performing one additional conventional triaxial test for understanding the failure strain and extrapolating the data to that point. They conducted undrained experiments on high plasticity silt from the Western coast of Australia. The specimen is sheared up to 3% axial strain for the first loading-reconsolidation cycles following Nambiar et al. (1985) recommendations. However, at the last stage, they continued the shearing up

to 25%, where the failure plane is appeared. The deviator stress at failure is obtained at this stage. Using Kondner's approach at the final stage, the axial strain at failure is attained and all the available data in previous steps are extrapolated to that axial strain. Using this method, an additional conventional triaxial test is not necessary, axial strain at failure is known and accordingly, the failure stress can be calculated for each cycle. Loading at the third stage is continued, and the failure stress is noted (Figure 2.5).

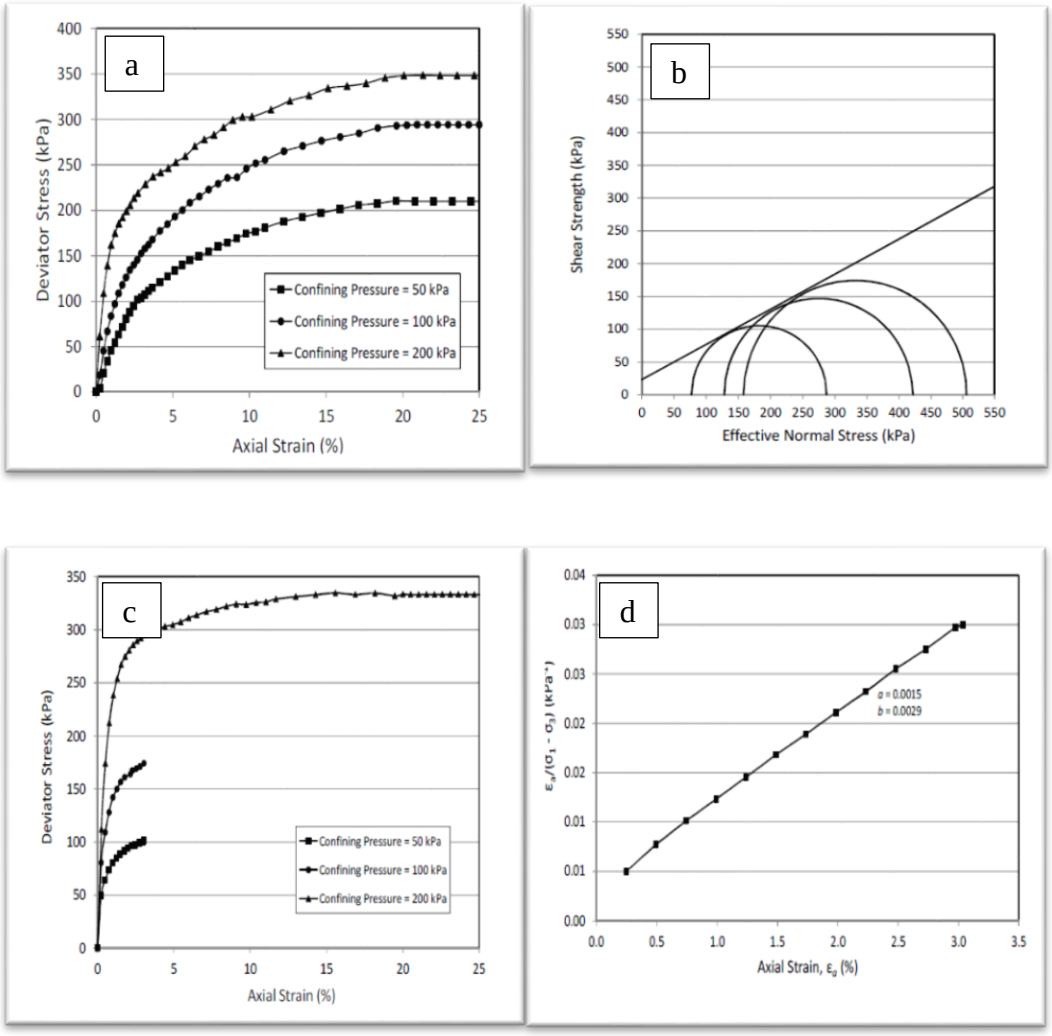

*Figure 2.5.*Cconventional and multi-stage test results. a) stress-strain relation of single-stage b) failure envelope from single-stage tests c) stress-strain relation of multi-stage test and continuing the shearing step at the third stage d) Linearization of data using Kondner method (Shaheen and Cargeeg, 2011)

In the late 1980s, Soranzo (1988) performed multistage consolidated undrained triaxial tests on normally consolidated alluvial and overconsolidated colluvial soil formations. He pointed out that the results of multi-stage are in perfect agreement with single-stage. Employing the normalized stress axis with consolidation pressure, the results of multi-stage and single-stage are almost the same (Figure 2.6). The researcher noted that when a softening behavior is observed at very low strains (less

than 4%), as in the case of brittle behavior of heavily overconsolidated fissured clays, cemented, or highly sensitive clays, this procedure cannot be applied. However, suppose the brittle behavior is expected at higher strains (about 5% -6%). In that case, a multi-stage triaxial test can be implemented up to small strains, and some numerical interpretations can be considered (i.e., Kondner's hyperbolic model) to evaluate the strength parameters.

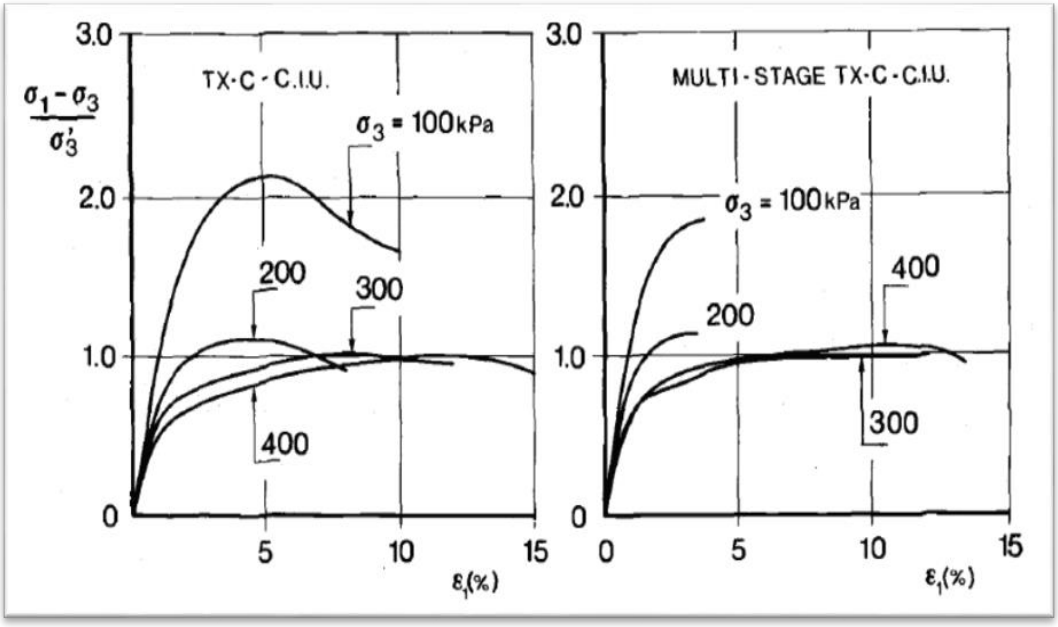

Figure 2.6. Normalized deviatoric stress versus axial strain curves for traditional and multi-stage triaxial tests (Soranzo, 1980)

Saeedy & Mollah (2009) applied the multi-stage procedure on Kuwait sand to obtain both drained and undrained strength parameters. Using the conventional triaxial test, they observed that the strength parameters vary significantly from one specimen set to another. Friction angle and cohesion obtained from different soil specimens are in the range of 2°-14° and 0-100 kPa, respectively. Also, sample preparation is challenging and costly in the case of cemented Kuwait soil and saturated sand. Therefore, the multi-stage testing procedure was employed to assess the strength parameters of Kuwait sand. In multi-stage tests, the shearing is stopped for the first

two cycles when the difference between two consecutive deviator stress measurements show a negligible difference (less than 0.05%). A reconsolidation stage follows it under a higher cell pressure. They continued the shearing up to 20% axial strain for the third cycle.

It is reported that the multi-stage and single-stage triaxial results are in good agreement in terms of failure stresses. However, the axial strains, the pore pressure change in the undrained test, and the volumetric behavior in the drained test do not follow the same pattern for multi-stage and conventional triaxial tests (Figure 2.7). The reason is that the pore pressure change and volumetric behavior mainly depend on the physical condition of the specimen before the shearing stage.

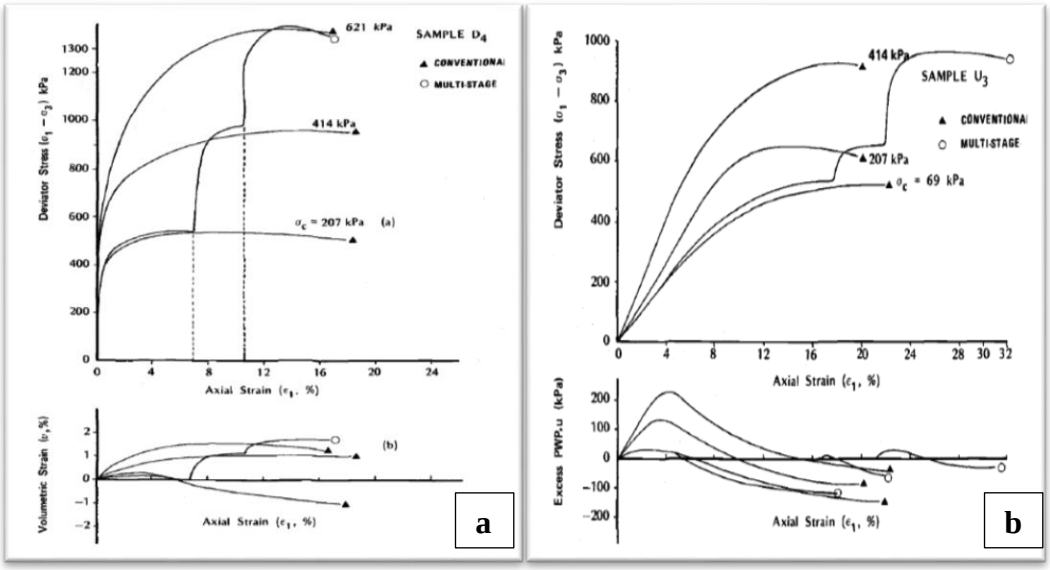

Figure 2.7. a) Stress-axial strain and volumetric strain-axial strain relationships in drained test b) Stress-axial strain and excess pore pressure-axial strain relationships in undrained test (Saeedy & Mollah ,2009)

Gräsle (2011) performed a multi-step test on Mont Terri Opalinus clay to overcome the problems of sample variability and scarcity. The study investigated linear elastic behavior, peak and residual strength of Opalinus clay. It is asserted that although the

multi-stage procedure is applicable for many soil samples (i.e., Opalinus clay), serious considerations are needed for brittle materials. Moreover, it is noted that due to the creation of micro-cracks, even at very low axial strains at each loading stage, lower strength is expected as the experiment continues for the latter cycles. Opalinus clay can hold four cycles to attain peak strength. After four cycles, a decrease in strength is observed, and it is reduced toward the residual strength. Figure 2.8 shows the three cycles of multi-stage results for linear elastic, peak, and residual strength in octahedral stress space.

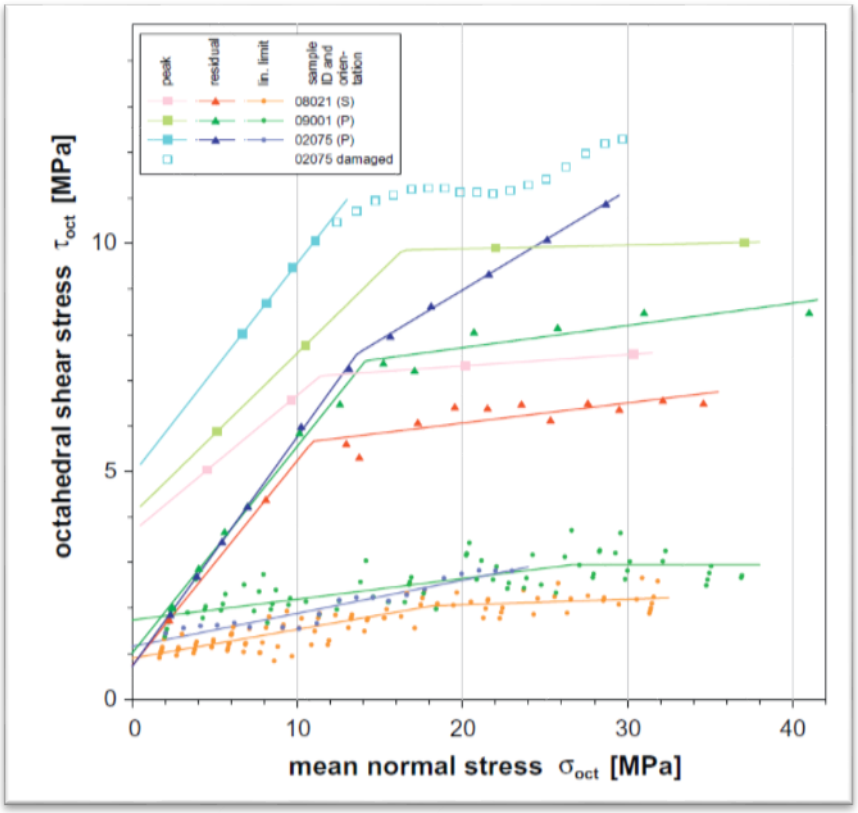

Figure 2.8. Results of three multi-stage strength tests displayed in octahedral stress space (Gräsle, 2011)

Alyousif (2015) performed multi-stage drained tests on sand specimens. This work introduced two new approaches to stop the shearing and consolidating under higher

pressure. **1.** Minimum slope **2.** Maximum curvature. In these techniques, the shearing is ceased where the deviatoric stress-axial strain plot has the lowest slope (about 8%) and the highest curvature. They also employed the cycled or sustained loading approaches introduced by Ho and Fredlund (1982). The study results are provided in Figures 2.9, 2.10 and 2.11. Also are tabulated in Table. 2.1. As it can be seen, the minimum slope cycled loading multi-stage procedure gives the closest results to the actual single-stage triaxial test results. Furthermore, it is highlighted that the sustained loading method (for both minimum slope and, maximum curvature approaches) gives unrealistic results compared to single-stage triaxial test results.

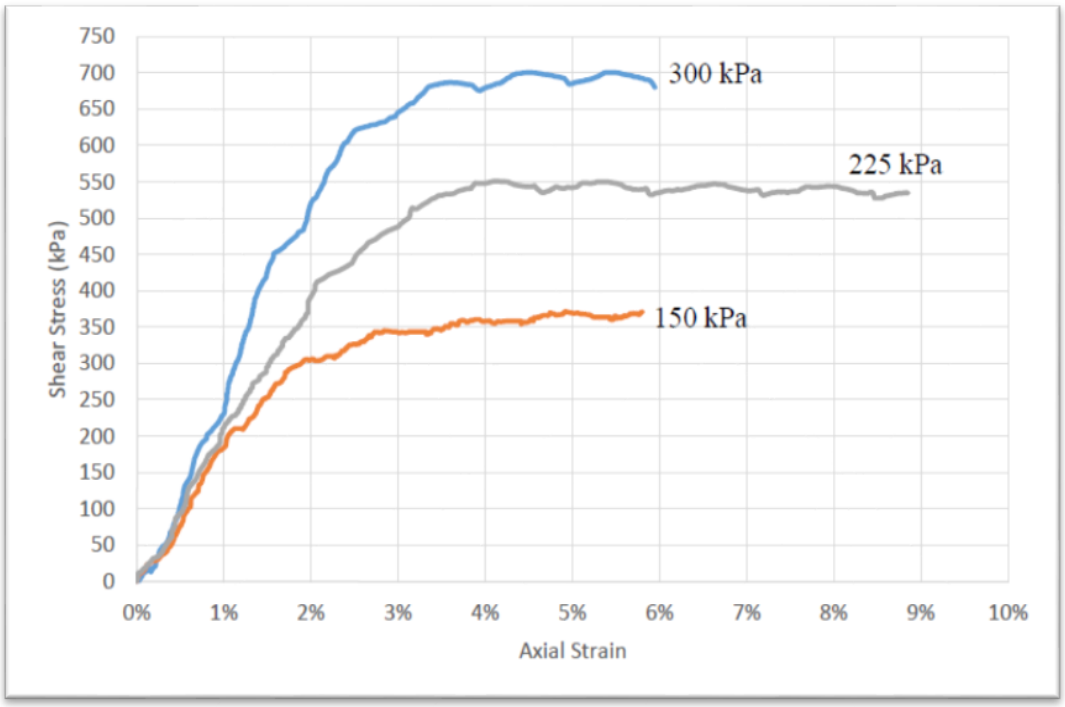

Figure 2.9. Single-stage drained test results for validation purposes

(Alyousif, 2015)

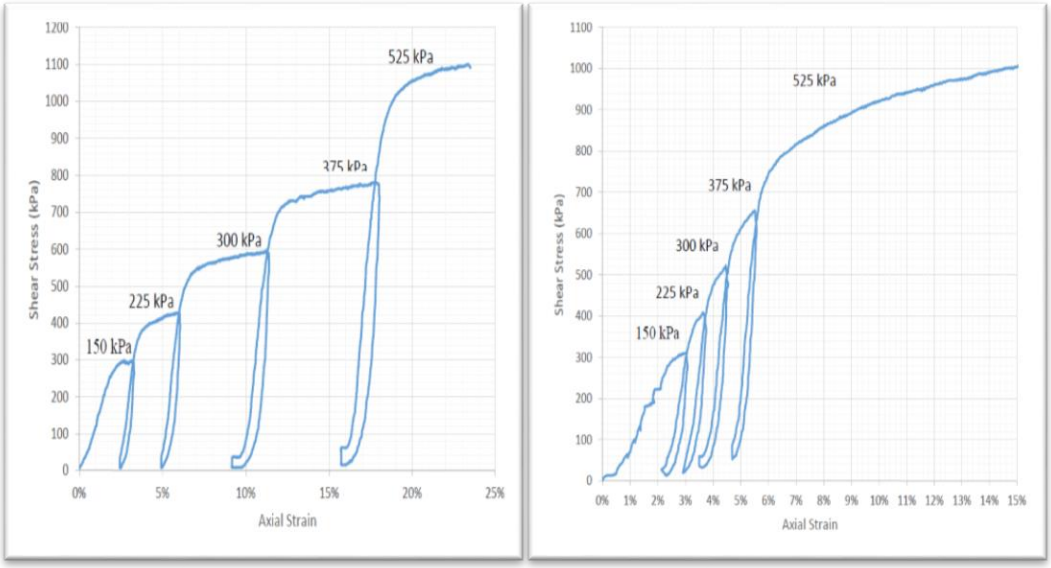

Figure 2.10. Multi-stage cycled loading a) minimum slope technique b) maximum curvature technique (Alyousif, 2015)

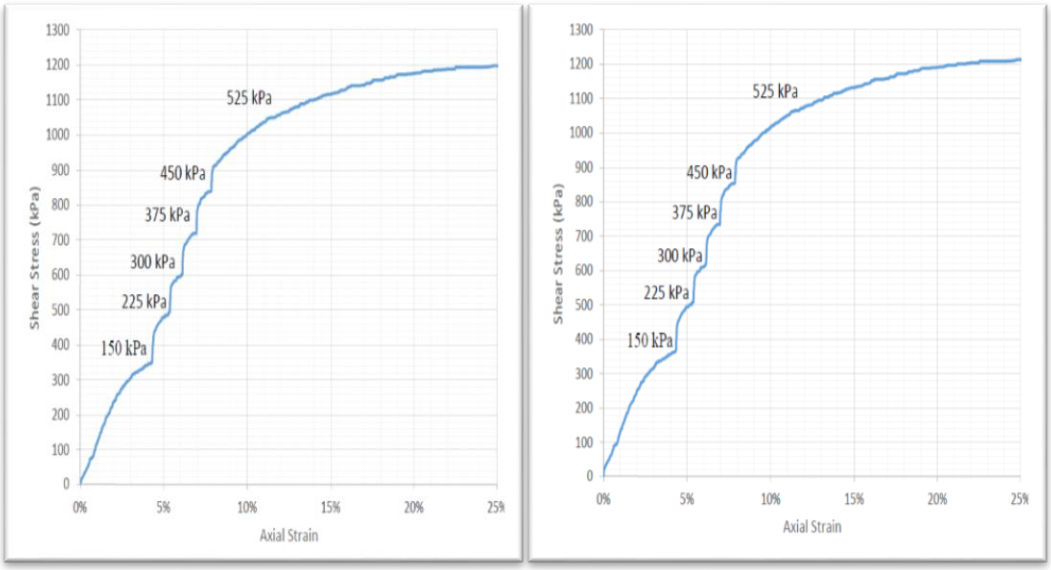

Figure 2.11. Multi-stage sustained loading a) minimum slope b) maximum curvature (Alyousif, 2015)

Table 2.1. Single-stage and multi-stage test results (Alyousif, 2015)

	Number of tests	Fiction angle (ϕ')	Cohesion (kPa)
Single-stage	3	33	0
Minimum Slope Cyclic	1	32	0
Maximum Curvature Cyclic	1	28	0
Minimum Slope Sustained	1	28	30
Maximum Curvature Sustained	1	27	35

A recent study by Kayaturk et al. (2021) on clayey soil shows promising results of multi-stage compared to conventional triaxial. In this work, drained tests were performed, and the specimen was sheared up to 4.5% axial strain. In addition to the method proposed by Nambiar et al., 1985, they proposed a new method to find the stress at failure through the available stress-strain data until 4.5% strain. They implemented a 2-parameter logarithmic equation to predict the stress at failure following Eq.5.

$$y = y_0 + a\ln x \qquad \textit{Eq. 5}$$

Where $\boldsymbol{x}$ is axial strain, $\boldsymbol{y}$ is deviatoric stress, $\boldsymbol{a}$ and $\boldsymbol{y_0}$ are the equation constants. The study results for conventional triaxial, multi-stage using Kondner's method and the curve fitting approach are presented in Figure 2.12.

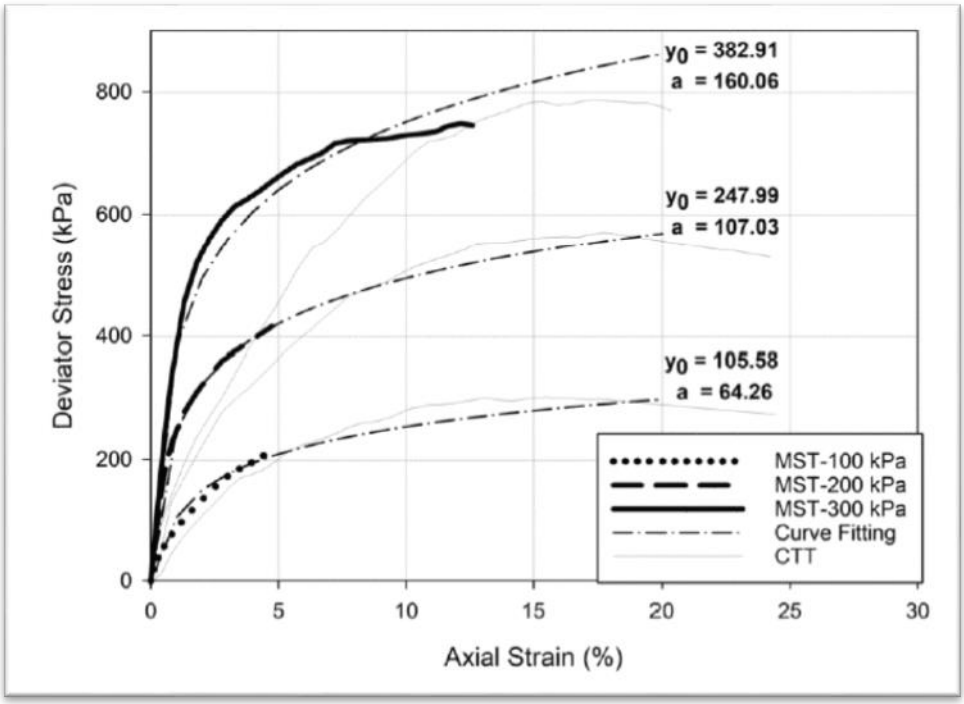

Figure 2.12. Stress-axial strain curves of the conventional triaxial, multi-stage test and curve-fitting approach (Kayaturk et al., 2021)

Multi-stage is a handy method for particular tests when exactly identical specimens are needed to assess soil parameters. Multi-stage was used on unsaturated soil samples (Khosravi et al., 2012), cemented mixed soil samples (Taheri et al., 2012), or on methane-bearing sediment samples (Choi et al., 2018), in which preparing identical specimens were either impossible or extremely expensive or time-consuming. Multi-stage triaxial addresses the issues associated with soil variability and scarcity of replicates (Banerjee et al., 2020).

2.2 Ankara Clay Characteristics

According to the available literature, Ankara clay's general characteristics and properties are listed in Table 2.2. In Chapter 3, the laboratory experiments are conducted on samples of Ankara clay.

Table 2.2. Ankara clay properties from different studies and locations in Ankara

	Clay Percent (%)	LL (%)	PI (%)	G_s	Classification
(Erguler & Ulusay, 2003)	11 – 75	44 – 103	17 – 67	2.60	–
(Avsar et al., 2005)	26 – 67	51 – 93	24 – 51	–	CH and MH
(Avsar et al., 2009)	39 – 60	75 – 112	42 – 75	–	CH
(Ispir, 2011)	45	58 – 66	29 – 35	2.6	MH – CH
	60 – 67	59 – 68	31 – 40	2.63	CH
	45.6 – 50	50 – 52	27 – 31	2.71	CH
	51.3 – 52	54 – 56	32 – 34	2.65	CH
(Akgün et al., 2017)	61.5 – 65.6	52.2 – 62.9	34.8 – 38.2	2.6 – 2.8	CH
	43.2 – 85	40.2 – 49.3	23.8 – 32.1	2.7 – 2.78	CL
	51.8 – 80.1	47.3 – 81.8	26.3 – 36.7	2.68 –2.84	MH-CH-CL
(Çokça & Tilgen, 2010)	67.9	48	27	2.73	CL
(Binal et al., 2016)	36	88.7	53.7		CH

CHAPTER 3

TESTING MATERIAL AND PROCEDURES

This chapter consists of three main sections. First, the testing material and its characteristics are explained by employing laboratory tests following the American Society for Testing and Materials (ASTM). Subsequently, the sample preparation and maintenance will be discussed, and finally, testing setups for both drained and undrained tests will be demonstrated.

3.1 Testing Material

In this study, reconstituted Ankara clay is used to investigate the applicability of the multi-stage triaxial compression test procedures. Ankara clay is one of the dominant formations in Ankara, the capital of Turkey. According to the literature, it is problematic soil due to its characteristics. Knowledge of its highly variable physical and mechanical properties is essential for many local projects. The following subsections provide detailed information about the physical properties of Ankara clay according to the American Society for Testing and Materials (ASTM).

3.1.1 Specific Gravity (G_s)

The specific gravity of soil (G_s) is defined as the ratio of the mass of its solids at a particular volume to the mass of the distilled water at the same volume. The ASTM D854 − 02 standards, method B: *Procedure for Oven-Dried Specimen*, is considered.

At the end of three test repetitions, the specific gravity of the soil solids using a water pycnometer is found as 2.65±0.04 where the standard deviation of results is in an acceptable range. The results are provided in Table 3.1. Figure 3.1 shows the pycnometer with water and soil together with the beaker of water and a thermometer in it taken during the experiment.

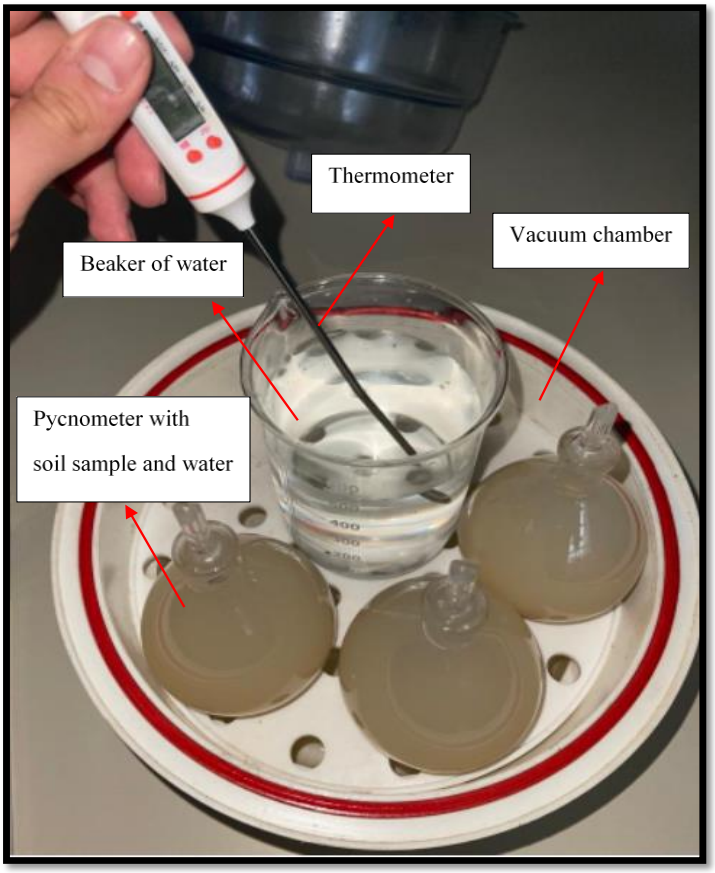

Figure 3.1. Specific gravity test, a picture of three pycnometers, water beaker and thermometer in the vacuum chamber

Table 3.1. Results of Specific Gravity Test with Water Pycnometer

Sample No.	1	2	3
Mass of empty pycnometer (gr)	74.723	75.429	76.807
Mass of pycnometer with soil (gr)	110.274	110.001	114.592
Mass of pycnometer with soil and water (gr)	350.951	348.503	351.071
Mass of pycnometer full of water (gr)	328.981	326.963	327.339
Volume of pycnometer (ml)	254.854	252.141	251.144
Volume of water in pycnometer with soil (ml)	241.241	239.029	237.057
Volume of solids (ml)	13.612	13.063	14.087
Mass of solids (gr)	35.551	34.572	37.785
G_s	2.616	2.651	2.687
Stardard Deviation (%)		3.5	
Average, G_s		2.65	

3.1.2 Particle Size Distribution of Fine-Grain Soils

To specify the particle size distribution of Ankara Clay, sieve analysis is conducted following ASTM D6913 − 04. The amount of soil sample for the test is prepared by quartering following the ASTM C702/C702M) standard presented in Figure 3.2. It is observed that all soil sample is finer than sieve No. 10 (2 mm diameter). Therefore, particle size distribution is investigated by hydrometer test for fine-grained soils according to ASTM D7928 − 17 standards for air-dried soil samples on 50 gr Ankara clay. The picture showing the hydrometer test apparatus taken during the experiment is shown in Figure 3.3. The result of the hydrometer test is shown in Figure 3.4. Based on its grain size distribution, this soil is classified as a fine-grained soil.

Figure 3.2. Quartering for sample preparation

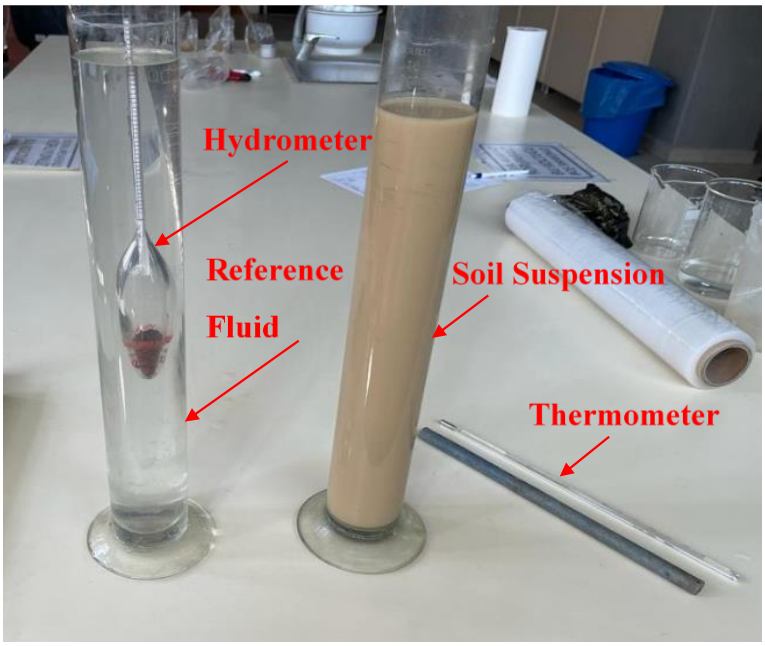

Figure 3.3. Hydrometer test apparatus

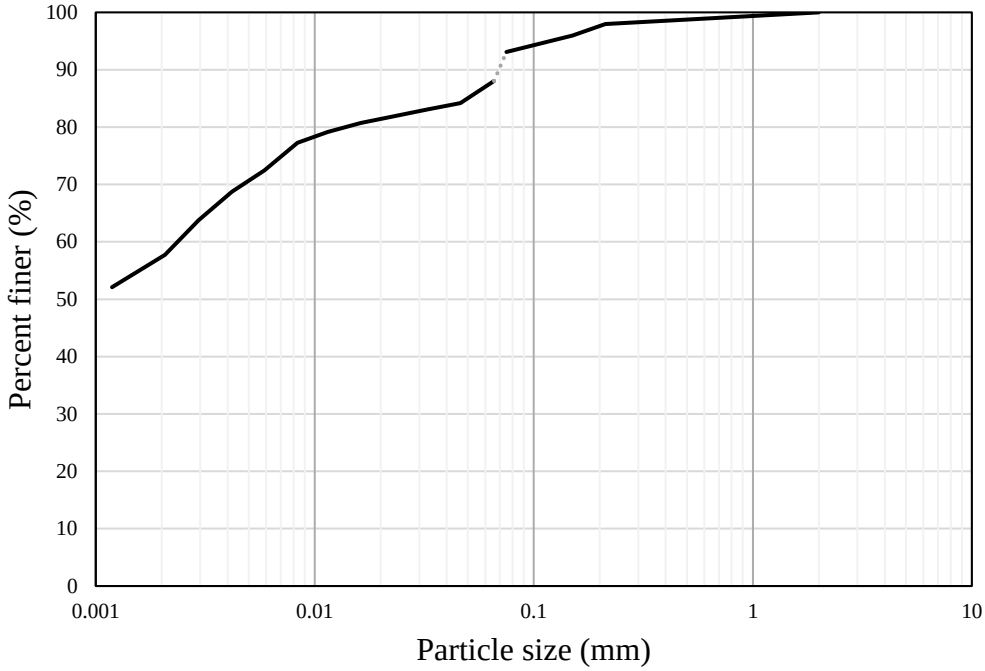

Figure 3.4. Particle size distribution for Ankara clay

3.1.3 Liquid Limit, Plastic Limit and Plasticity Index

Atterberg limits are the boundaries between the fine-grained soils' different consistencies, namely, solid, semi-solid, plastic, and fluid-like (Figure 3.5). By increasing the water content of the soil, the distance between fine soil particles increases and the mechanical behavior of the soil changes. Atterberg limits are used for different purposes, including specifying the engineering properties and classification of the soil. Moreover, the liquid limit of the Ankara clay sample is needed to be used in reconstituted sample preparation in this study, which will be discussed in the coming sections.

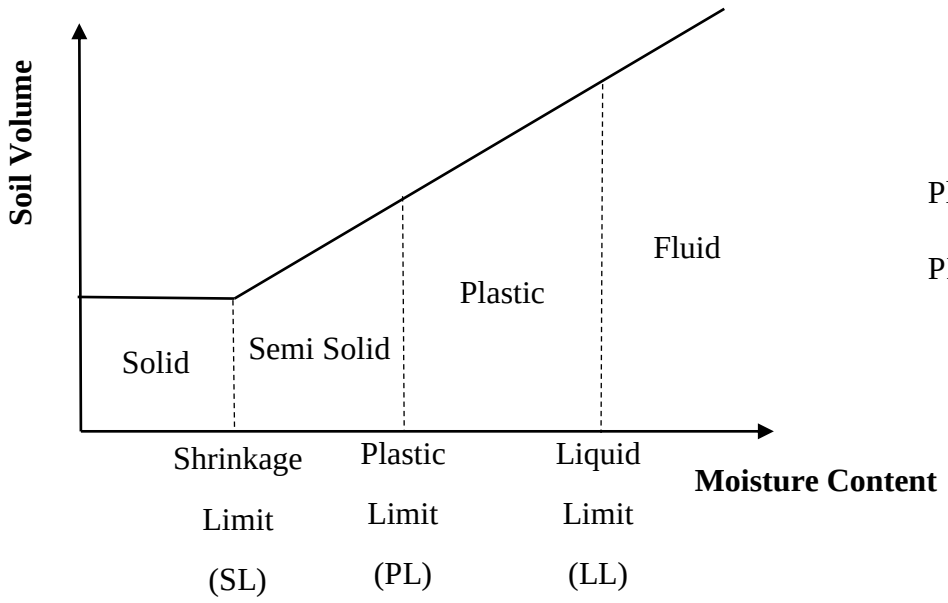

Plasticity Index:

PI = LL - PL

Figure 3.5. Moisture content against fine-grained soil state

According to the ASTM D4318-17 standard, liquid and plastic limits are investigated. For liquid limit assessment wet to dry approach is implemented and using Eq. 6 suggested by ASTM for the one-point method, the LL is calculated as 71%. However, using the three-point method, LL is measured as 70 % for 25-drops. Therefore, the liquid limit for Ankara clay is noted as 70%.

$$LL^n = \omega_n \left(\frac{N^n}{25}\right)^{0.121} \qquad \text{Eq. 6}$$

The results of the liquid limit test are provided in Table 3.2. In Figure 3.6, the Casagrande test apparatus for the liquid limit experiment is shown.

Table 3.2. Results of the liquid limit test using three-point method for 25 drops

Test Number	Number of drops	Water content (%)
1	15	73
2	27	69
3	50	66
Liquid Limit	25	LL=70%

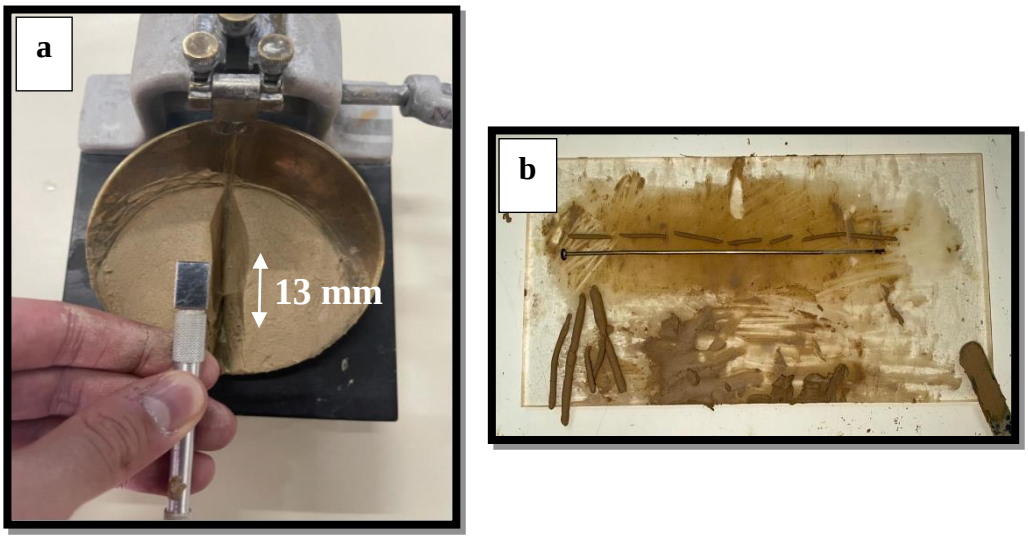

Figure 3.6. Atterberg limits test a) liquid limit after 25 drops b) plastic limit after rolling the clay sample to 3 mm diameter

The plastic limit of Ankara clay is measured as 30%. As a result, the plasticity index is calculated as 40%, and following Table 3. 3, the soil is classified as high plasticity clay according to the USCS classification system (ASTM D2487 − 17).

Table 3.3. Ankara clay properties and classification

G_s	2.65
Liquid Limit (%)	70
Plastic Limit (%)	30
Plasticity Index (%)	40
Clay Percent (%)	58
Soil Activity	0.69
USCS Classification	CH

3.2 Sample Preparation

To perform the triaxial compression test on Ankara clay, first, it is necessary to prepare the identical soil specimens. Soil specimen dimension of 35 mm x 70 mm is chosen. The following steps are taken for reconstituting a clay sample by consolidating it from slurry:

- ✓ First, water was added to the clay sample up to the liquid limit.
- ✓ The soil and water together were placed in a plastic container and were mixed until no particles were flocculated and clustered. The homogenous slurry was then checked by hand for any possible flocculation (Figure 3.7).

Figure 3.7. Soil and water mixed to the liquid limit for sample preparation

- ✓ Two layers of filter paper were located at the bottom of a 30 cm x 30 cm tank (Figure 3.8). Inner walls were lubricated by vaseline to minimize the effect of wall friction during the consolidation. The sample slurry was poured into the consolidation tank with care to avoid air entrapment and two layers of filter papers were located on top of it. The height of the slurry in the tank was about 12 cm in order to have specimens with at least 80 mm height after consolidation.
- ✓ The top plate of the tank is placed, covering the filter papers. Vertical load is applied on this plate by a pneumatic piston that is connected to the air pressure compressor to apply 50 kPa pressure on the soil sample (Figure 3.9).
- ✓ There are a few holes on both the top and bottom of the tank for water drainage through filter papers. After applying the vertical load by a pneumatic piston on the top plane, water drainage from the holes at first day can be seen in Figure 3.8.

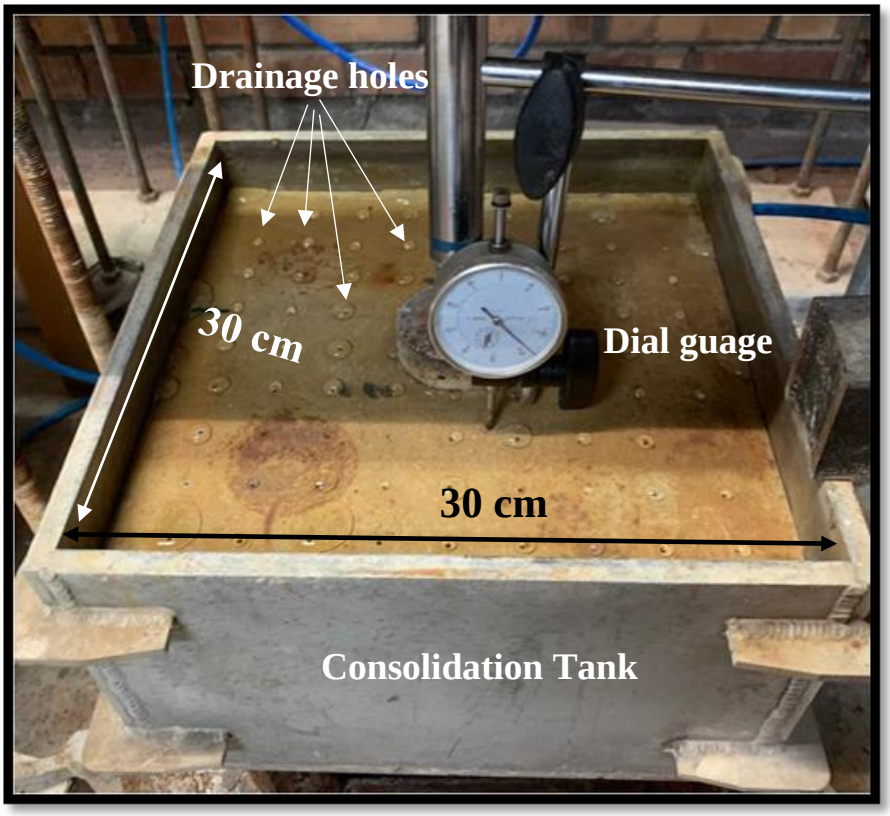

Figure 3.8. Dimensions and water drainage from the top holes of the test tank under 50 kPa pressure

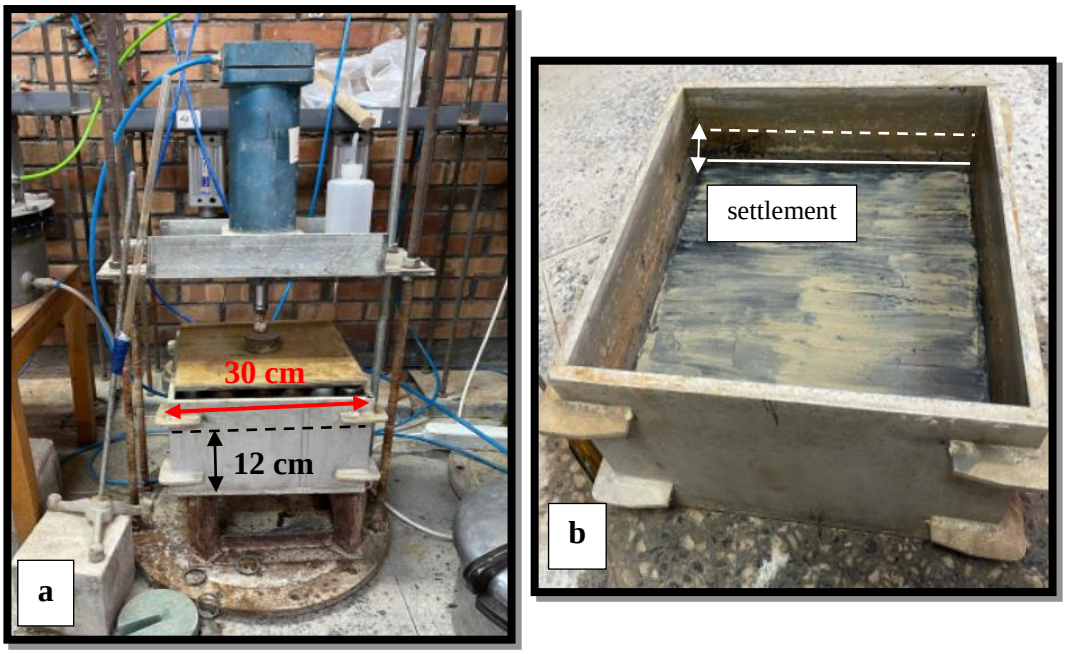

Figure 3.9. a)Test tank under 50 kPa pressure before consolidation b) Test tank after consolidation

- ✓ By assembling a dial gauge on the top cap, the amount of sample consolidation was measured continuously until no change in dial gauge was observed for five consecutive days.
- ✓ After removing the top plate and filter papers, clay specimens were obtained using cylindrical sample extractors. The extractors are placed on the soil sample and the top plate is located in them. By applying pressure on the plate, the extractors are driven in the soil sample. The extractors are taken out of the tank. Soil specimens slowly pushed out of the extractor and 36 reconstituted high plasticity clay specimens are obtained. Then specimens were placed in a humid container (a desiccator jar where a pool of water replaces desiccant under the perforated base) and sealed by vasseline to prevent any humidity loss, as shown in Figure 3.10. In order to componsate any humidity loss in the container, water is sprayed in the container regularly.

Therefore, it is made sure that the water content of soil specimens are kept constant during the whole study.

- ✓ After consolidation and specimen extraction, the remaining consolidated clay's water content was measured from different locations and heights in the test tank. The tank's area is divided into four sections and from top and bottom of each section two samples for water content chack was extracted (Figure 3.11). Moreover, all the remained soil sample in collected in a larger tray and water content is controled. It is observed that the variation of water content at different zones is in an acceptable range, as are written in Table 3.4 (less than 5%).

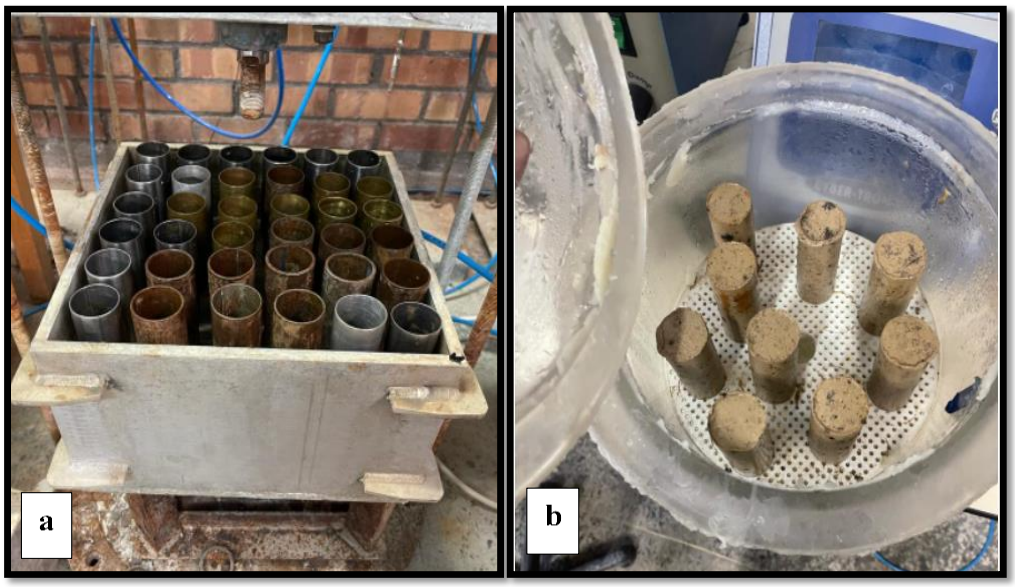

Figure 3.10. a) locating cylindrical specimen extraction before applying pressure and penetration b) maintenance of clay specimens in a desiccator

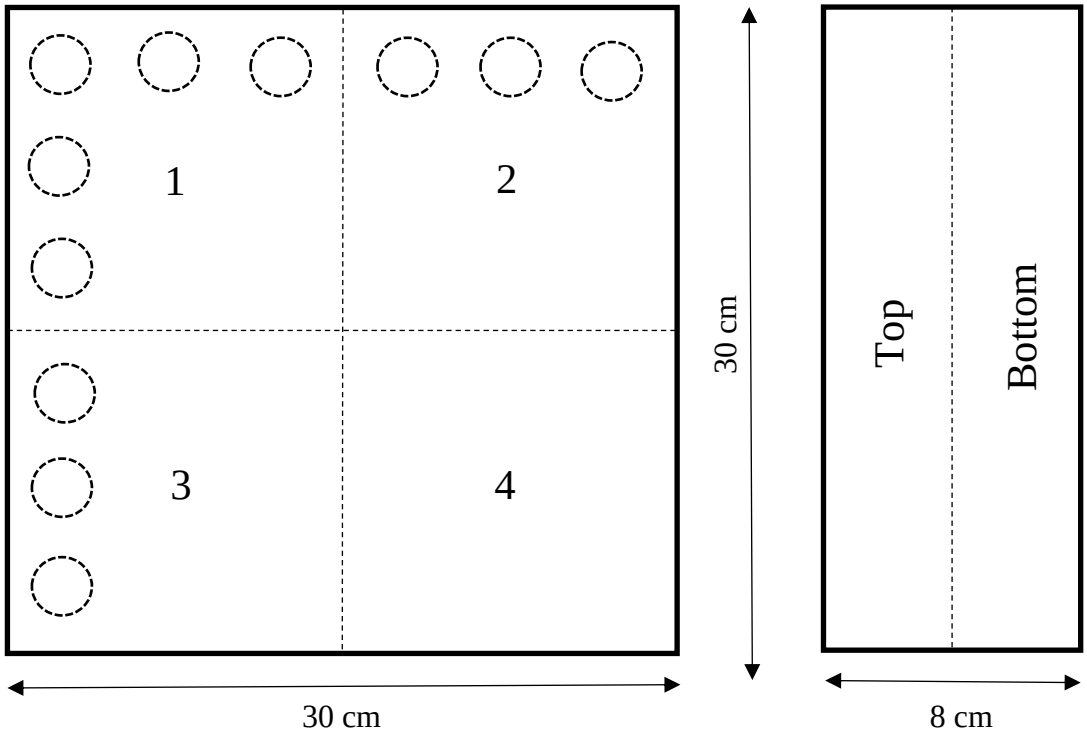

Figure 3.11. Water content check from four sections at top and bottom of the test tank

Table 3.4. Water content check from the tank after consolidation

		M_{tray} (gr)	$M_{wet\ sample}$ (gr)	$M_{dry\ sample}$ (gr)	M_{water} (gr)	Water content (%)
1	Top	22.01	52.60	42.05	10.55	52
	Bot	30.72	50.52	43.73	6.77	52
2	Top	30.40	59.28	49.55	9.73	51
	Bot	30.72	60.06	50.16	9.9	51
3	Top	75.94	153.21	127.02	26.19	51
	Bot	76.73	157.71	130.24	27.47	51
4	Top	76.42	156.82	130.02	26.8	50
	Bot	139.64	229.13	198.90	30.23	51
All remains		310.96	985.54	759.28	226.26	50

3.3 Triaxial Test Equipment

This section introduces the testing setups for undrained and drained triaxial experiments. The next chapter deals with the procedures and assumptions in drained and undrained triaxial tests.

Figure 3.12 and Figure 3.13 show the test setup used for the triaxial drained and undrained test, respectively. For the drained test, a fully automated testing setup was used, whereas for the undrained test the manual testing setup was utilized. Instead of the pore pressure transducer, a null indicator was used in the manual test setup to measure the pore pressure in the specimen and was controlled by a pressure gauge. Furthermore, the volume of the water in or out of the specimen is measured by a Double Burette. Both experiments are conducted in Soil laboratory of Middle East Technical University, Ankara, Turkey.

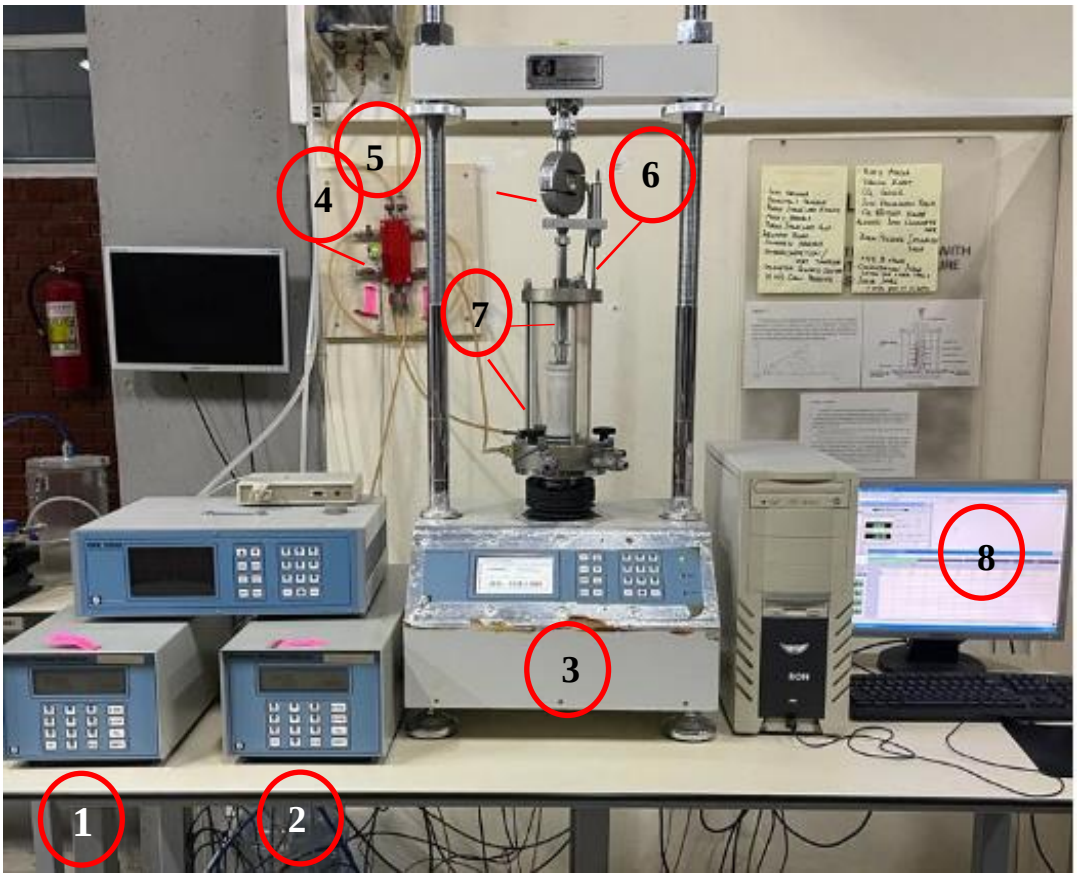

Figure 3.12. The testing setup used for CD triaxial tests

1. Cell pressure Automatic Pressure Controller (APC) with water reservoir for water volume change calculations
2. Backpressure Automatic Pressure Controller (APC) with water reservoir for water volume change measurements
3. Load frame and axial motor used for shearing stage
4. Pore pressure measurement device
5. Load cell for measuring the deviatoric stress
6. Axial displacement transducer
7. Triaxial cell and the loading rod on the specimen during the shearing stage
8. Controlling software

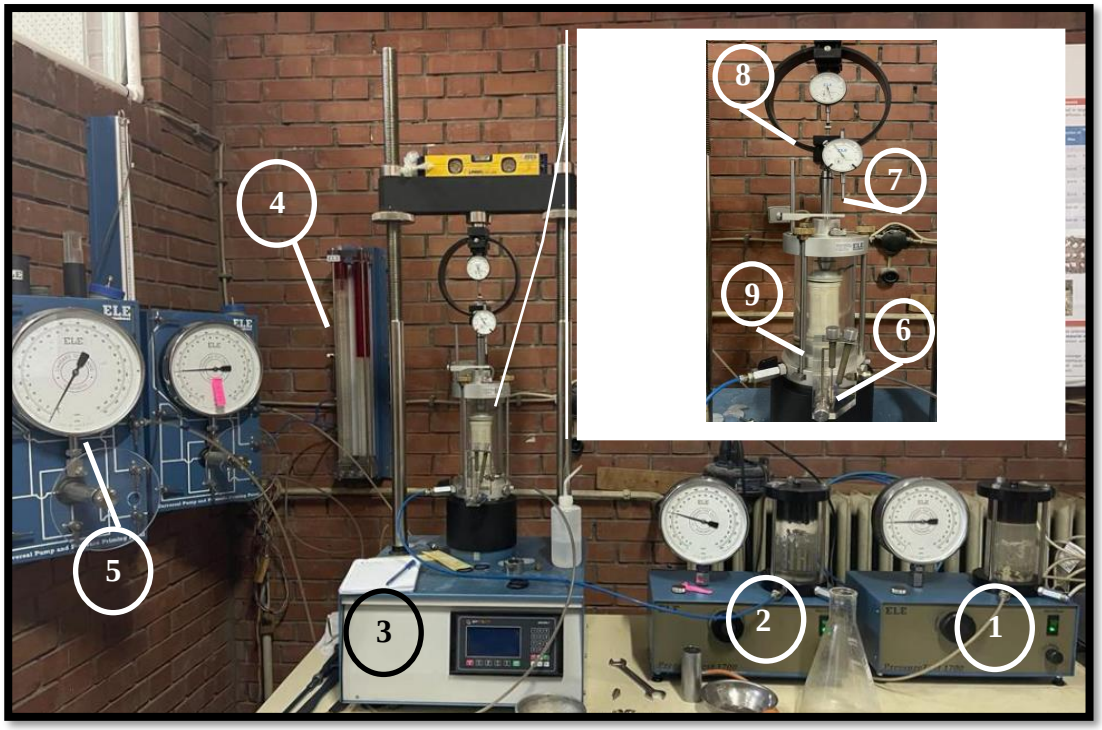

Figure 3.13. The testing setup used for CU triaxial tests

1. Backpressure control unit
2. Cell pressure control unit
3. Load frame and axial motor used for shearing stage
4. Double burette for measuring the drained water volume
5. Pressure gauge for pore water pressure measurement through the null indicator
6. Mercury null indicator
7. Dial gauge for axial deformation measurement
8. Load cell
9. Triaxial cell filled with water and the specimen

3.4 Triaxial Test Procedures

This subsection of the study deals with the triaxial compression test stages and important assumptions and considerations for consolidated drained (CD) and consolidated undrained (CU) tests. The results of the experiments will be spresented in section 4 to compare with those of the multi-stage triaxial test.

All the necessary steps for the consolidated drained and undrained triaxial test are discussed in the following subsections based on ASTM D7181 − 20 and ASTM D4767 − 11 standards.

3.4.1 Preparation Procedures

- Measure the specimen height and diameter from three different points and note the average height and diameter for the initial area and volume calculations.
- Weigh the cylindrical clay specimen and calculate the wet density.
- Moisturize the side drain filter paper and roll it around the clay specimen so that the side drain can touch the top and bottom filter papers for better drainage.
- Make sure that porous stone and filter paper are saturated and put them on the pedestal. Place the clay specimen on them and put the other porous stone and filter paper above it.
- Stretch the rubber membrane over the membrane stretcher by sucking air with a dust-blowing ball and placing it around the mounted specimen (Figure 3.14).
- Place the triaxial cell on the base and fill it with water.

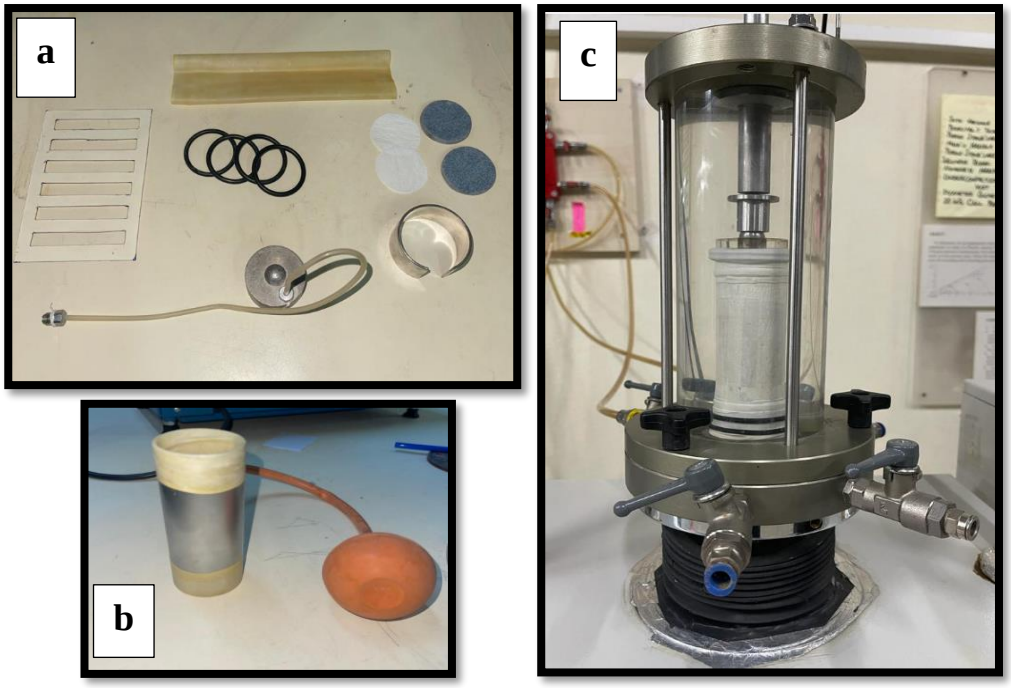

Figure 3.14. Triaxial test apparatus a) a picture of side drain, four o-rings, rubber membrane, two porous stones, filter papers, o-ring stretcher and top cap. b) membrane stretcher and dust blowing ball c) mounted specimen in triaxial cell ready for the test

3.4.2 Saturation Stage

The first stage of the triaxial test is the specimen's saturation by pressurizing the trapped air bubbles in the whole test setup and replacing them with water. It is vital to keep the effective stress constant, thereby avoiding prestressing the specimen or allowing it to swell. The saturation of the clay specimen is a function of pressure and time (Lambe & Whitman, 1969). For this purpose, the following steps are followed:

- increase the cell pressure and back pressure simultaneously. The cell and back pressure difference shouldn't be higher than 30 kPa or lower than 10 kPa (ASTM D4767 – 11).

- In order to prevent overconsolidation of the specimen at two ends, the cell pressure and back pressure are increased incrementally. Therefore, the pressure is distributed throughout the specimen. For each increment, increase cell and back pressures by 50 kPa every one hour up to 350 kPa backpressure. This value is obtained experimentally after the first test. Reconstituted clay specimens have relatively high water content (close to the liquid limit). Therefore, after 24 hours the specimen becomes saturated under 350 kPa as is observed for the first specimen.
- The soil specimen waits under 350 kPa backpressure for 24 hours.
- Close the drainage valve, increase the cell pressure by 70 kPa and check the change in pore water pressure.
- Investigate for pore pressure coefficient B as the portion of pore water pressure changes to cell pressure change (Skempton, 1984).
- If the B value is higher than 95%, the specimen is considered fully saturated. If not, open the drainage valve, increase the back pressure and cell pressure and wait for another 24 hours.
- Repeat the last two steps until a B value of higher than 95% is achieved. All the triaxial tests in this study are performed on clay specimens with a B value of at least 95% and considered fully saturated.

3.4.3 Consolidation Stage

The main objective of this stage is to pressurize the specimen to drain the water and consolidate the specimen to the desired effective consolidation stress. Moreover, the consolidation data will be used to calculate the shearing rate. During the shearing in the drained test, the pore pressure should not change, and the shearing speed must be slow enough to allow the drainage of the water from the specimen. The procedure is summerized below:

- After the saturation stage, close the drainage valve and increase the cell pressure to a desired effective consolidation stress. This study examined

effective consolidation pressures of 100 kPa, 200 kPa, 400 kPa and 600 kPa. For example if the specimen becomes saturated at 350 kPa back pressure and 370 kPa cell pressure, at this stage increase the cell pressure to 450 kPa to consolidate the specimen under 100 kPa effective stress.

- Open the drainage valve and simultaneously start the clock. Record the amount of drained water as an indicator of volume change at specific time intervals.
- Draw the volume change against either the square root of time or the logarithm of time. Determine the time of 50% or 90% of consolidation.
- For this study, two consolidation data are shown in Figure 3.15 and Figure 3.16, and the shearing rate for drained and undrained tests is calculated.

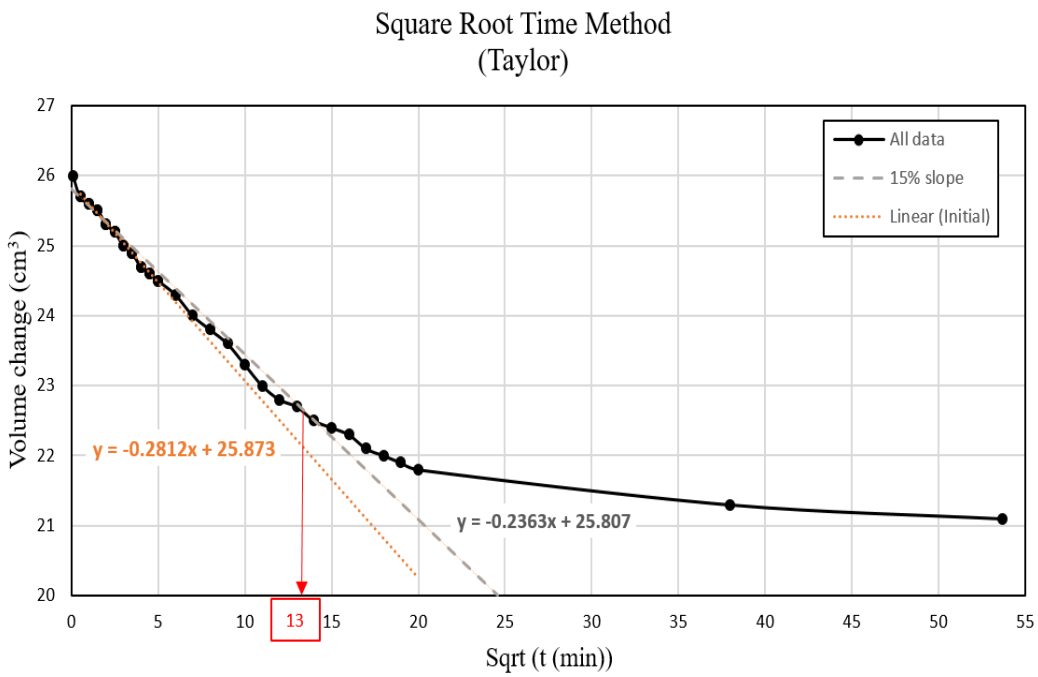

Figure 3.15. Consolidation data obtained from a specimen under 100 kPa consolidation pressure for the shearing rate assessment using the Square Root Time method

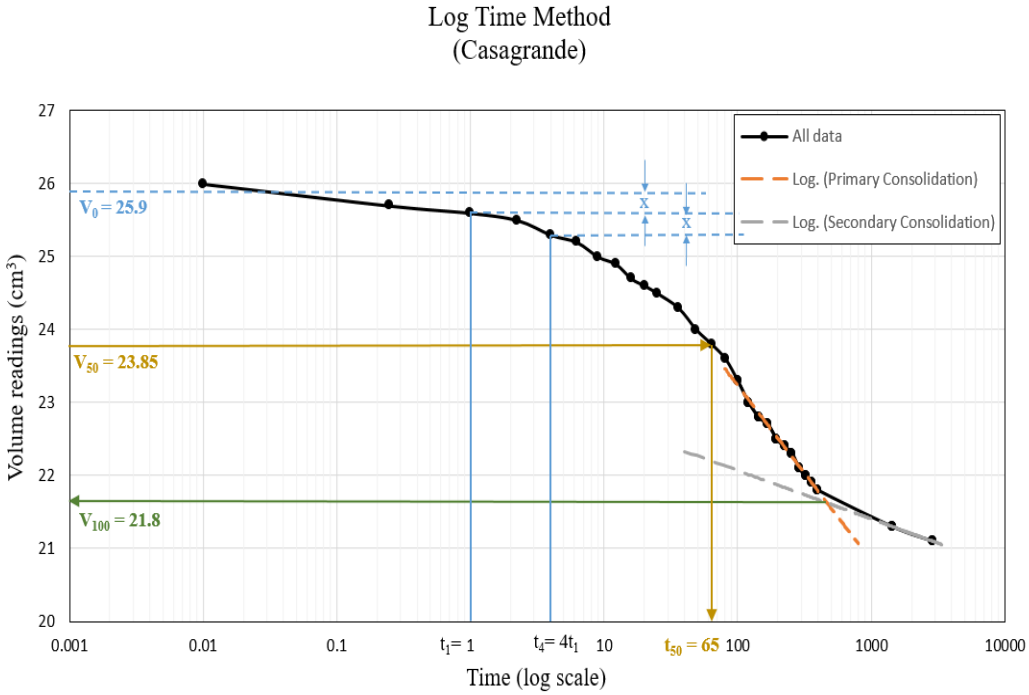

Figure 3.16. Consolidation data under 100 kPa consolidation pressure for the shearing rate assessment using the Log Time method

- In order to make sure that the consolidation is ended, in addition to the proposed equations, the volume change in 24 hours is measured, and if it is negligible, the consolidation stage would be finished.

3.4.4 Shearing Stage

During the shearing stage, the specimen is axially loaded to the failure. Each specimen, consolidated under different effective consolidated stress, gives one stress-strain relation. For each of them, one mohr circle at failure is drawn. After at least three tests, the failure envelope tangent to three circles is fitted and strength parameters are obtained.

The results of the four consolidated drained and undrained triaxial tests are presented in chapter 4.

Since the drainage is allowed in the drained test, the pore pressure remains constant and the amount of drained water measures volume change of the specimen.

On the other hand, no volume change is expected from the specimen in undrained test since the drainage valve is closed and pore water pressure is being measured.

3.4.4.1 Shearing Rate

- Using **Square Root Time** and **Log of Time** suggested by Taylor (1948) and Casagrande & Fadum, (1940) (Eq. 7 and Eq. 8), respectively, following the ASTM D2435 - 04 standard, find the shearing rate.

  Undrained test:

  $$\dot{\epsilon} \geq \frac{4\%}{10\ t_{50}} \qquad \textit{Eq. 7}$$

  Drained test:

  $$\dot{\epsilon} \leq \frac{4\%}{16\ t_{90}} \qquad \textit{Eq. 8}$$

  $\dot{\epsilon}$: shearing rate

  t_{50}: Time for 50% consolidation, obtained from Log Time method

  t_{90}: Time for 90% consolidation, obtained from Root Time method

- From Figure 3.15, t_{90} is calculated as 169 min and utilizing Eq. 8, the shearing rate is 0.001 mm/min for drained test. However, the specimen was sheared at a 0.005 mm/min rate in all the drained tests. It should be noted that during the shearing stage for the drained triaxial test, no excess pore pressure was observed.
- The shear rate for undrained test is calculated using Eq. 7 and the method suggested by Casagrande (log time) shown in Figure 3.16. Note that there is

no limitation for the shear rate for the CU test since the excess pore pressure is measured during the shearing stage.

- Figure 3.16 gives a shearing rate of 0.005 mm/min. However, the authors decided to shear the specimens with a 0.5 mm/min rate for all the CU tests in agreement with ASTM D4767 − 11.

Information about the Square Root Time and Log of Time methods is provided in (Craig, 2004) and (Das, 2019).

3.4.4.2 Corrections

At every data point, three corrections are necessary to be applied; namely filter paper strips correction, rubber membrane correction and specimen's cross-sectional area.

Eq. 9 and Eq. 10 are provided by ASTM D7181 – 20 for filter paper corrections at every data point. The computed value should be subtracted from the calculated stress.

For axial strain above 2%:

$$\frac{K_{fp}P_{fp}}{A_c} \qquad \textit{Eq. 9}$$

For axial strain 2% or less:

$$\frac{50\epsilon_a K_{fp}P_{fp}}{A_c} \qquad \textit{Eq. 10}$$

K_{fp}: *a* load carried by filter paper per unit length of the perimeter (0.19 N/mm used in this study)

P_{fp}: perimeter covered by filter paper (65 mm used in this study)

A_c: the cross-sectional area after the consolidation stage

ϵ_a: axial strain

The rubber membrane around the soil specimen imposes a confinement effect on the specimen and causes an increase in soil strength. Rubber membrane correction

proposed by (Henkel & Gilbert, 1952) should be computed for every data point from Eq. 11 during the shearing according to ASTM D7181 – 20.

$$\frac{4E_m t_m \epsilon_a}{D_c} \qquad \textit{Eq. 11}$$

D_c: diameter of the specimen after consolidation

E_m: young's modulus for the membrane material (1.4 MPa used in this study)

t_m: the thickness of the membrane (0.3 mm used in this study)

As shearing proceeds, the cross-sectional area of the specimen is altered and should be recalculated. The corrected cross-sectional area is computed using the Eq. 12 proposed for a parabolic specimen profile by Toker (2007) for each data point. For the area correction calculations, Eq. 13 is recommended by ASTM D4767 – 11. However, by measuring the cross-sectional area of the specimen, it is concluded that Eq. 12 represents the actual cross area more accurately for our experiments. In the light of this discussion, the author decided to proceed with Eq. 12 for the area correction calculations at every data point.

$$A_c = \frac{A_0}{16}\left(\sqrt{30 \times \frac{1-\epsilon_v}{1-\epsilon_a} - 5} - 1\right)^2 \qquad \textit{Eq. 12}$$

$$A_c = \frac{A_0}{1-\epsilon_a} \qquad \textit{Eq. 13}$$

A_c: corrected area

ϵ_v: volumetric strain

ϵ_a: axial strain

3.5 Multi-stage Test Procedures

In this work, three different procedures are employed and compared to the conventional triaxial test results. The necessary backgroud about the literature is mentioned in Chapter 2. For each of the following procedures, Cycled and Sustained loading conditions are also examined to assess their applicability of them on reconstituted high plasticity Ankara clay.

3.5.1 Rational Procedure

In this procedure, at each shearing stage, the axial load is applied on the specimen until 2% axial strain. A linear relation is expected in $\varepsilon_a/(\sigma_1-\sigma_3)$ vs. ε_a space until 2% axial strain. Subsequently, using Kondner hyperbolic model, the stress and pore water pressure at failure are calculated. From the cell pressure and pore pressure at failure, σ'_3 can be calculated. σ'_1 is calculated from the σ_1-σ_3 at failure. p' and q' are also calculated using Eq. 14 and Eq. 15. In case of the drained test the pore water pressure is constant at all data points. Figure 3.17 demonstrates the results of first shearing stage in undrained test under 100 kPa effective consolidation pressure.

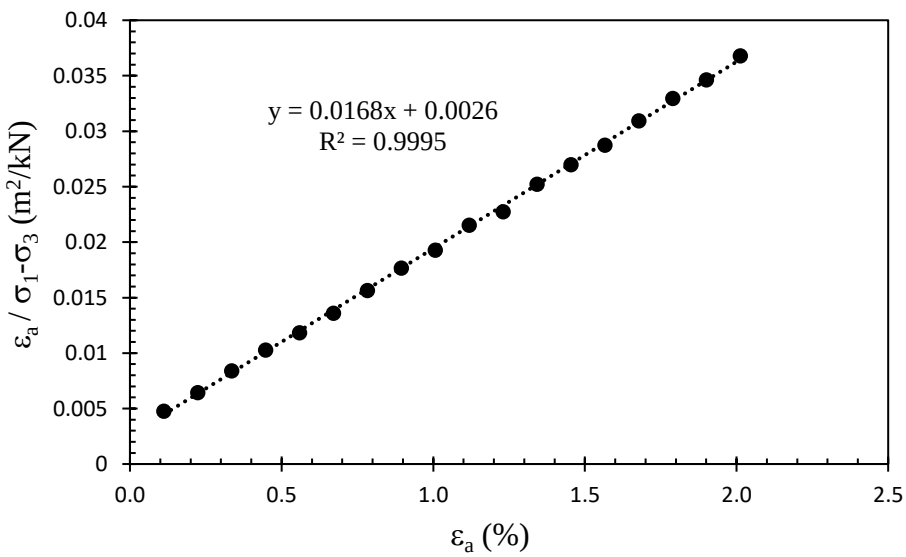

Figure 3.17. Transformed stress-axial strain relation

$$p' = \frac{(\sigma'_1 + \sigma'_3)}{2} \qquad \textit{Eq. 14}$$

$$q' = \frac{\sigma'_1 - \sigma'_3}{2} \qquad \textit{Eq. 15}$$

From Figure 3.17, b is equal to 0.0168 and 1/b is equal to 59.52 kPa, which is the deviatoric stress at failure.

From Figure 3.18, the pore water pressure at failure can be calculated as 481.5 kPa and therefore all needed parameters are available to calculate the p' and q'.

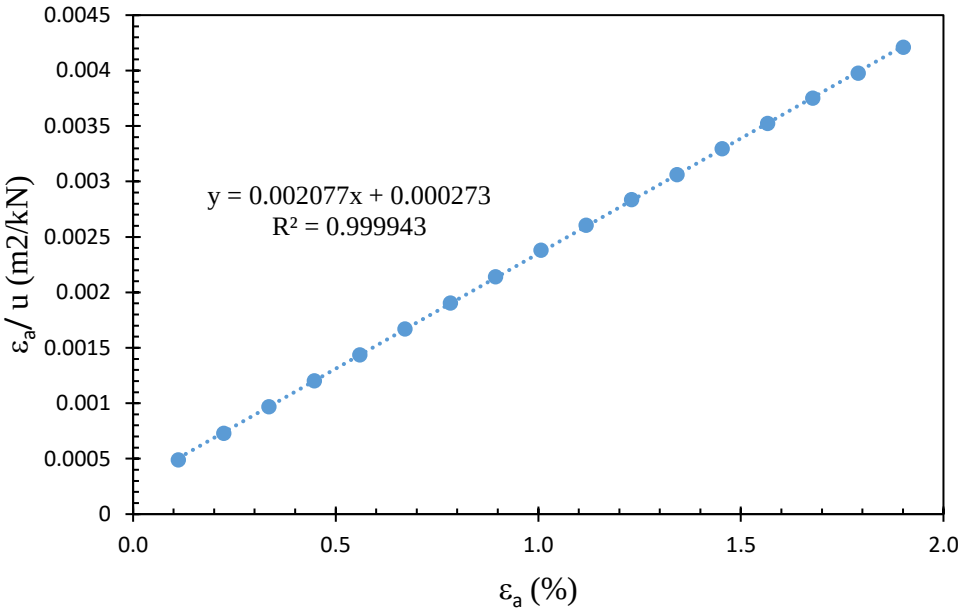

Figure 3.18. Transformed pore water pressure-axial strain relation

The effective consolidation pressure should be doubled at each sequence; however, due to the limited capacity of available pressure tanks, the author decided to use 600 kPa instead of 800 kPa effective consolidation pressure at the last reconsolidation-shearing cycle.

3.5.2 Minimum Slope

In this procedure, the stress-strain curve is drawn and at each data point, the slope of the curve is examined between two data points. To avoid capturing a local failure plane, a line passing two points with 0.6 axial strain intervals is drawn. In other word, a line passing the recent data point and the fifth data point before it (for example, a line between the first and sixth data points, another line from the second and seventh data points). An ideal curve is provided in Figure 3.19 with various lines and slopes. The shearing is continued until the slope becomes minimum (close to zero). After that point, if the negative slope is observed (red line in Figure 3.19), immediately the shearing is stopped and reconsolidation under higher effective stress is started.

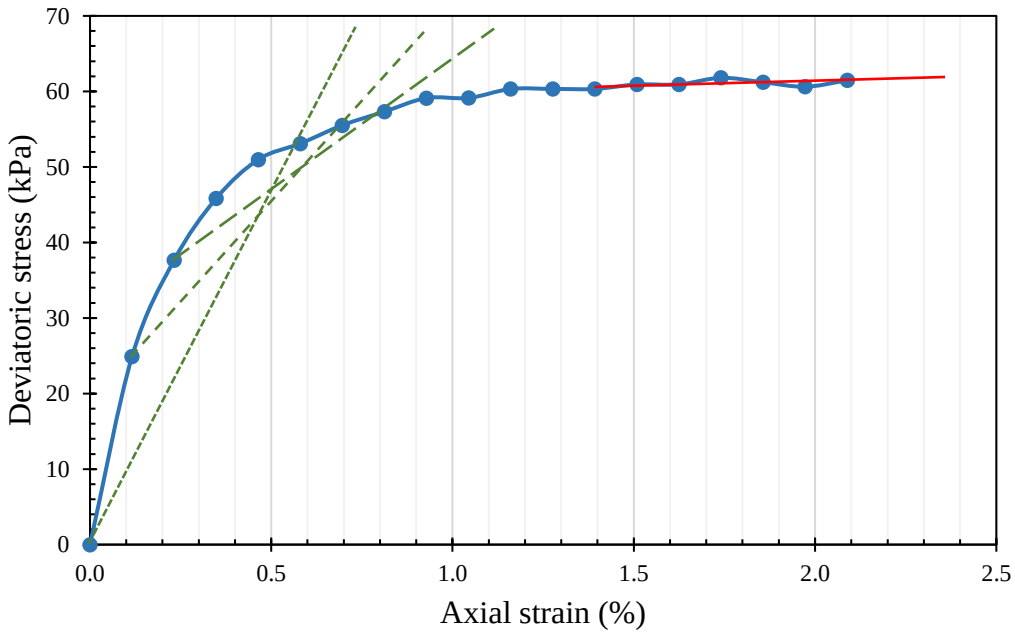

Figure 3.19. Representative plot for minimum slope assessment on the curve

3.5.3 Maximum Curvature Procedure

This procedure is associated by drawing a circle through three points on the stress-strain curve. The maximum curvature of the figure is achieved when the drawn circle

has the minimum radius. Figure 3.20 shows a curve and drawn two circles. The shearing stage is stopped immediately after observing an increase in the radius of the fited circle. To overcome the scaling problems, the axial strain is multiplied by 100 at each data point. The radius of the black circle is higher than the red circle. In other word the curvature of the curve at ninth point (circle passing through the 7th, 8th and 9th data points) is maximum. However, after the red circle, data points become linear and the curvature of the figure at the tenth point (circle passing the 8th, 9th and 10th data points) becomes very low. At this point, the shearing stage is stopped and reconsolidation begins.

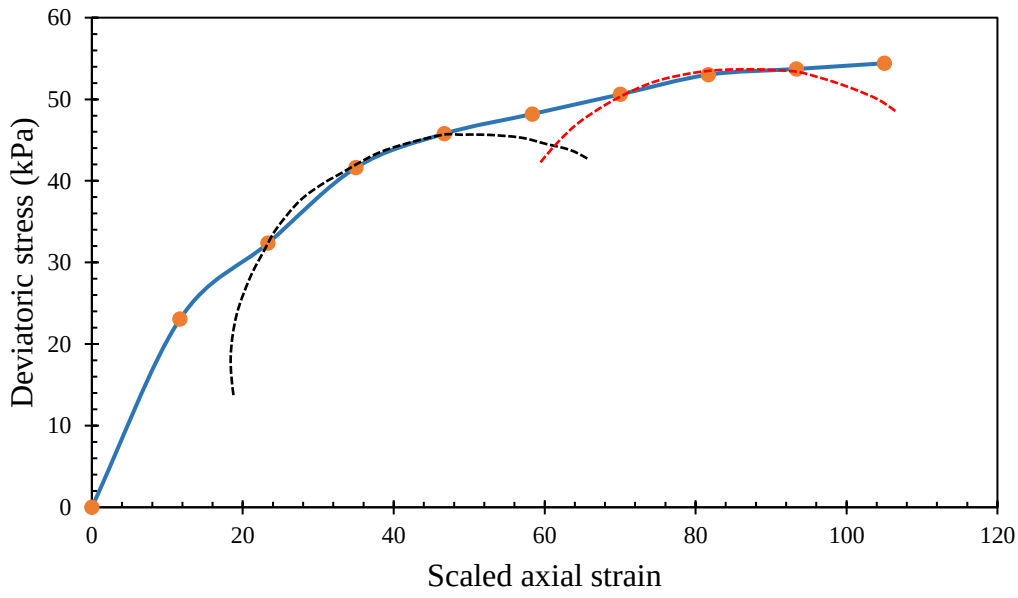

Figure 3.20. Scaled curve and fitted circles at different points

CHAPTER 4

RESULTS OF EXPERIMENTS

In this chapter, the results of the experiments are presented and compared to assess the applicability of each multi-stage triaxial procedure and select the most compatible one with reconstituted Ankara clay soil sample.

Chapter 4 is divided into two parts. The first part shows the results of single-stage and multi-stage undrained experiments. Subsequently, the single-stage and multi-stage drained test results are provided. Table 4.1 presents a list of conducted tests and code for each test.

Six multi-stage triaxial approaches were investigated on the reconstituted Ankara clay under drained and undrained conditions. The outcome of the multi-stage tests is compared to those of single-stage conventional triaxial test by considering the shear strength parameters. Moreover, the maximum possible number of shear-reconsolidation sequences at each approach is examined. The same testing setup for single-stage and multi-stage tests is used for each drainage condition with the assumptions and considerations as are explained in chapter 3.

Table 4.1. Conducted single-stage and multi-stage triaxial tests on Ankara clay

Test Type	Loading	Test Code
Single-Stage (validation test)	4 specimens	CTC
Multistage Rational Procedure	Cycled	RPC
Multistage Rational Procedure	Sustained	RPS
Multistage Minimum Slope	Cycled	MSC
Multistage Minimum Slope	Sustained	MSS
Multistage Maximum Curvature	Cycled	MCC
Multistage Maximum Curvature	Sustained	MCS

4.1 Consolidated Undrained (CU) Test Results

In this section, the results of undrained experiments are presented. Isotropically consolidated undrained tests are conducted on four specimens under 100 kPa, 200 kPa, 400 kPa, and 600 kPa effective confining pressures. The failure is achieved when the peak deviatoric stress is observed on the deviatoric stress-axial strain curve.

4.1.1 Undrained single-stage Test Results

Initially, the water content of specimens was measured as 50%. The single-stage stress-axial strain relation and excess pore water pressure vs. axial strain are shown in Figure 4.1 and Figure 4.2, respectively. In Table 4.2, the results of single-stage tests at failure are written .The modified failure envelope, together with slope and intercept for single-stage undrained tests are presented in Figure 4.3 and strength parameters are calculated afterwards.

Table 4.2. Initial and final water content for undrained single-stage triaxial test

		M_{wet} (gr)	M_{dry} (gr)	M_{tray} (gr)	Water content
100 kPa	initial	273.250	222.92	127.22	0.525
	final	267.437	222.92		0.465
200 kPa	initial	226.389	174.56	72.189	0.506
	final	215.874	174.56		0.403
400 kPa	initial	283.040	229.76	127.24	0.519
	final	268.42	229.76		0.377
600 kPa	initial	277.390	226.29	127.23	0.515
	final	262.018	226.29		0.360

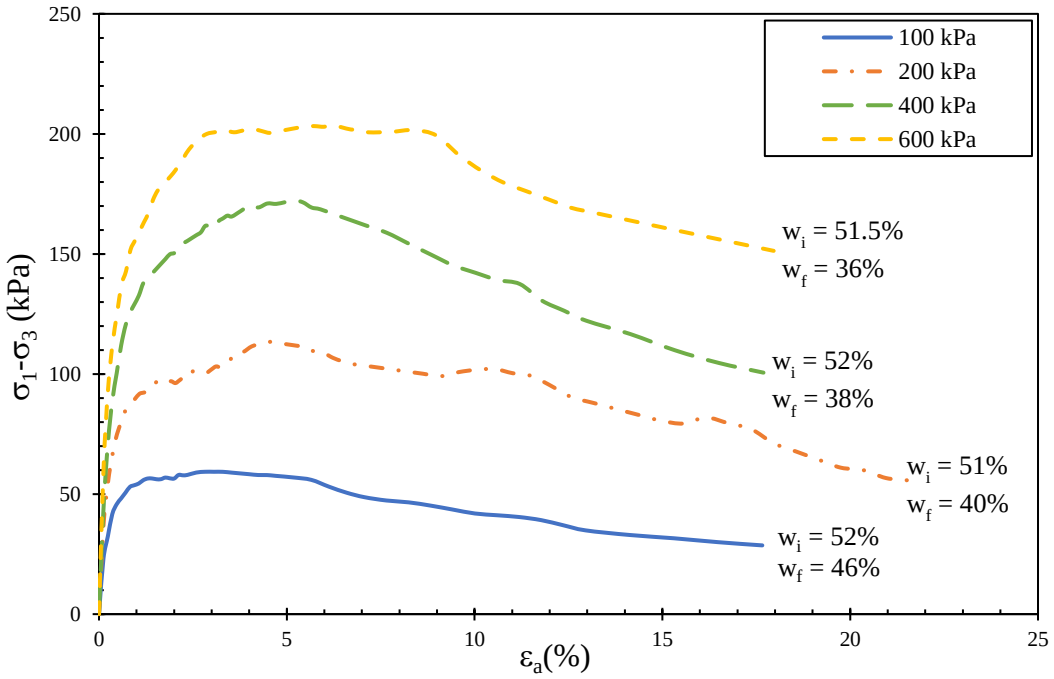

Figure 4.1. Deviatoric stress - axial strain for single-stage undrained tests

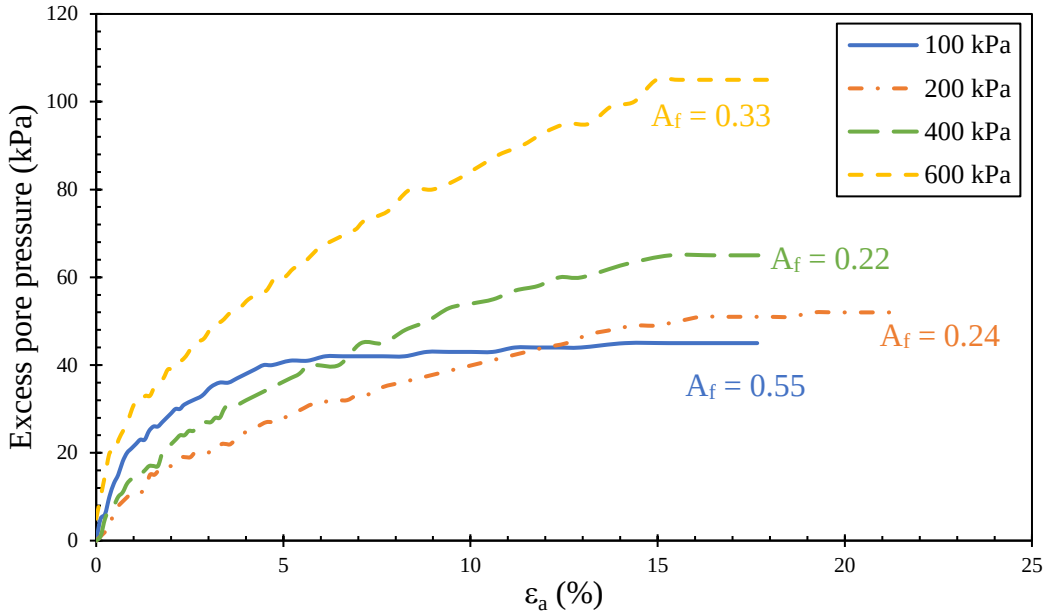

Figure 4.2. Excess pore water pressure vs. axial strain for single-stage undrained test

Table 4.3. Pore pressure and deviatoric stress at failure, initial and secant elastic moduli for single-stage tests

	u_f (kPa)	$(\sigma_1-\sigma_3)_f$ (kPa)	p' (kPa)	q (kPa)	E'_0 (MPa)	E'_{50} (MPa)
100 (kPa)	445	59.3	96.6	29.6	19.7	13.8
200 (kPa)	497	113.4	229.7	56.7	30.8	22.9
400 (kPa)	572	172.3	449.1	86.1	36.7	24.9
600 (kPa)	618	203.6	633.8	101.8	50.3	30.9

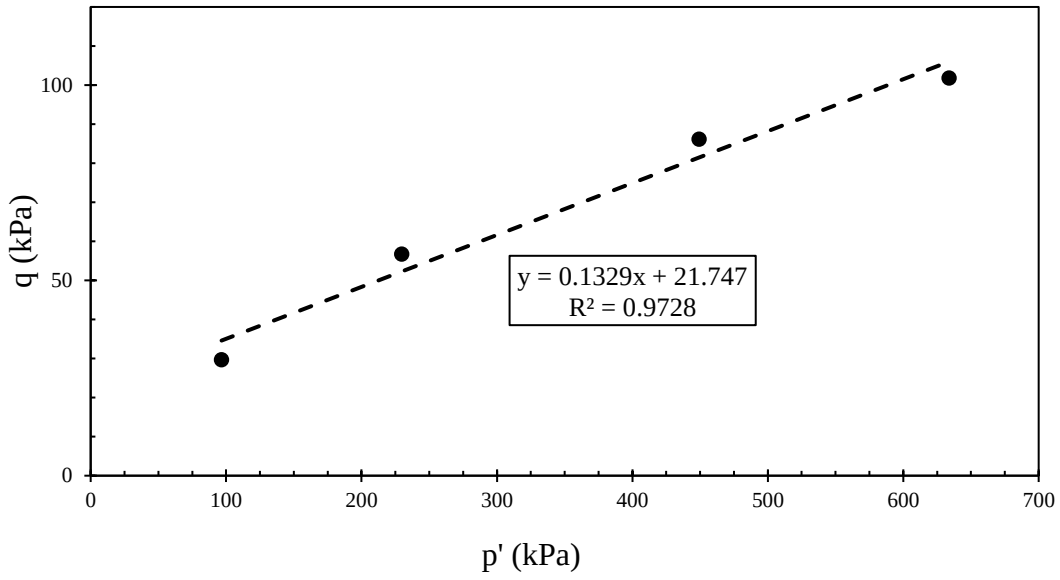

Figure 4.3. Modified failure envelope for undrained single-stage tests

From the modified failure envelope equation, the internal friction angle and cohesion are calculated as **7.6**° and **22 kPa**.

4.1.2 Undrained RPC Test Results

Following the proposed Rational Procedure by Nambiar et al. (1985), the specimen is sheared up to 2% axial strain and by interpretation of the results, the strength parameters are calculated as it is explained in chapter 3.5. Figure 4.4 and Figure 4.5 depict the results of the RPC test in ε_a/u vs. ε_a and $\varepsilon_a/(\sigma_1-\sigma_3)$ vs. ε_a spaces for 100 kPa, 200 kPa, 400 kPa and 600 kPa effective confining pressures, respectively. Stress-axial strain and excess pore pressure vs. axial strain relationships are demonstrated in Figures 4.6 and 4.7 accordingly. Using the equations of four lines, the stresses at failure are estimated and presented in Table 4.3 and modified failure envelope is drawn in Figure 4.8.

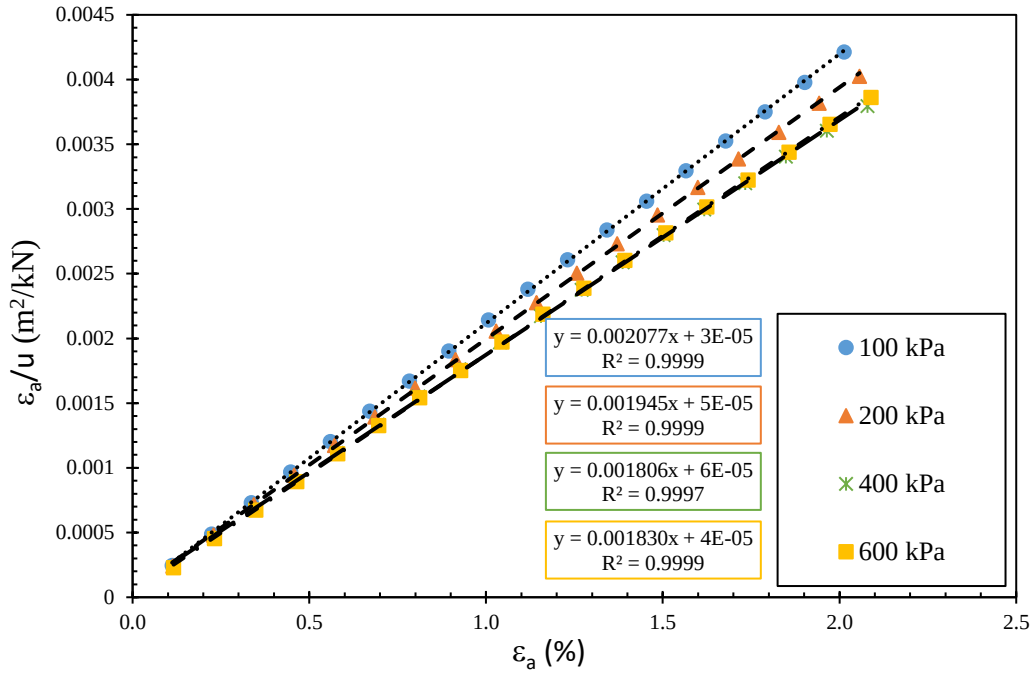

Figure 4.4. Transformed pore water pressure vs. axial strain relationship for undrained RPC test

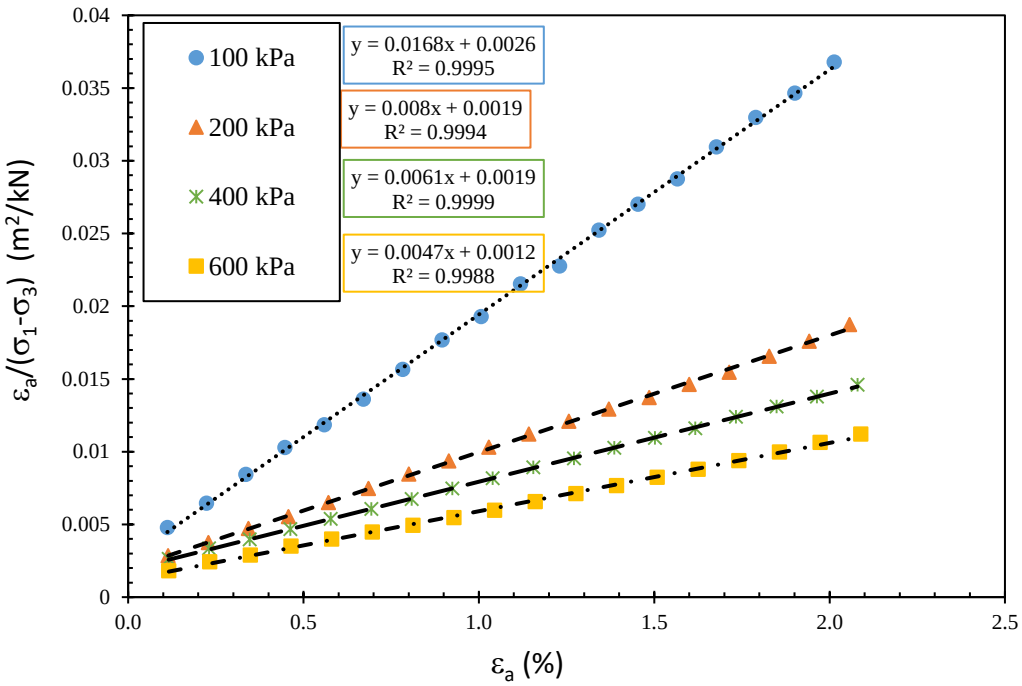

Figure 4.5. Transformed stress-axial strain relationship for undrained RPC test

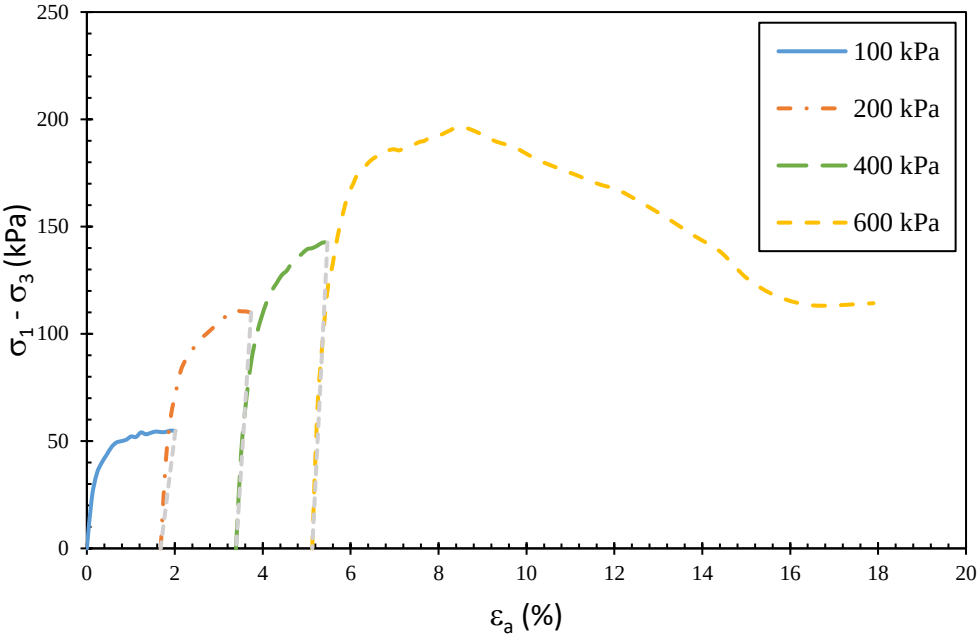

Figure 4.6. Stress-axial strain relationship for undrained RPC test

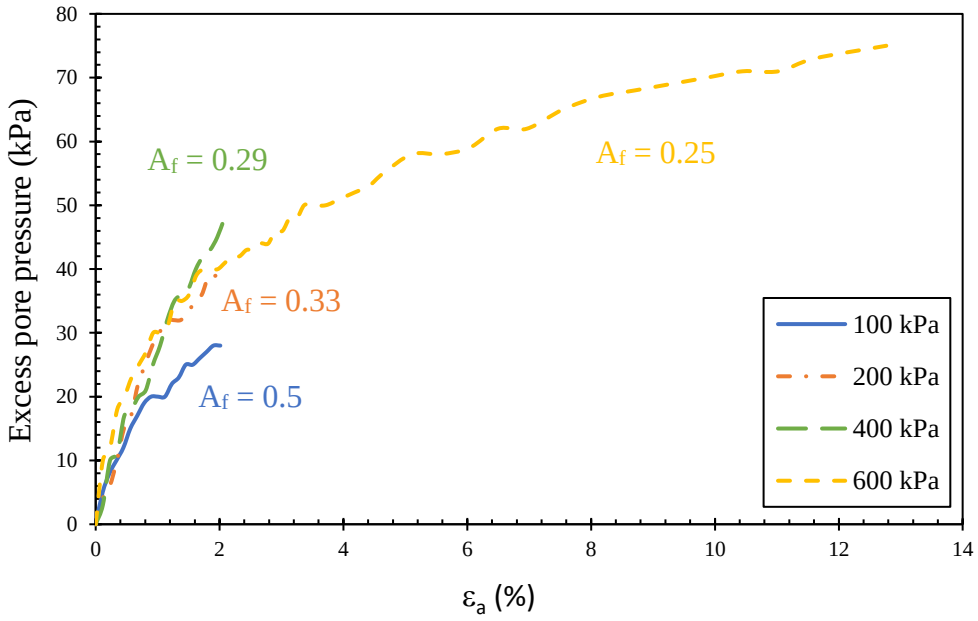

Figure 4.7. Excess pore water pressure vs. Axial strain for undrained RPC test

Table 4.4. Predicted pore pressure and stress at failure, initial and secant elastic moduli for undrained RPC test

	b_u	u_f (kPa)	b	$(\sigma_1-\sigma_3)_f$ (kPa)	p' (kPa)	q (kPa)	E'_0 (MPa)	E'_{50} (MPa)
100 (kPa)	0.002077	481.4	0.0168	59.5	98.3	29.7	20.9	15.4
200 (kPa)	0.001945	514.1	0.0080	125	218.4	62.5	35	23.7
400 (kPa)	0.001806	553.7	0.0061	163.9	428.3	81.9	38.2	24.8
600 (kPa)	0.001830	546.4	0.0047	212.7	659.9	106.3	55.2	31.1

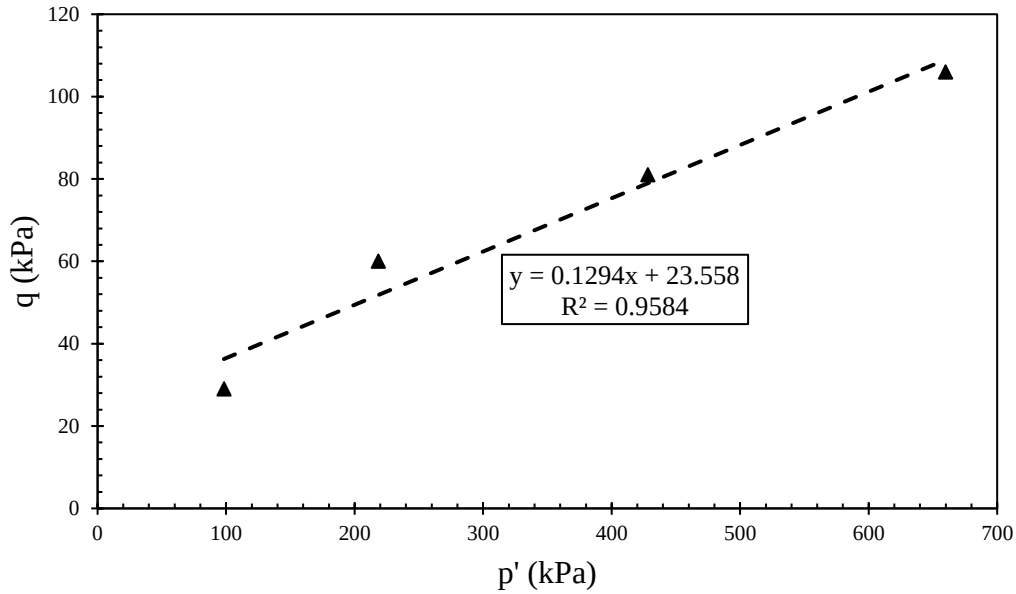

Figure 4.8. Modified failure envelope for RPC test

Considering the failure envelope equation in Figure 4.8, the reconstituted Ankara clay's internal friction angle and cohesion using the RPC method are predicted as **7.4**° and **23 kPa,** respectively.

4.1.3 Undrained RPS Test Results

The same Rational procedure as explained in chapter 3.5 is followed without removing the deviatoric load after each shearing phase. Therefore, a lower strength is expected from the specimen at latter shearing-reconsolidation cycles. Figure 4.9 and Figure 4.10, Figure 4.11 and Figure 4.12 demonstrate the results of the RPS test in ε_a/u vs. ε_a, $\varepsilon_a/(\sigma_1-\sigma_3)$ vs. ε_a, σ_1-σ_3 vs. ε_a and excess pore pressure vs. ε_a space for 100 kPa, 200 kPa, 400 kPa and 600 kPa effective confining pressures, respectively. Table 4.4 provides the estimated stresses at failure and in Figure 4.13, the modified failure envelope is drawn.

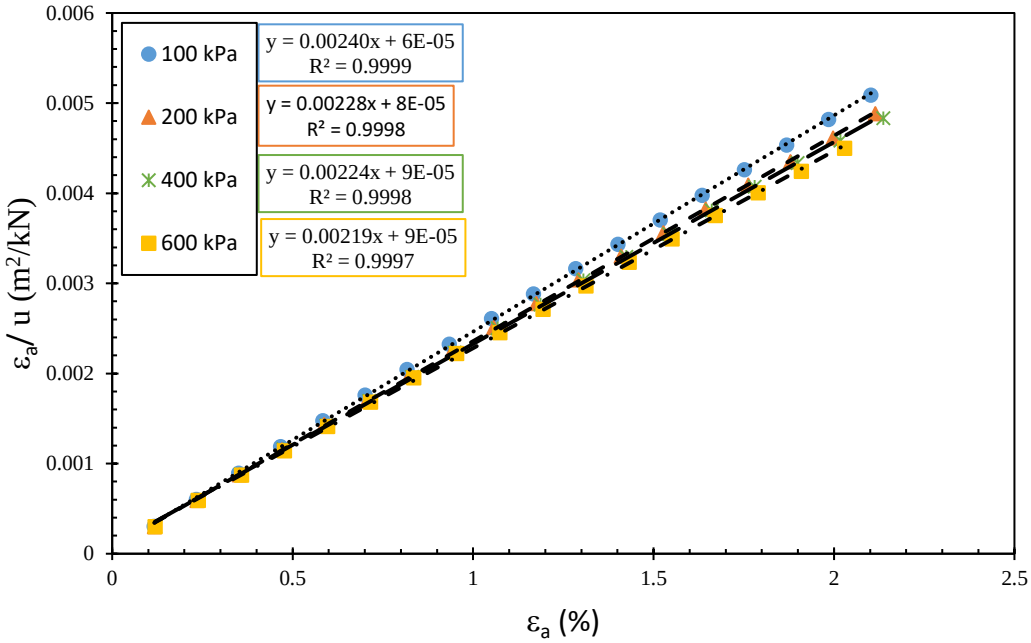

Figure 4.9. Transformed pore water pressure vs. axial strain relationship for undrained RPS test

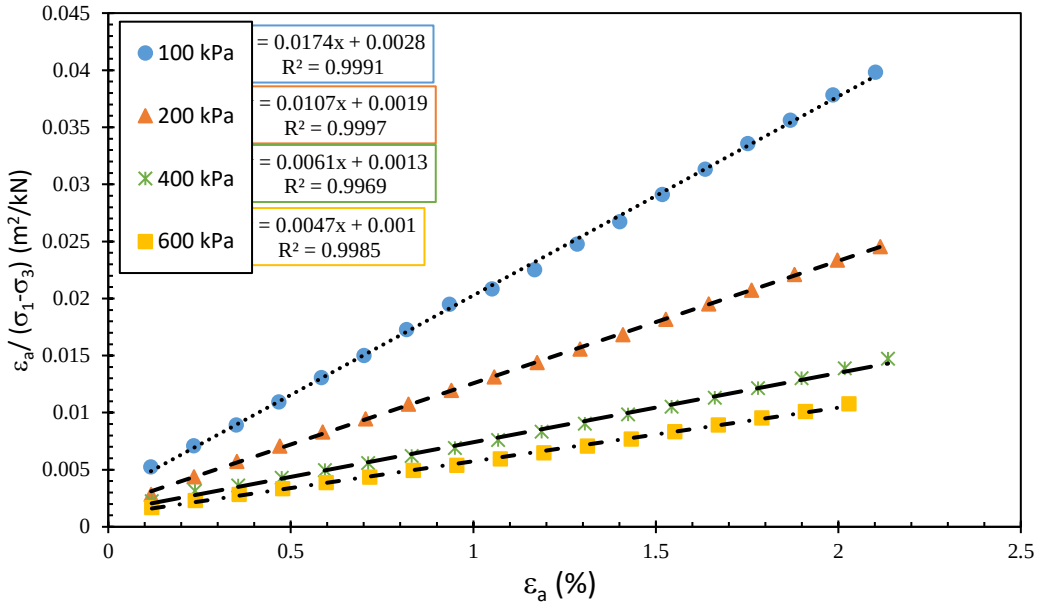

Figure 4.10. Transformed stress-axial strain relationship for undrained RPS test

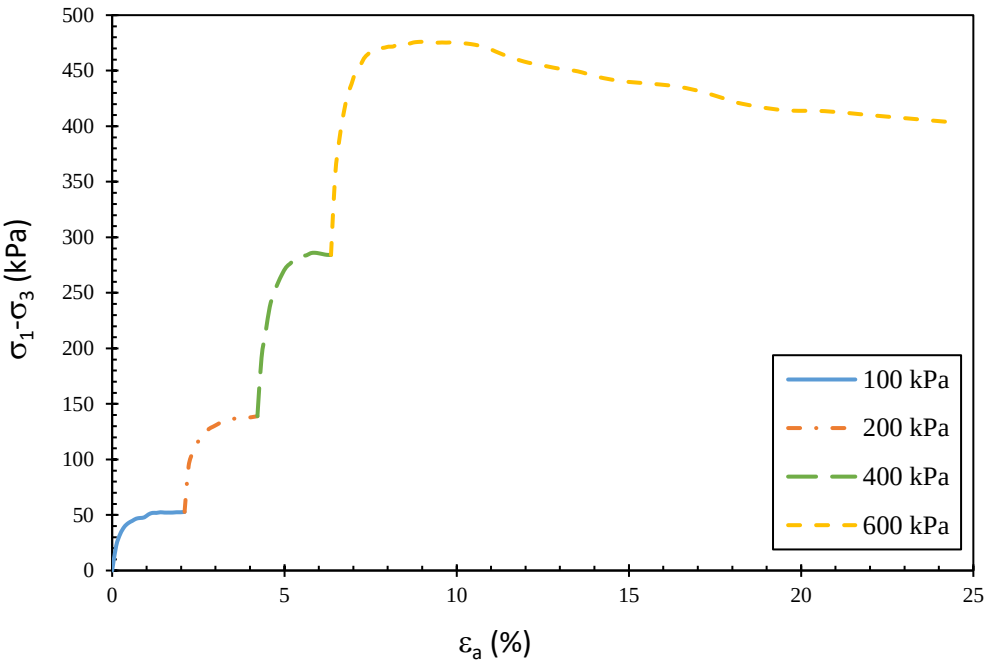

Figure 4.11. Stress-axial strain relationship for undrained RPS test

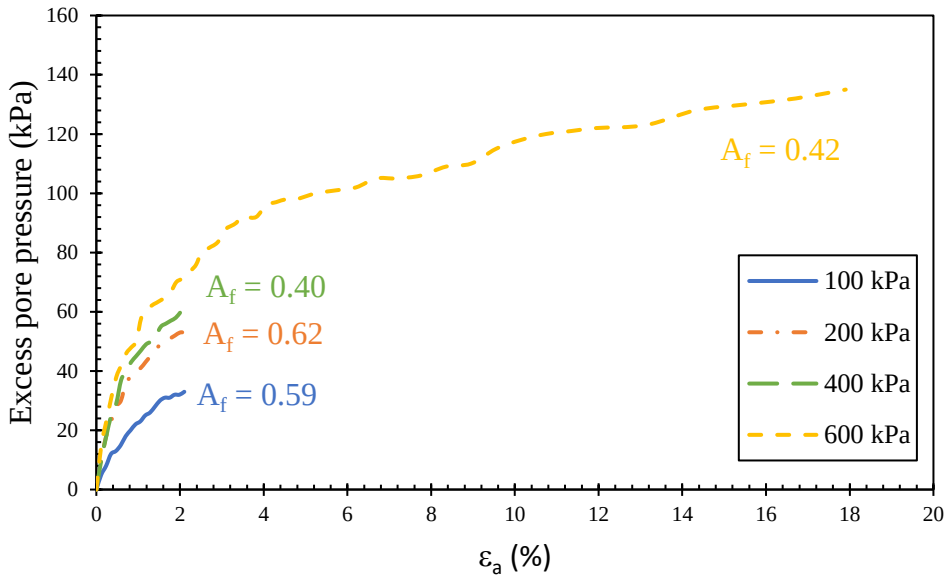

Figure 4.12. Excess pore pressure vs. Axial strain for undrained RPS test

Table 4.5. Predicted pore pressure and stress at failure, initial and secant elastic moduli for undrained RPS test

	b_u	u_f (kPa)	b	$(\sigma_1-\sigma_3)_f$ (kPa)	p' (kPa)	q (kPa)	E_0' (MPa)	E'_{50} (MPa)
100 (kPa)	0.00240	416.7	0.0174	57.5	92.1	28.7	19	12.3
200 (kPa)	0.00228	438.6	0.0107	93.5	188.1	46.7	35.2	19.8
400 (kPa)	0.00224	446.4	0.0061	163.9	415.5	81.9	44.3	23
600 (kPa)	0.00219	456.6	0.0047	212.8	629.8	106.4	59.7	40.1

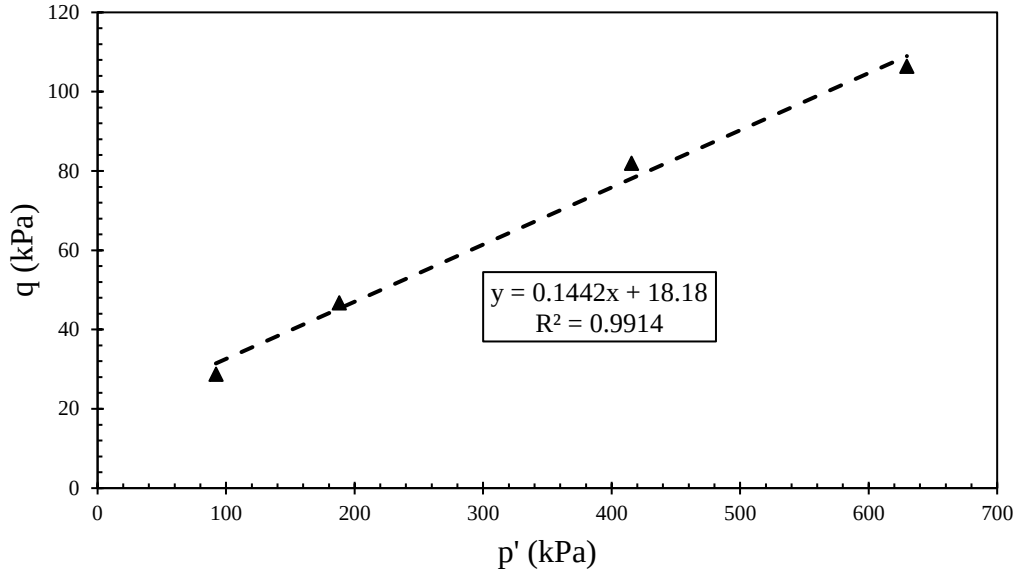

Figure 4.13. Modified failure envelope for RPS test

Considering the failure envelope equation in Figure 4.13, the reconstituted Ankara clay's internal friction angle and cohesion using the RPS method are predicted as **8.3**° and **18 kPa,** respectively.

4.1.4 Undrained MSC Test Results

In this approach, the shearing is stopped when the slope of the stress–axial strain figure becomes minimum. Mostly, this minimum slope is followed by a decrease in strength where the slope becomes negative. The experiment should be ceased before the start of this decrease. Deviatoric stress–axial strain and excess pore pressure vs. axial strain are plotted in Figure 4.14 and 4.15 respectively. The results of the MSC are tabulated in Table 4.6, and the modified failure envelope is drawn in Figure 4.16.

Due to an unexpected accident, the experiment couldn't be continued for the fourth sequence and only three points were available to draw the failure envelope.

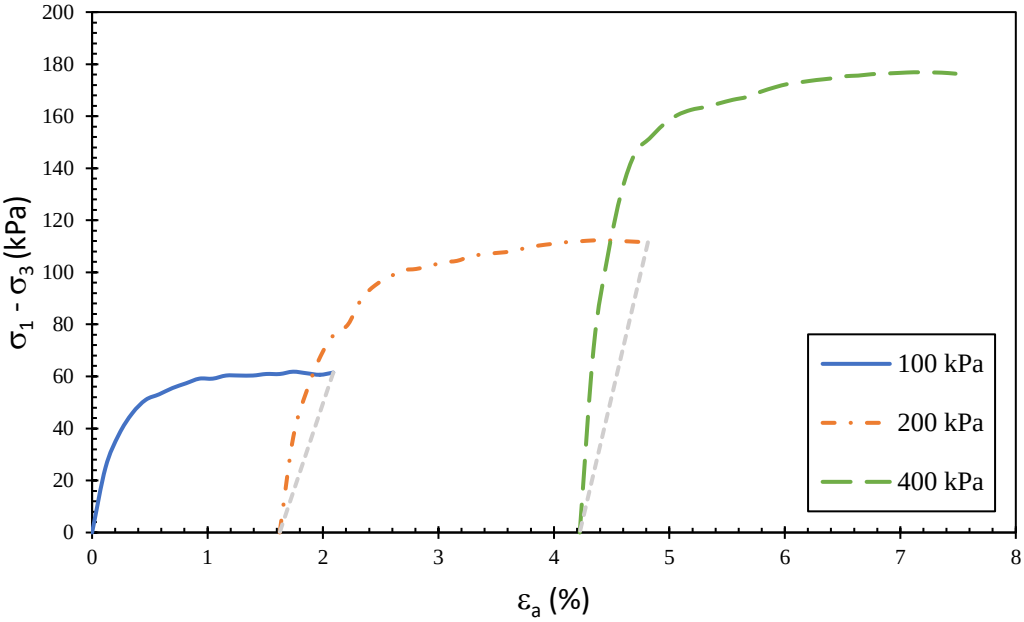

Figure 4.14. Deviatoric stress–axial strain for undrained MSC test

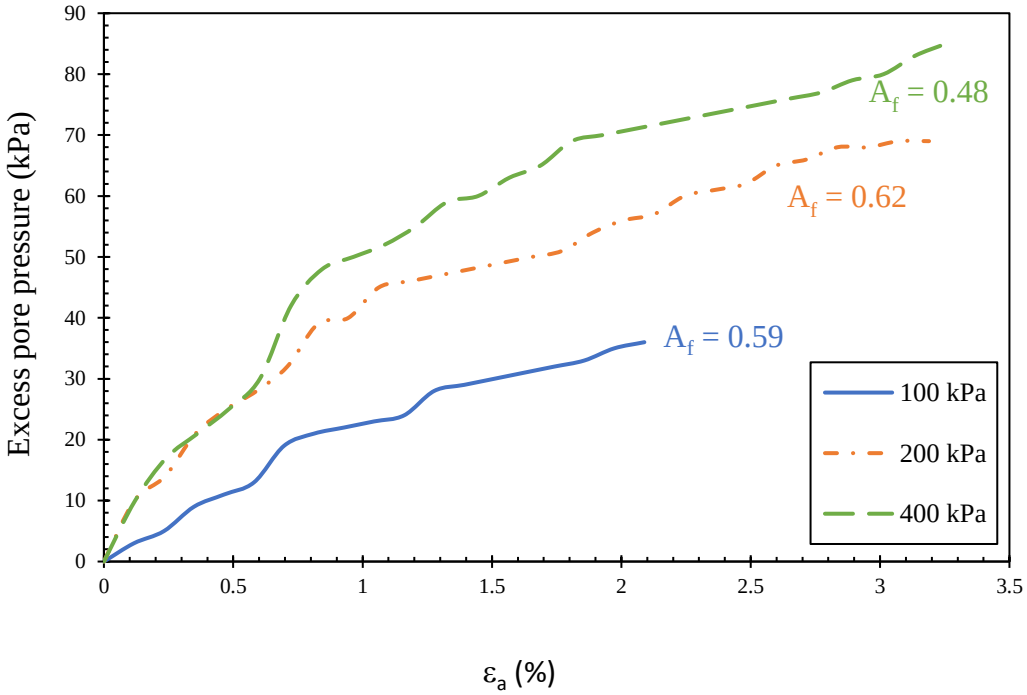

Figure 4.15. Excess pore pressure vs. axial strain for undrained MSC test

Table 4.6. Pore pressure, deviatoric stress, initial and secant elastic moduli at failure for undrained MSC test

	u_f (kPa)	$(\sigma_1-\sigma_3)_f$ (kPa)	p' (kPa)	q (kPa)	E_0' (MPa)	E'_{50} (MPa)
100 (kPa)	386	61.5	94.7	30.7	21.4	15.3
200 (kPa)	419	111.8	186.8	55.8	31.1	21.1
400 (kPa)	433	176.7	405.4	88.4	58	44

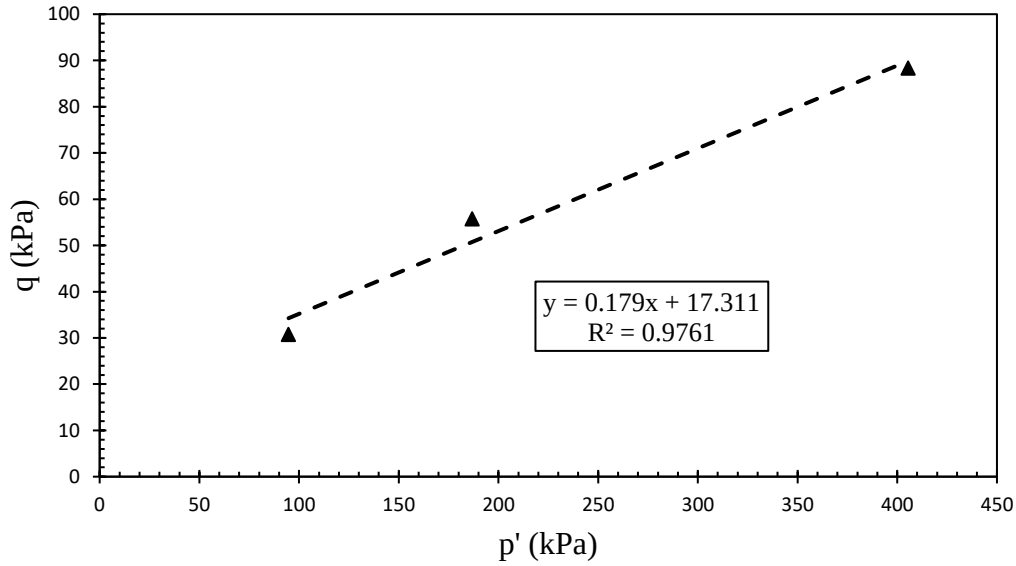

Figure 4.16. Modified failure envelope for undrained MSC test

Considering the modified failure envelope equation in Figure 4.16, the reconstituted Ankara clay's internal friction angle and cohesion using the MSC method are estimated as **10.3**° and **17.6 kPa,** respectively.

4.1.5 Undrained MSS Test Results

In Figure 4.17 and Figure 4.18, the deviatoric stress–axial strain and excess pore pressure vs. axial strain are demonstrated. The results of the MSS testing procedure are shown in Table 4.7. Implementing the MSS approach, reconstituted Ankara clay sample can withstand a maximum of 3 shear-reconsolidation sequences and at the fourth shearing step, the specimen shows a dramatic strength reduction compared to the CTC test results. Therefore, considering the first three cycles, the modified failure envelope is drawn in Figure 4.19 and the strength parameters are reported afterward.

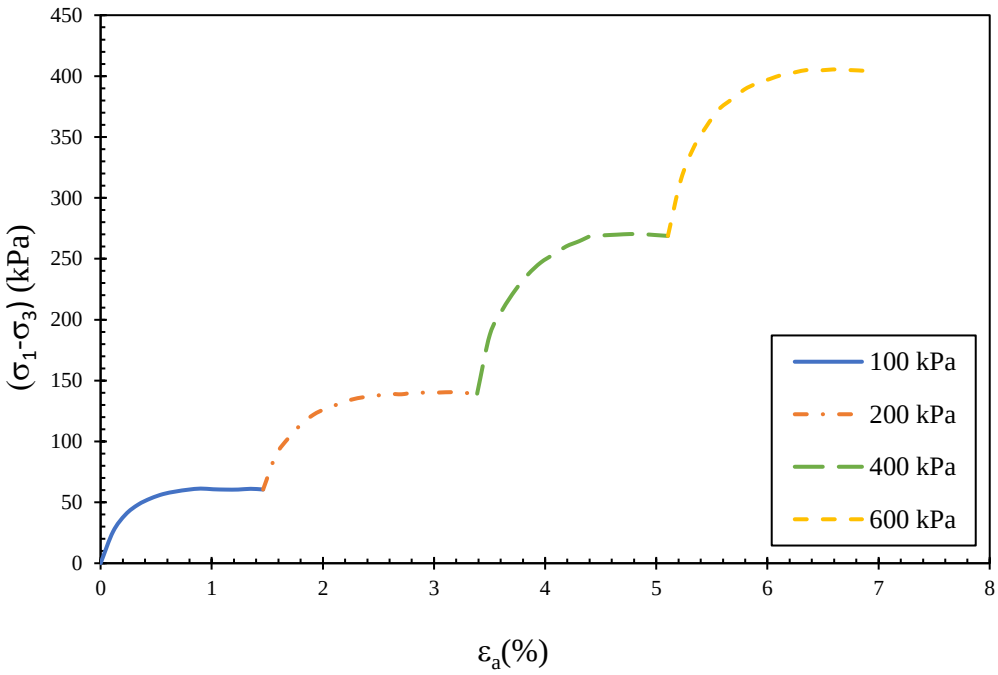

Figure 4.17. Deviatoric stress–axial strain for undrained MSS test

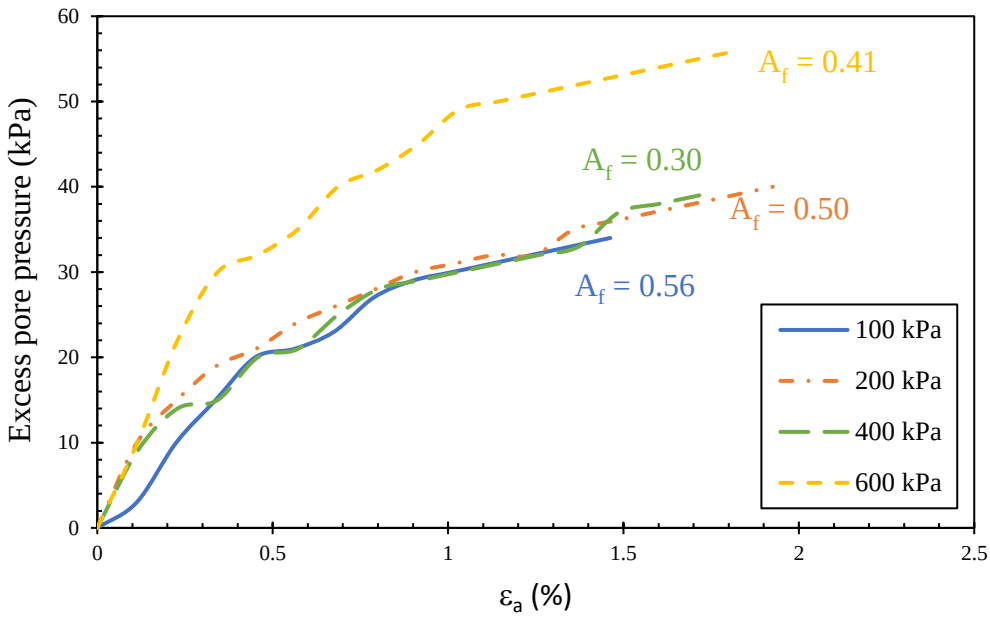

Figure 4.18. Excess pore pressure vs. axial strain for undrained MSS test

Table 4.7. Pore pressure and deviatoric stress at failure and initial and secant elastic moduli for undrained MSS test

	u_f (kPa)	$(\sigma_1-\sigma_3)_f$ (kPa)	p' (kPa)	q (kPa)	E_0' (MPa)	E'_{50} (MPa)
100 (kPa)	414	60.5	97.5	30.5	23.1	16.6
200 (kPa)	420	79.3	200.7	39.7	24.6	17.7
400 (kPa)	418	130.2	427.1	65.1	42.3	30.8
600 (kPa)	436	135.9	612.9	67.9	39.6	32.1

In Figure 4.19, red doted line shows the failure envelope if we include the fourth cycle in the calculations. However, the fourth data point was omitted, the failure

envelope was drawn through three points, and strength parameters were found using the dashed line.

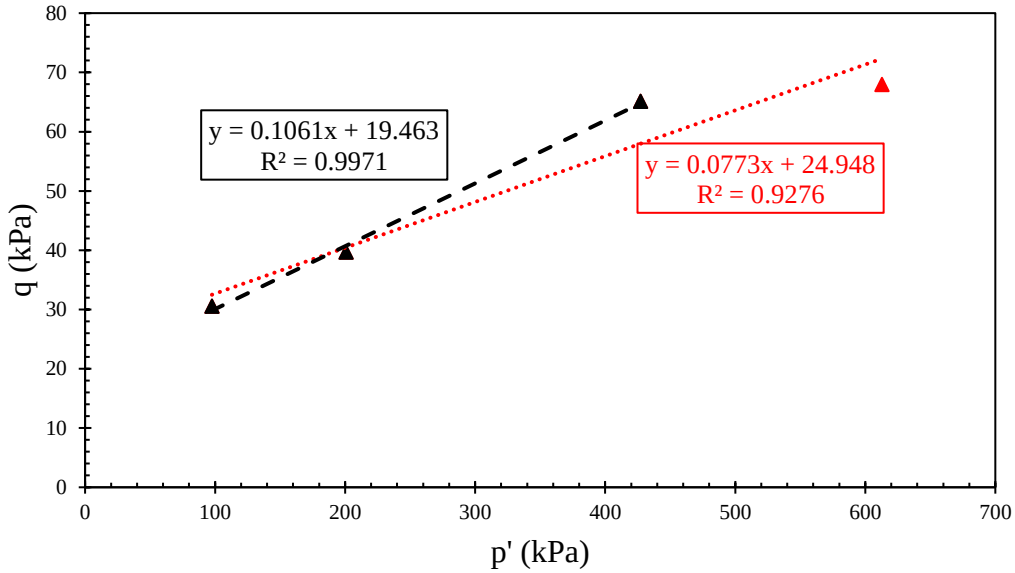

Figure 4.19. Modified failure envelope for undrained MSS test

Regardless of the fourth sequence, considering the failure envelope's equation in Figure 4.19, the reconstituted Ankara clay's undrained internal friction angle and cohesion using the MSS method are predicted as **6**° and **19.6 kPa,** respectively.

4.1.6 Undrained MCS Test Results

The deviatoric stress–axial strain and excess pore pressure vs. axial strain are demonstrated in Figures 4.20 and 4.21, followed by Table 4.8, presenting the results of the undrained MCS approach. The modified failure envelope is shown in Figure 4.22 and the strength parameters are noted.

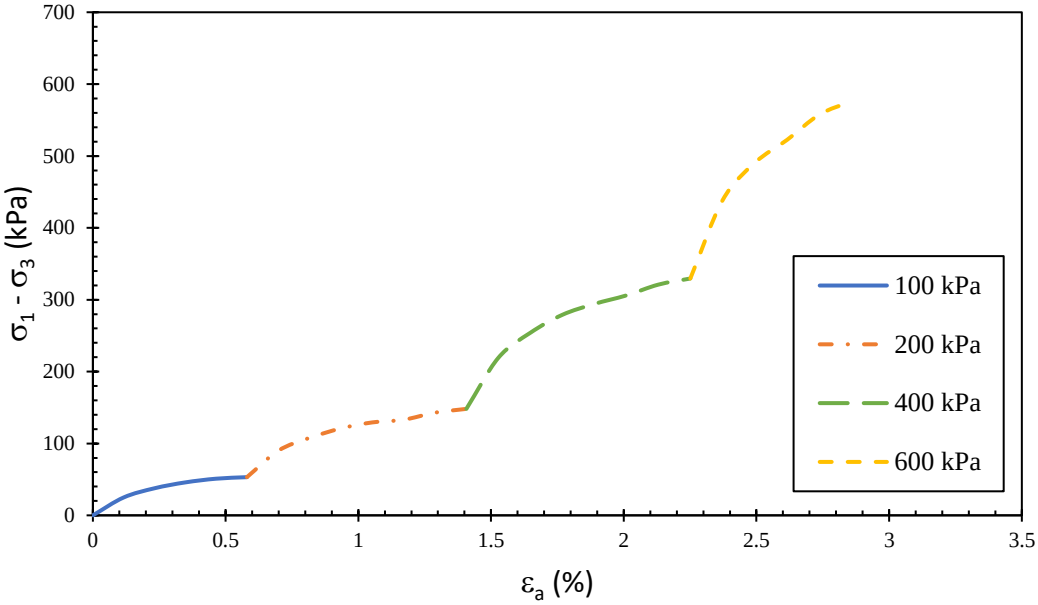

Figure 4.20. Deviatoric stress–axial strain for undrained MCS test

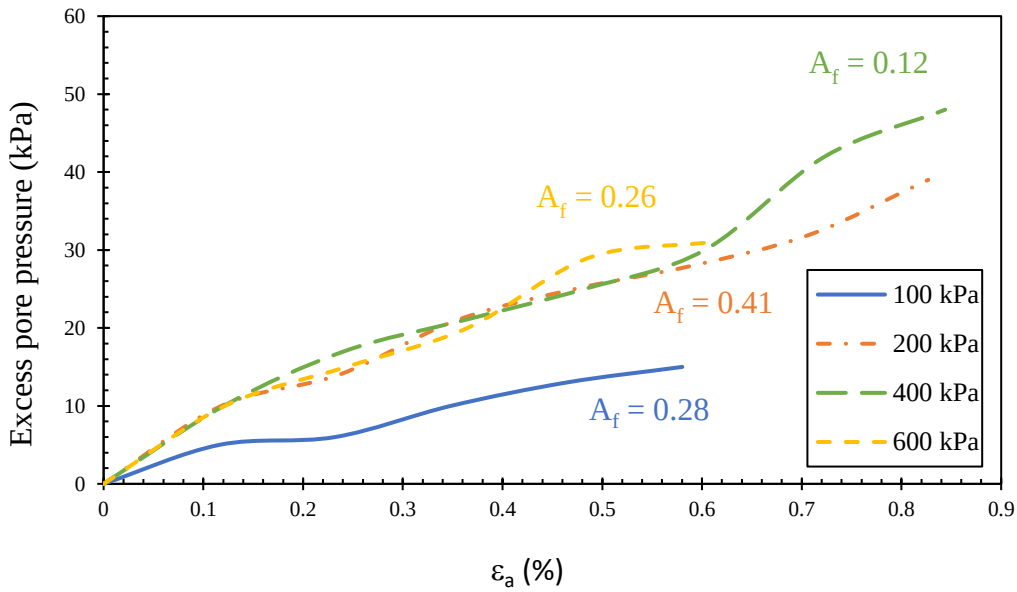

Figure 4.21. Excess pore pressure vs. axial strain for undrained MCS test

Table 4.8. Pore pressure and deviatoric stress at failure, initial and secant elastic moduli for undrained MCS test

	u_f (kPa)	$(\sigma_1-\sigma_3)_f$ (kPa)	p' (kPa)	q (kPa)	E_0' (MPa)	E'_{50} (MPa)
100 (kPa)	369	55.5	108.8	27.8	21.4	20.3
200 (kPa)	389	95.0	208.5	47.5	31.1	25
400 (kPa)	398	181.4	442.7	90.7	58.9	47.6
600 (kPa)	381	246.7	492.3	123.3	89.5	76.8

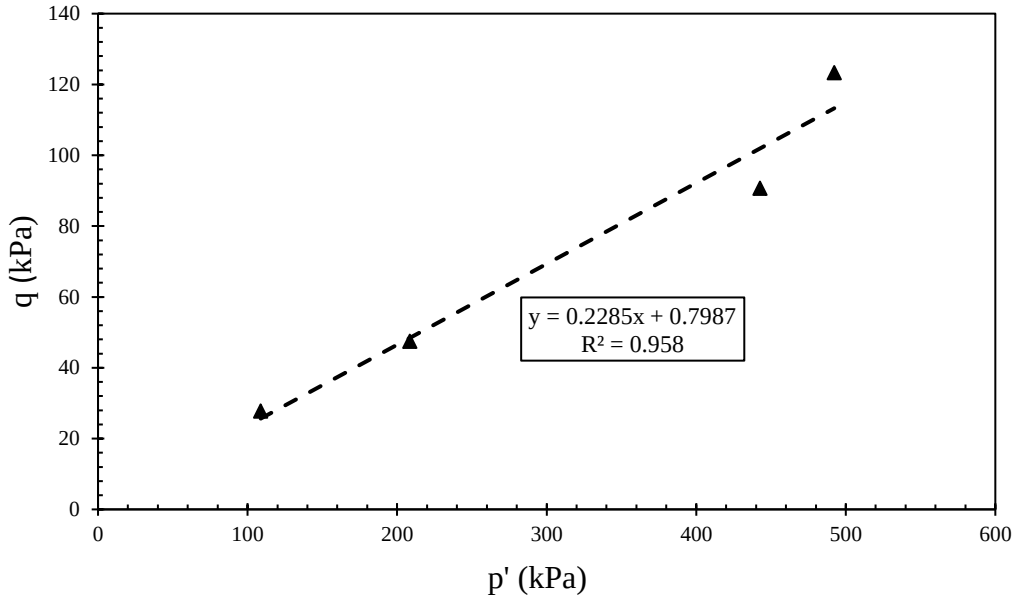

Figure 4.22. Modified failure envelope for undrained MCS test

Considering the modified failure envelope's equation in Figure 4.22, the reconstituted Ankara clay's internal friction angle and cohesion using the MCS method are estimated as **13.2**° and **1 kPa,** respectively.

4.1.7 Undrained MCC Test Results

The stress–axial strain relationship for four cycles of the MCC test is shown in Figure 4.23. Excess pore pressure vs., axial strain is demonstrated in Figure 4.24 and the results are listed in Table 4.9. The modified failure envelope is drawn in Figure 4.25 and the strength parameters are written afterward. Note that in the Maximum Curvature method, the minimum radius is measured and due to the creation of local failure planes, the peak strength couldn't be measured with this approach. However, since the shearing is stopped at very low axial strains, the reconstituted Ankara clay specimen is in the elastic range and withstands up to 4 cycles with no significant strength reduction.

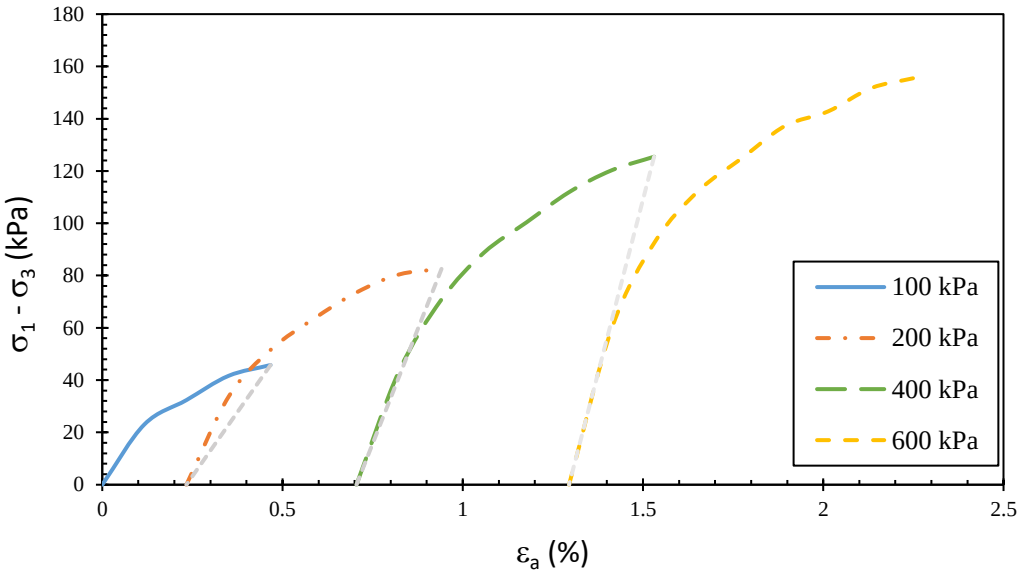

Figure 4.23. Deviatoric stress–axial strain for undrained MCC test

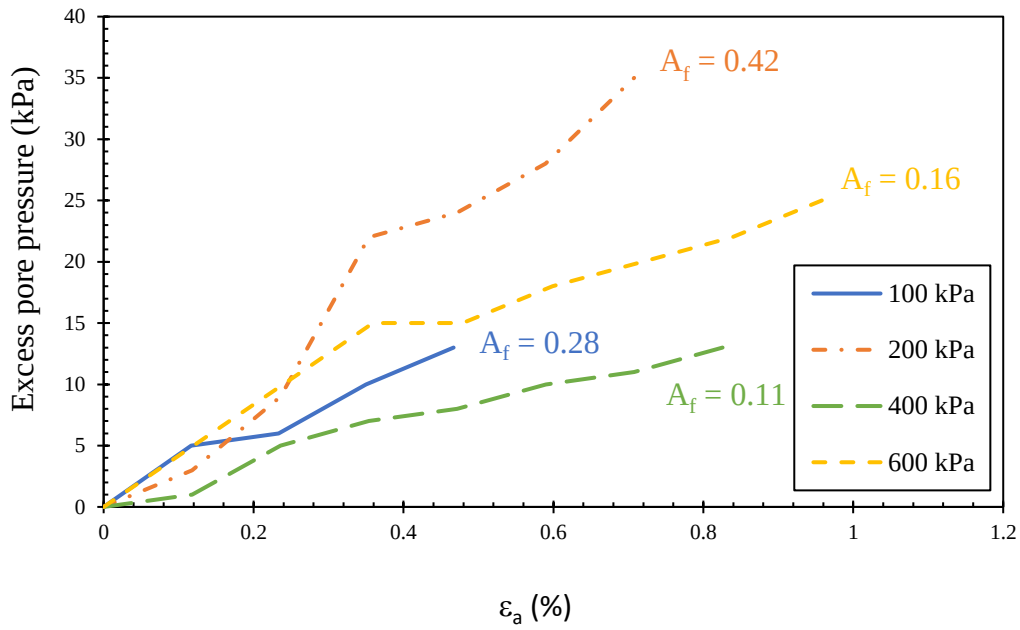

Figure 4.24. Excess pore pressure vs. axial strain for undrained MCC test

Table 4.9. Pore pressure and deviatoric stress at failure, elastic and secant elastic moduli for undrained MCC test

	u_f (kPa)	$(\sigma_1-\sigma_3)_f$ (kPa)	p' (kPa)	q (kPa)	E_0' (MPa)	E'_{50} (MPa)
100 (kPa)	423	45.7	109.9	22.9	20.4	14.1
200 (kPa)	485	82.5	206.3	41.3	28.7	24.1
400 (kPa)	548	125.5	449.7	62.7	36.7	32.8
600 (kPa)	580	155.6	647.8	77.8	50.3	45.5

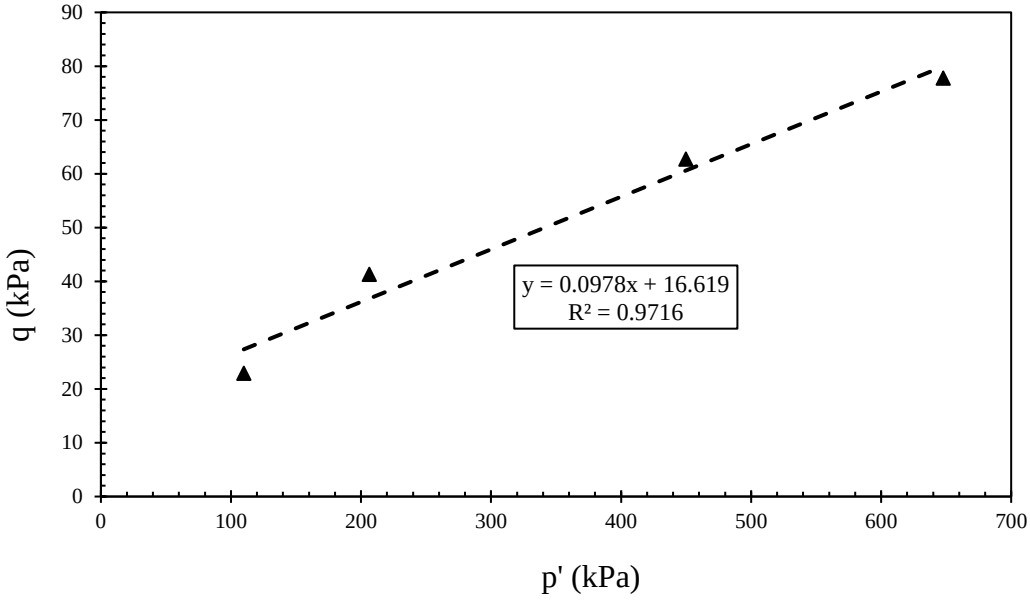

Figure 4.25. Modified failure envelope for undrained MCC test

Considering the failure envelope equation in Figure 4.25, the reconstituted Ankara clay's internal friction angle and cohesion using the MCC method are predicted as **5.6**° and **16.7 kPa,** respectively.

4.2 Drained Test Results

In this section, the results of drained experiments are shown. Consolidated drained (CD) CTC tests are conducted on four specimens under 100 kPa, 200 kPa, 400 kPa and 600 kPa effective consolidation pressures, and CD multi-stage tests are conducted under the same effective confining stresses using one specimen as it was provided in section 4.1.

4.2.1 Drained single-stage Test Results

The consolidated drained tests are conducted according to the procedure explained in 3.4. Since, in drained tests, the water from the specimen can drain, no excess pore

pressure is expected during the test. On the other hand, the volume of the specimen is not preserved and must be measured at each data point.

As discussed in chapter 3, the shearing rate for the drained test was assumed as 0.005 mm/min and during the experiments, no excess pore pressure was observed.

Since the fully automated testing setup is used for drained tests, the results depend on the resolution of the proving ring. The proving ring that is used in the experiments has a resolution of 4 N. Therefore, for example the values between 4 N and 8 N cannot be measured and 5 N, 6 N and 7 N all are recorded as either 4 N or 8 N. In order to overcome this issue, the acquired data from each test first went through a smoothing process. Figure 4.26 demonstrates the raw data from the testing setup and smoothens data by averaging the values of deviatoric stress. To average the data, seven data points before and seven data points after a specific data point are considered and the average of the all 15 points is the result. This process is followed throughout the study for drained tests.

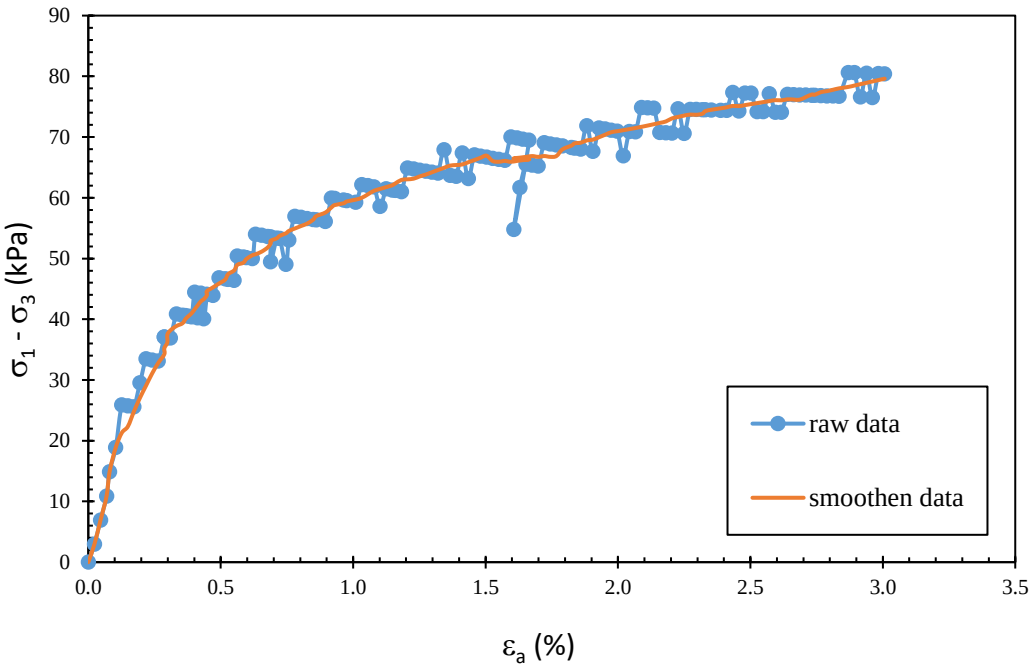

Figure 4.26. Representation of raw data and smoothen data acquired from automatic test setup for drained tests

Results of deviatoric stress–axial strain and volumetric strain vs. axial strain under 100 kPa, 200 kPa, 400 kPa, and 600 kPa effective confining stresses are shown in Figure 4.27 and Figure 4.28, respectively. Table 4.10 shows the calculation of the water content before and after the triaxial compression test at each effective confining pressure.

Table 4.10. Initial and final water content for drained single-stage triaxial test

		M_{wet} (gr)	M_{dry} (gr)	M_{tray} (gr)	Water content
100 kPa	initial	295.03	239.74	127.23	0.491
	final	288.532	239.74		0.433
200 kPa	initial	282.336	230.234	127.23	0.505
	final	273.165	230.234		0.416
400 kPa	initial	283.546	230.545	127.23	0.512
	final	270.905	230.545		0.390
600 kPa	initial	284.708	233.177	127.23	0.486
	final	270.531	233.177		0.352

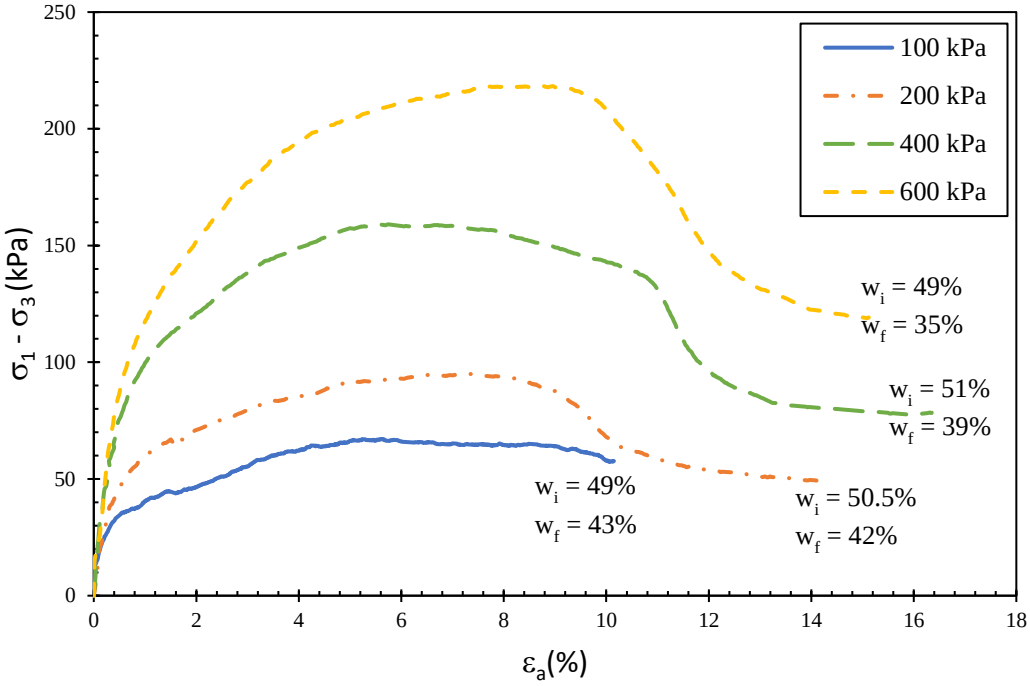

Figure 4.27. Smoothen deviatoric stress–axial strain for drained single-stage tests

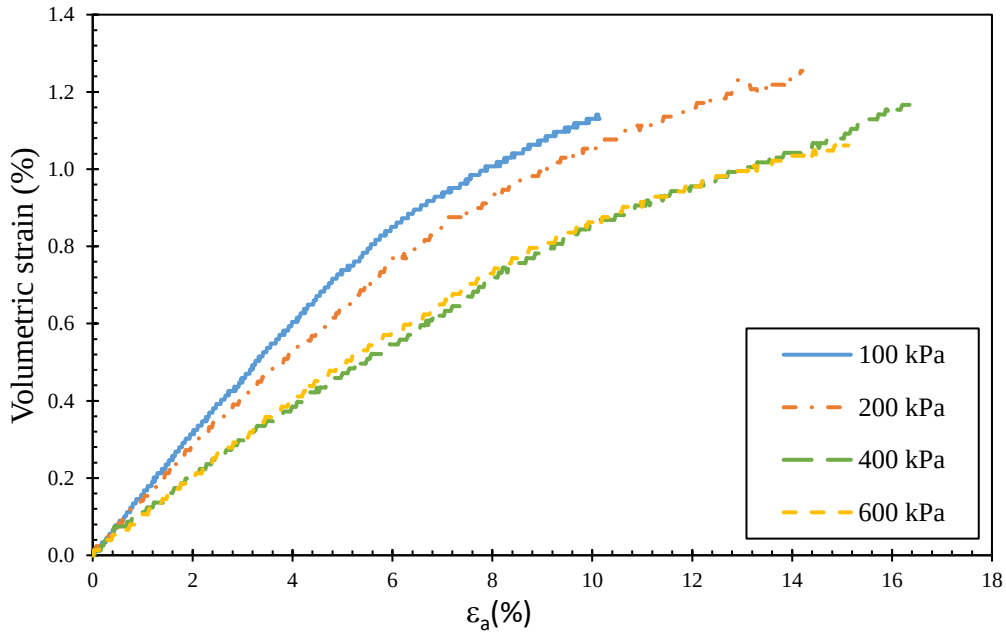

Figure 4.28. Volumetric strain vs. axial strain for drained single-stage tests

The modified failure envelope for the drained single-stage test is reported in Figure 4.29. Using the envelope's equation, the strength parameters are calculated and will be used for validating the multi-stage test results.

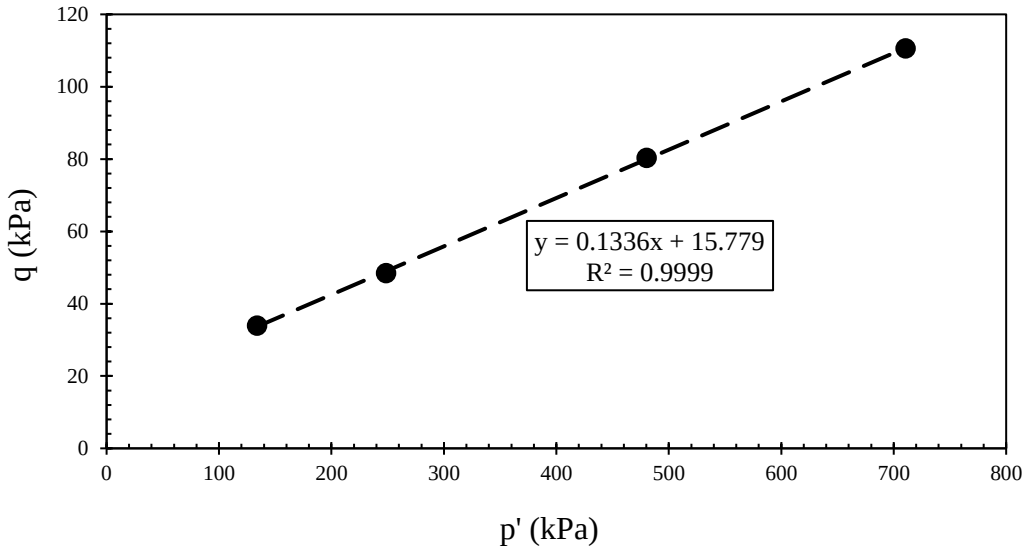

Figure 4.29. Modified failure envelope for drained single-stage tests

The friction angle and cohesion are calculated from the modified failure envelope equation as **7.7**° and **16 kPa**.

4.2.2 Drained RPC Test Results

The reconstituted Ankara clay specimen is sheared up to 2% axial strain at each consolidation pressure. Subsequently, the deviatoric stress at failure is calculated using the transformed relationship of $\varepsilon_a/(\sigma_1-\sigma_3)$ vs. ε_a. Figure 4.30, Figure 4.31 and Figure 4.32 depict the transformed stress–axial strain, deviatoric stress–axial strain and volumetric strain vs. axial strain relationships for drained RPC. Table 4.11 presents the interpreted parameters at failure. The modified failure envelope with the equation is drawn in Figure 4.33 and the strength parameters obtained from this method are reported afterward.

As it was noted before, due to the resolution of the proving ring that is used in the triaxial testing setup, the recorded values are scattered slightly from the line. However, as it can be seen from Figure 4.30, the minimum R^2 for the best fit line is about 92% which is acceptable and the smoothing process is not applied in this section.

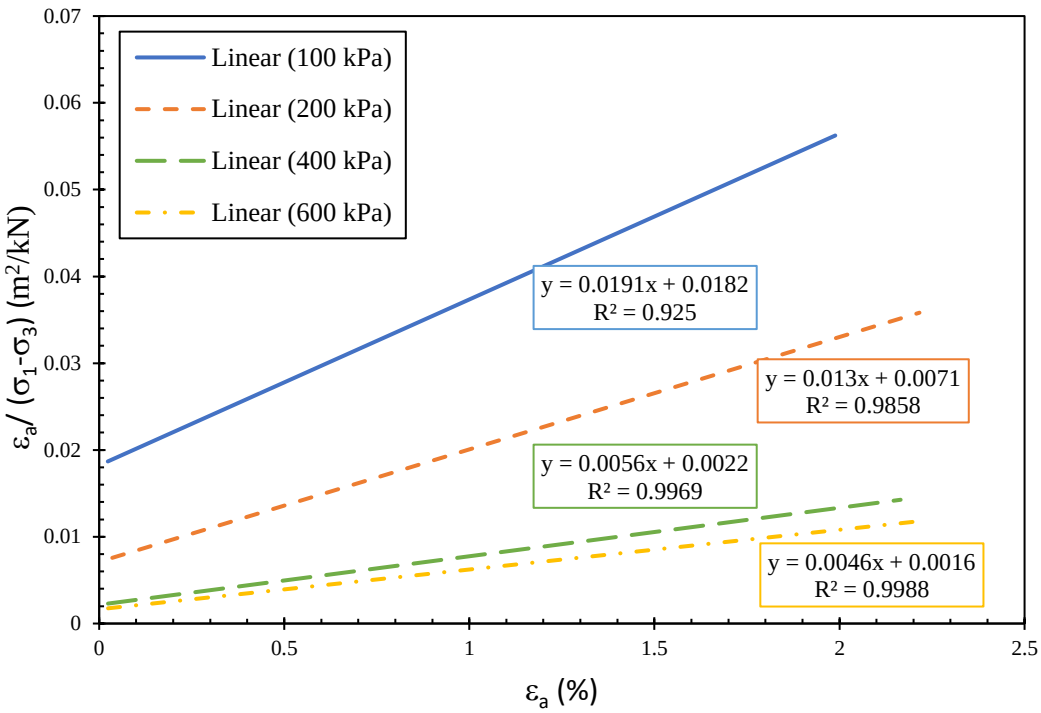

Figure 4.30. Transformed stress–axial strain relationship for drained RPC

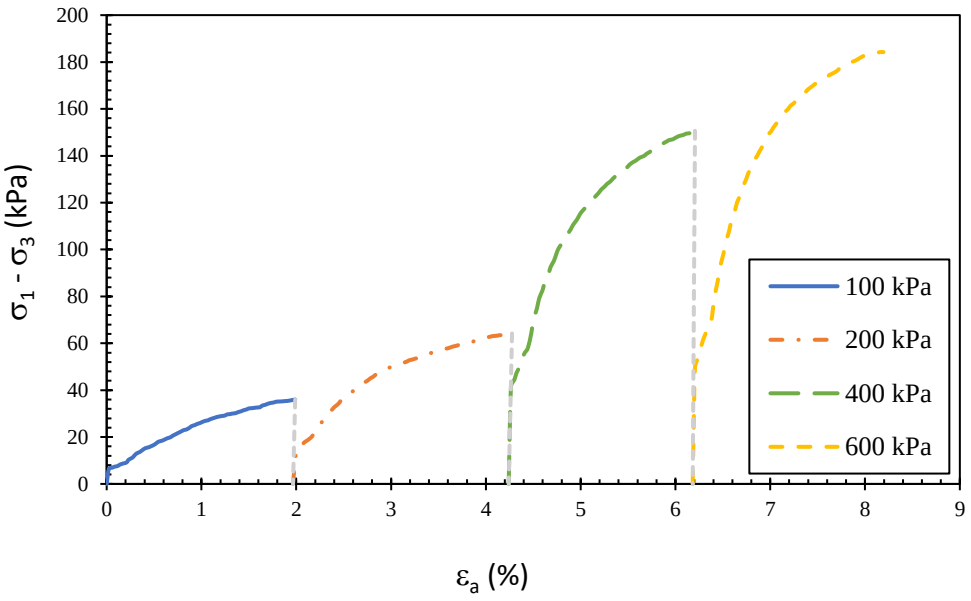

Figure 4.31. Deviatoric stress–axial strain relationship for drained RPC test

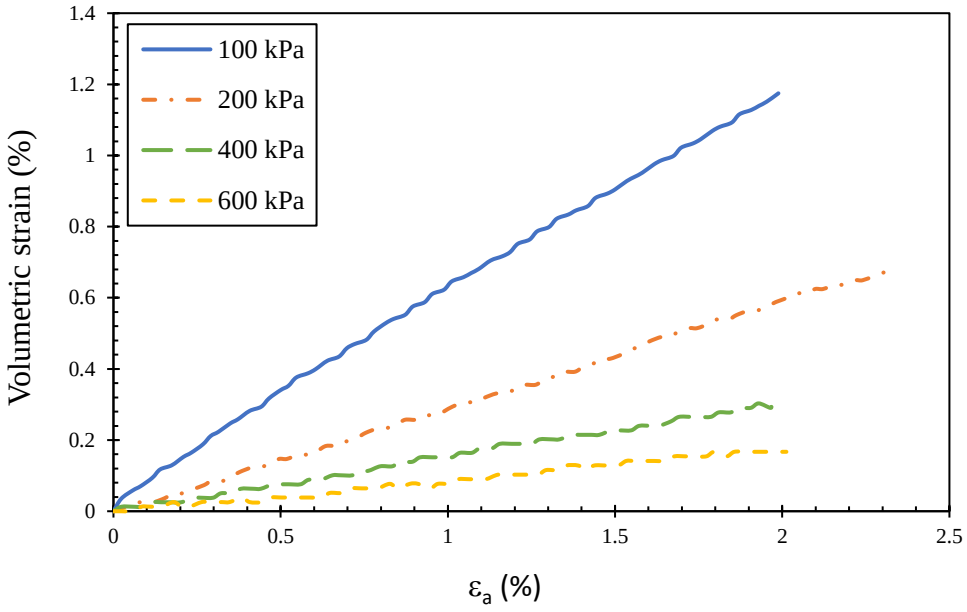

Figure 4.32. Volumetric strain vs. axial strain relationship for drained RPC test

Table 4.11. Predicted deviatoric stress at failure, initial and secant elastic moduli for drained RPC tets

	u (kPa)	b	$(\sigma_1-\sigma_3)_f$ (kPa)	p' (kPa)	q (kPa)	E_0' (MPa)	E'_{50} (MPa)
100 (kPa)	400	0.0191	52.4	126.2	26.2	17	2.6
200 (kPa)	400	0.013	76.9	238.5	38.5	22.7	6.2
400 (kPa)	400	0.0056	178.6	489.3	89.3	48.2	24.2
600 (kPa)	400	0.0046	217.4	708.7	108.7	70.9	28.3

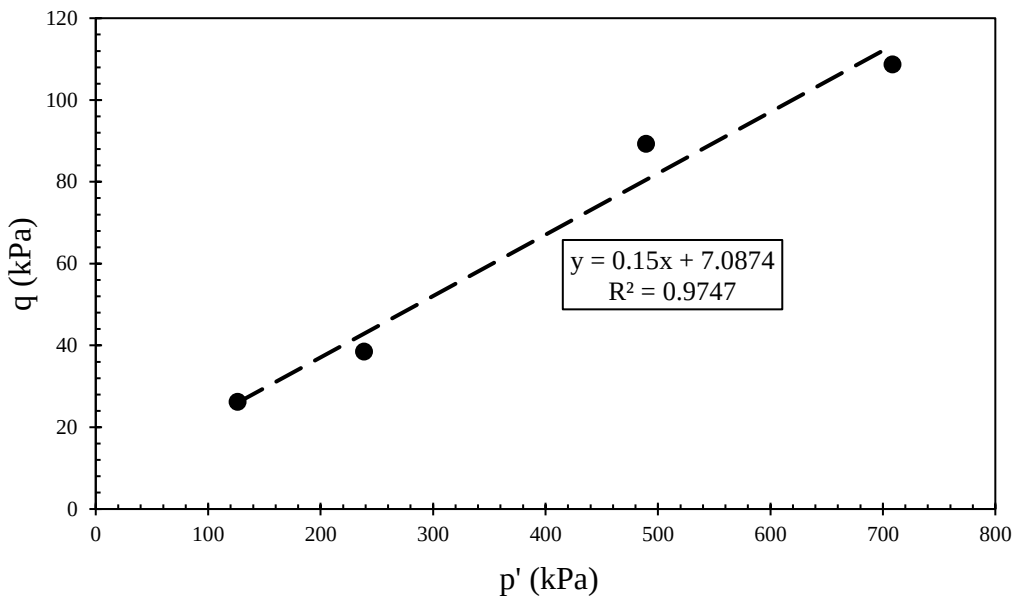

Figure 4.33. Modified failure envelope for drained RPC test

Considering the failure envelope equation in Figure 4.33, the reconstituted Ankara clay's internal friction angle and cohesion using the RPC method are predicted as **8.6**° and **7.2 kPa,** respectively.

4.2.3 Drained RPS Test Results

Figure 4.34 demonstrates the results of the RPS test in $\varepsilon_a/(\sigma_1-\sigma_3)$ vs. ε_a space for 100 kPa, 200 kPa, 400 kPa, and 600 kPa effective consolidation pressures, respectively. In Figures 4.35 and 4.36, deviatoric stress-axial strain and volumetric strain vs. axial strain are demonstrated. Table 4.12 provides the estimated parameters and in Figure 4.37, the modified failure envelope is drawn.

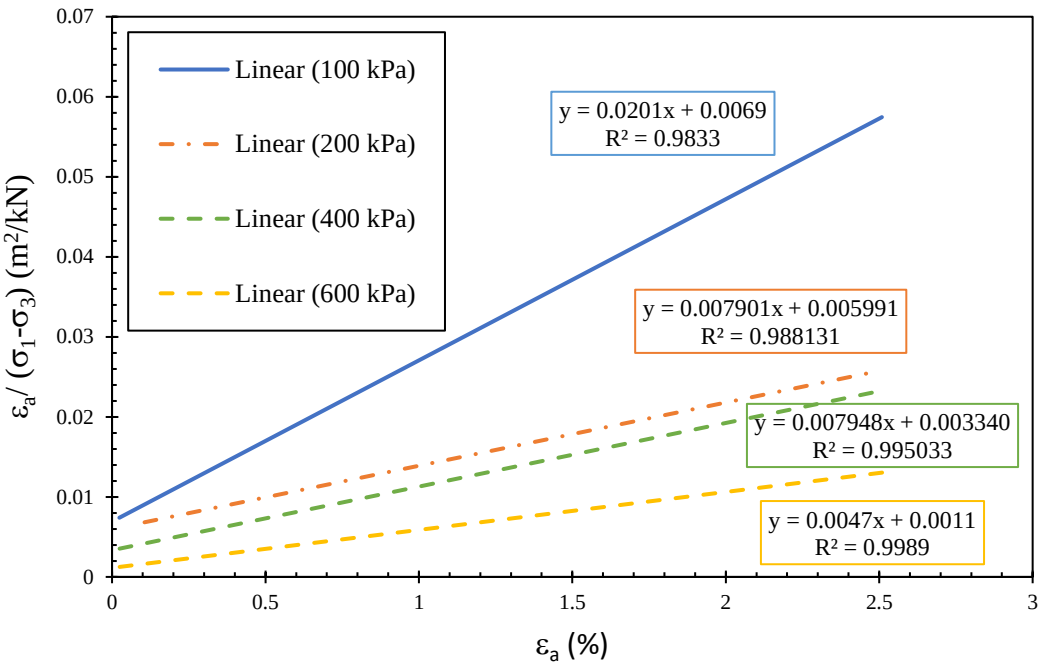

Figure 4.34. Transformed stress–axial strain relationship for drained RPS test

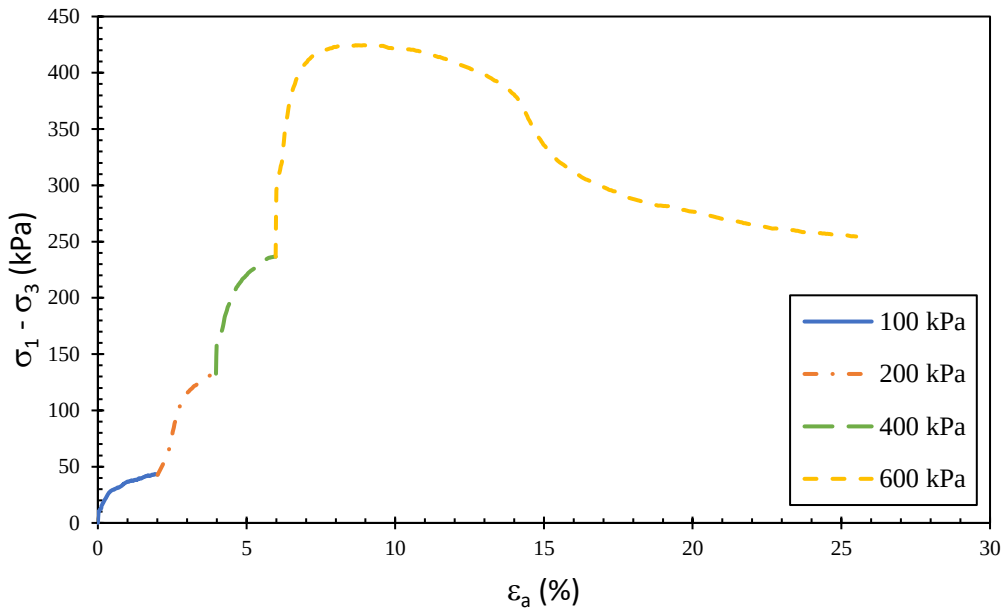

Figure 4.35. Deviatoric stress–axial strain relationship for drained RPS test

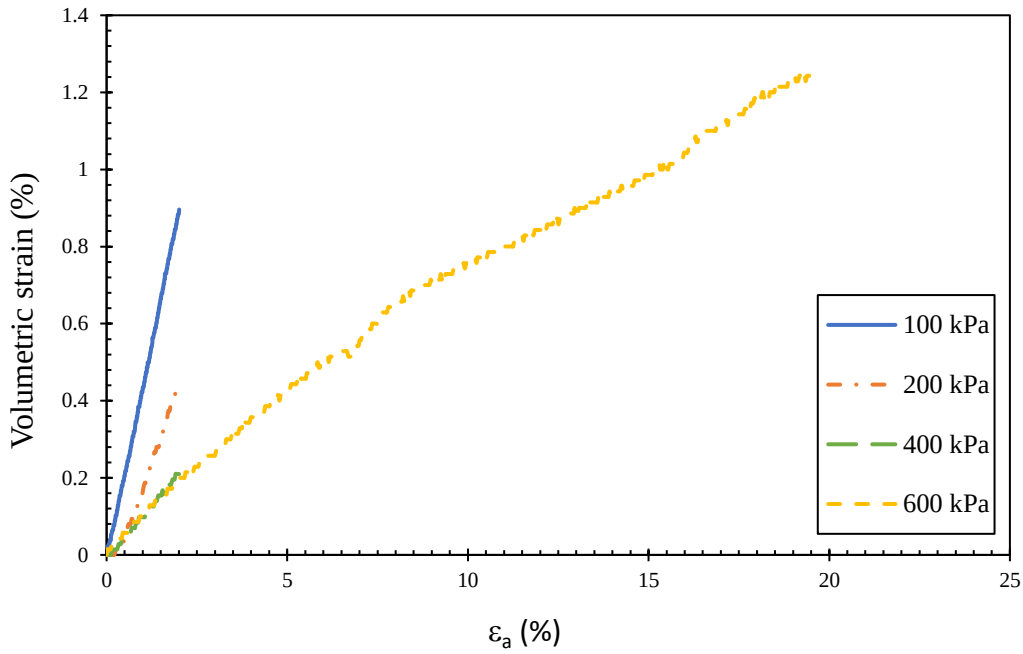

Figure 4.36. Volumetric strain vs. axial strain relationship for drained RPS test

Table 4.12. Predicted deviatoric stress at failure, initial and secant elastic moduli for drained RPS test

	u_f (kPa)	b	$(\sigma_1-\sigma_3)_f$ (kPa)	p' (kPa)	q (kPa)	E_0' (MPa)	E'_{50} (MPa)
100 (kPa)	500	0.0201	49.75	124.9	24.9	17.1	7.7
200 (kPa)	500	0.007901	126.57	263.3	63.3	17.4	8
400 (kPa)	500	0.007948	125.82	462.9	62.9	50	13.8
600 (kPa)	500	0.0047	212.77	706.4	106.4	87.5	35.7

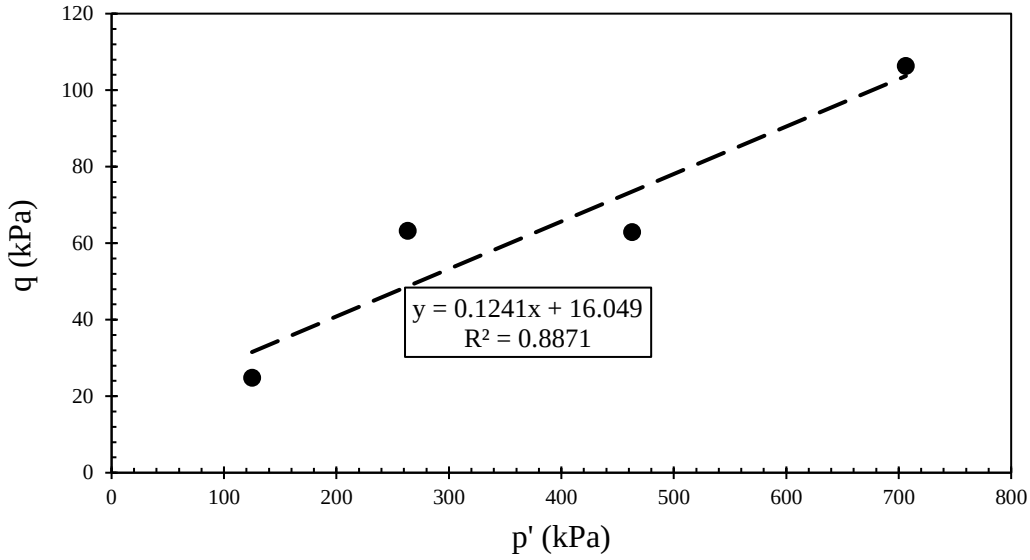

Figure 4.37. Modified failure envelope for drained RPS test

Considering the failure envelope equation in Figure 4.37, the reconstituted Ankara clay's internal friction angle and cohesion using the RPC method are calculated as **7.1**° and **16.2 kPa,** respectively.

4.2.4 Drained MSC Test Results

The deviatoric stress–axial strain relation and volumetric strain vs. axial strain in the Minimum Slope approach with the cycled loading approach are shown in Figure 4.38 and Figure 4.39. Deviatoric stresses and other parameters are reported in Table 4.13. The modified failure envelope is drawn in Figure 4.40 and strength parameters are noted afterward.

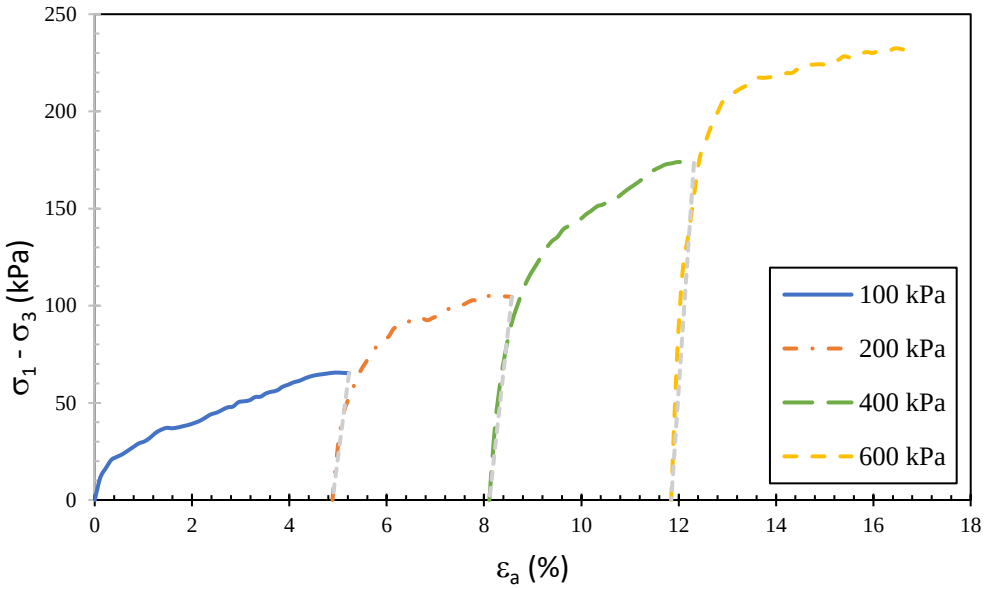

Figure 4.38. Deviatoric stress–axial strain for drained MSC test

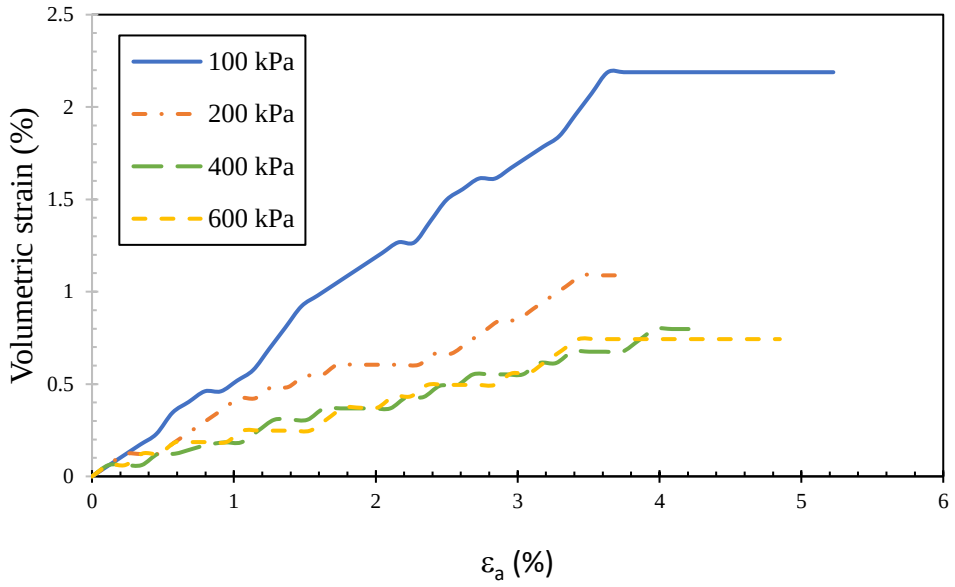

Figure 4.39. Volumetric strain vs. axial strain relationship for drained MSC test

Table 4.13. Predicted deviatoric stress at failure, initial and secant elastic moduli for drained MSC test

	u_f (kPa)	$(\sigma_1-\sigma_3)_f$ (kPa)	p' (kPa)	q (kPa)	E_0' (MPa)	E'_{50} (MPa)
100 (kPa)	350	65.2	132.6	32.6	10	2.8
200 (kPa)	350	104.5	252.2	52.2	24.5	15.1
400 (kPa)	350	173.5	486.7	86.7	32.6	21.6
600 (kPa)	350	231.5	715.7	115.7	61.8	50.3

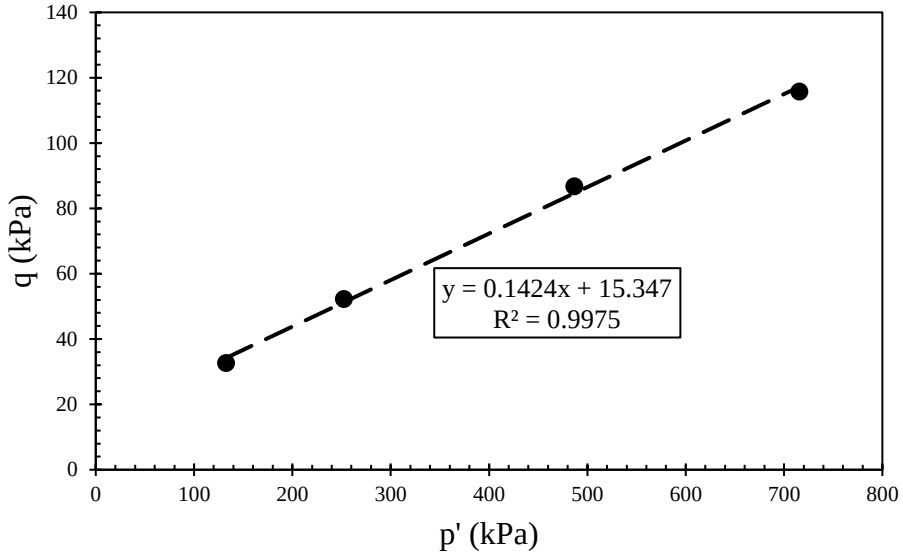

Figure 4.40. Modified failure envelope for drained MSC test

From the equation on Figure 4.40, the reconstituted Ankara clay's internal friction angle and cohesion are estimated as **8**° and **15.5 kPa,** respectively.

4.2.5 Drained MSS Test Result

The deviatoric stress–axial strain in Minimum Slope method with a sustained loading approach is depicted in Figure 4.41. The expected stresses at failure are reported in Table 4.14 and the modified failure envelope is drawn in Figure 4.42. The strength parameters are written afterward.

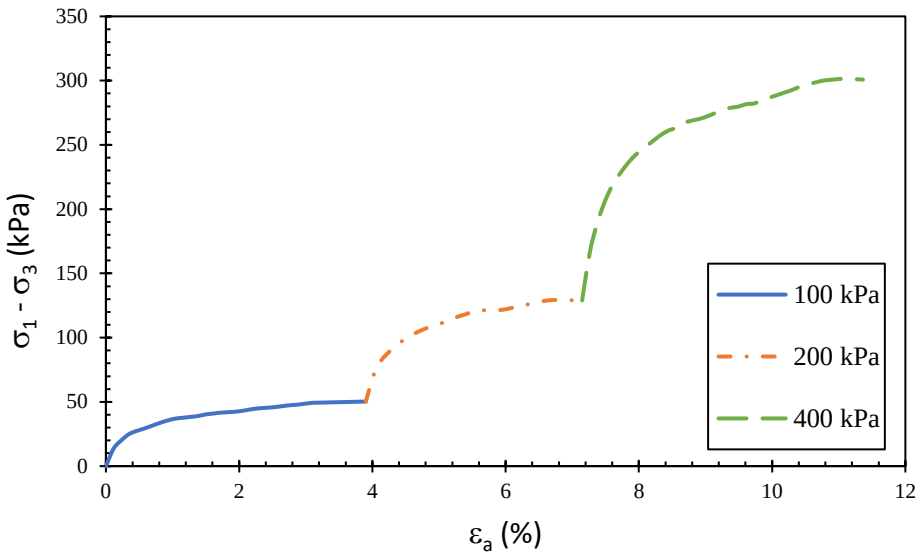

Figure 4.41. Deviatoric stress–axial strain for drained MSS test

Table 4.14. Predicted deviatoric stress at failure, initial and secant elastic moduli for drained MSS test

	u_f (kPa)	$(\sigma_1-\sigma_3)_f$ (kPa)	p' (kPa)	q (kPa)	E_0' (MPa)	E'_{50} (MPa)
100 (kPa)	350	50.3	125.1	25.7	11.8	7.2
200 (kPa)	350	78.7	239.3	39.3	17.8	11.2
400 (kPa)	350	171.8	485.9	85.9	32.2	21.4

In this test, due to an unexpected electrical malfunction, the fourth cycle couldn't be completed. Therefore the result of three cycles is considered and the modified failure envelope is drawn in Figure 4.42.

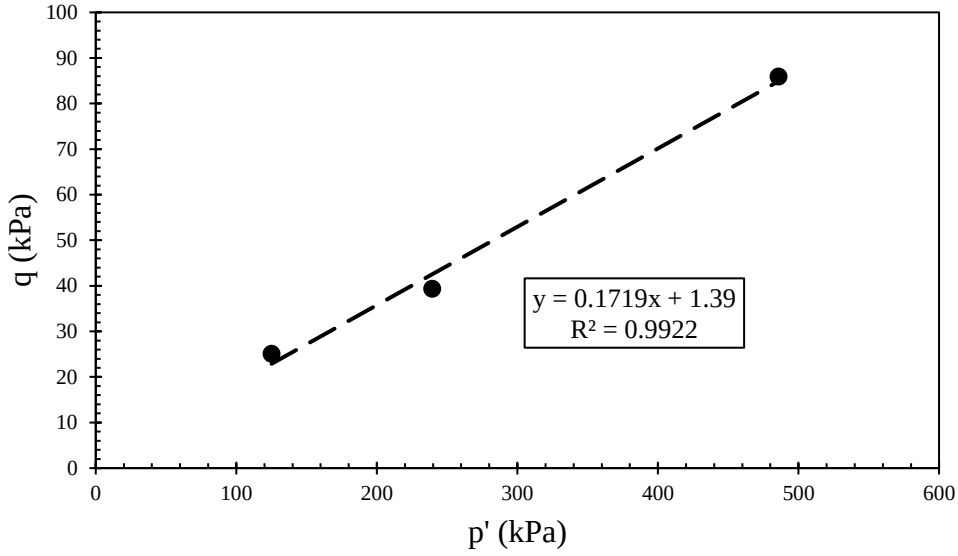

Figure 4.42. Modified failure envelope for drained MSS test

From the equation in Figure 4.42, the reconstituted Ankara clay's internal friction angle and cohesion are estimated as **10**° and **1.5 kPa,** respectively.

CHAPTER 5

DISCUSSION AND CONCLUSION

5.1 Conclusions of the Study

The main objective of this study is to examine the applicability of multi-stage triaxial compression test procedures on reconstituted normally consolidated Ankara clay. First, a set of consolidated undrained (CU) and consolidated drained (CD) tests are conducted on four reconstituted Ankara clay specimens under 100 kPa, 200 kPa, 400 kPa, and 600 kPa confining pressures. Consequently, six approaches for undrained and four techniques for drained tests were implemented, and the results are compared to determine the most compatible and accurate procedure that is applicable on reconstituted high-plasticity Ankara clay soil samples.

The first approach was to shear the specimen at very low axial strains (2-4%) and interpret the results to find the deviatoric stress at failure using Koendner's hyperbolic method (RP). The second approach was to determine the slope of the deviatoric stress-axial strain curve and stop the shearing step when the slope of the plot is minimum (close to zero) (MS). The last approach was to numerically determine the curvature of the deviatoric stress-axial strain plot by fitting a circle at different data points and measuring the circle's radius. The shearing step is stopped when the curvature of the plot is maximum (minimum radius) (MC).

Furthermore, for each approach, two deviatoric loading conditions are considered. 1) Sustained loading, where the deviatoric stress is kept on the specimen after the shearing step and during the consolidation. 2) Cycled loading, where the deviatoric stress is removed from the specimen after each shearing stage and reapplied at the new confining stress level.

The single-stage consolidated undrained tests and six undrained multi-stage tests results are presented in Table 5.1. Accordingly, the most accurate procedure is the RPC approach. The interpretation of the data from RPC gives the closest strength parameters to those obtained from the single-stage tests.

Table 5.1. single-stage and multi-stage tests results for undrained experiments

	Test name	Internal Friction Angle (ϕ')	Cohesion (kPa)	Applicable Cycles
1	**CTC**	**7.6**	**22**	_
2	SSC	7.4	23	4
3	SSS	8.3	18	4
4	MSC	10.3	17.6	3
5	MSS	6	19.6	3
6	MCC	13.2	1	4
7	MCS	5.6	16.7	4

The single-stage drained tests and 4 multi-stage drained tests results are presented in Table 5.2. MSC gives the most accurate strength parameters compared to those obtained from the single-stage drained tests.

Table 5.2. single-stage and multi-stage test results for drained experiments

	Test name	Internal Friction Angle (ϕ')	Cohesion (kPa)	Applicable Cycles
1	**CTC**	**7.7**	**16**	_
2	RPC	8.6	7.2	4
3	RPS	7.1	16.2	4
4	MSC	8	15.5	4
5	MSS	10	1.5	3

From Table 5.1 and Table 5.2, the following conclusions can be attained:

5.1.1 Undrained Tests

- ✓ Sustained loading gives lower strength parameters. As is expected, sustaining the load on the specimen causes accumulation of the strain and a weaker recovery at reconsolidation stage.
- ✓ In undrained single-stage triaxial tests, the specimen fails at relatively low axial strains (3–5%). Therefore, the Rational procedure is more suitable for undrained tests, where the specimen undergoes 2% axial strain.
- ✓ Regarding the Minimum Slope method, since the shearing is continued until relatively high strains, the disturbance of the clay specimen is high enough that leads to a strength reduction in the fourth cycle. Therefore, this approach cannot apply for more than three cycles.
- ✓ The maximum Curvature approach gives the lowest strength parameters compared to other approaches. This approach is not applicable on reconstituted Ankara clay samples since the stress-axial strain curve shows

the maximum curvature at very low strains and the obtained strength parameters are far lower than expected.

- ✓ In multi-stage undrained test, RPC approach is applicable on normally consolidated reconstituted Ankara clay.
- ✓ All the reconstituted Ankara clay specimens show the brittle behavior as it is expected from the normally consolidated clays. Moreover, the sample preparation method used in this study can be used to prepare identical specimens in terms of water content, dimentions and stress state as were shown in section 3.
- ✓ Regarding the pore water pressure change at different approaches, RPC procedure cannot capture the exact A_f values. However, the results are in relatively good agreement reffered to single-stage undrained triaxial test results (Table 5.3).
- ✓ The RPC procedure gives the closest initial and secant elastic moduli compared to single-stage test results that are noted in Table 5.3.

Table 5.3. Initial and secant elastic moduli and A parameter at failure for single-stage triaxial and RPC multi-stage procedure

	Single-stage			RPC		
	E'_0	E'_{50}	A_f	E'_0	E'_{50}	A_f
100 kPa	19.7	13.8	0.55	20.9	15.4	0.5
200 kPa	30.8	22.9	0.24	35	23.7	0.33
400 kPa	36.7	24.9	0.22	38.2	24.8	0.29
600 kPa	50.3	30.9	0.33	55.2	31.1	0.25

- ✓ Natural Ankara clay is an over consolidated fissured clayey soil. In this study the reconstituted Ankara clay soil sample is prepared and tested. The main reason is to have enough identical soil samples. Therefore, the applicability of the multi-stage triaxial procedures are studied on reconstituted soil

samples and applicability of these procedures on natural over consolidated fissured Ankara clay is still a question.

5.1.2 Drained Tests

- ✓ In drained test, the specimen fails at 5–6% axial strains. Therefore, minimum slope approach is applicable in drained tests.
- ✓ Rational Procedure Cycled method is not applicable on Ankara clay under drained conditions. However, the Rational Procedure Sustained approach gives an acceptable result compared to single-stage test results.
- ✓ In all the drained tests the brittle behavior of the normally cosolidated reconstituted Ankara clay is observed. Moreover, no dilation in noted and the specimen in all tests contracts and the volume was decreased.
- ✓ In the Minimum Slope Cycled procedure, the specimen recovers after removing the axial load, and due to the soil hardening, the specimen can withstand up to four cycles without strength reduction.
- ✓ In multi-stage drained test, MSC approach is the best applicable procedure on reconstituted Ankara clay.
- ✓ Applicability of MSC procedure is recommended on reconstituted Ankara clay specimen. Natural Ankara clay is an over consolidated fissured clay, and applicability of this procedure on natural Ankara clay is still a question.

5.2 Future Studies

- ➢ Double the confining stress at the fourth step and investigate the specimen response.
- ➢ Investigate a new approach directly from the applied axial load change.
- ➢ Check the applicability of the multi-stage approaches on overconsolidated Ankara clay sample.

- Provide a comprehensive framework for multi-stage procedures in which Kondner's method is not applicable.

REFERENCES

Alyousif, M. (2015). *Development of computer-controlled triaxial test setup and study on multistage triaxial test on sand* (Master's thesis, Middle East Technical University).

Akgün, H., Türkmenoğlu, A. G., Met, İ., Yal, G. P., Koçkar, M. K. (2017). *The use of Ankara Clay as a compacted clay liner for landfill sites*. Clay Minerals, *52*(3), 391–412.

ASTM 2487 – 17. *Standard practice for classification of soils for engineering purposes* (unified soil classification system).

ASTM C 136 – 06. *Standard Test Method for Sieve Analysis of Fine and Coarse Aggregates*.

ASTM 6913 – 04. *Standard test methods for particle-size distribution (gradation) of soils using sieve analysis*. ASTM International.

ASTM D 4318 – 10. *Standard Test Methods for Liquid Limit, Plastic Limit, and Plasticity Index of Soils*. Report, *04*(March 2010), 1–14.

ASTM D4767 – 02. (2002). *Standard Test Method for Consolidated Undrained Triaxial Compression Test for Cohesive Soils*. ASTM International, West Conshohocken, PA, American Society for Testing and Materials, *3*(Reapproved 2020), 1–13.

ASTM D7181 – 20. (2015). *Standard Test Method for Consolidated Drained Triaxial Compression Test for Soils*. ASTM International.

ASTM D7928 – 21. *Standard Test Method for Particle-Size Distribution (Gradation) of Fine-Grained Soils Using the Sedimentation (Hydrometer) Analysis*. *ASTM International*, 1–25. https://doi.org/10.1520/D7928-17

ASTM D854 – 02. *Standard Test Methods for Specific Gravity of Soil Solids by Water Pycnometer*. In *Astm D854* (Vol. 2458000, Issue C, pp. 1–7).

Avsar, E., Ulusay, R., Erguler, Z. A. (2005). Swelling properties of Ankara (Turkey) clay with carbonate concretions. *Environmental and Engineering Geoscience*, *11*(1), 73–93. https://doi.org/10.2113/11.1.73

Avsar, E., Ulusay, R., & Sonmez, H. (2009). Assessments of swelling anisotropy of Ankara clay. *Engineering Geology*, *105*(1–2), 24–31. https://doi.org/10.1016/j.enggeo.2008.12.012

Banerjee, A., Puppala, A. J., Hoyos, L. R. (2020). Suction-controlled multistage triaxial testing on clayey silty soil. *Engineering Geology*, *265*(September 2019). https://doi.org/10.1016/j.enggeo.2019.105409

Binal, A., Bas, B., Karamut, O. R. (2016). Improvement of the Strength of Ankara Clay with Self-cementing High Alkaline Fly Ash. *Procedia Engineering*, *161*, 374–379. https://doi.org/10.1016/j.proeng.2016.08.577

Budhu, M. (2015). *Soil Mechanics Fundamentals*.

Casagrande, A., Fadum, R. E. (1940). Notes on soil testing for engineering purposes.

Choi, J. H., Dai, S., Lin, J. S., Seol, Y. (2018). Multistage Triaxial Tests on Laboratory-Formed Methane Hydrate-Bearing Sediments. *Journal of Geophysical Research: Solid Earth*, *123*(5), 3347–3357. https://doi.org/10.1029/2018JB015525

Çokça, E., Tilgen, H. P. (2010). Shear strength-suction relationship of compacted Ankara clay. *Applied Clay Science*, *49*(4), 400–404. https://doi.org/10.1016/j.clay.2009.08.028

Craig, R. F. (2004). *Craig's soil mechanics*. CRC press

Das, B. M. (2008). *Advanced soil mechanics* (Vol. 270). New York: Taylor & Francis.

Deák, F., Ván, P., Vásárhelyi, B. (2012). Hundred years after the first triaxial test. *Periodica Polytechnica Civil Engineering*, *56*(1), 115–122. https://doi.org/10.3311/pp.ci.2012-1.13

De Beer, I. E. (1950). The cell-test. *Geotechnique*, *2*(2), 162-172.

Erguler, Z. A., Ulusay, R. (2003). Engineering characteristics and environmental impacts of the expansive Ankara Clay, and swelling maps for SW and central parts of the Ankara (Turkey) metropolitan area. *Environmental Geology*, *44*(8), 979–992. https://doi.org/10.1007/s00254-003-0841-y

Gräsle, W. (2011). Multistep triaxial strength tests: Investigating strength parameters and pore pressure effects on Opalinus Clay. *Physics and Chemistry of the Earth*, *36*(17–18), 1898–1904. https://doi.org/10.1016/j.pce.2011.07.024

Head, K. H. (1982). Manual of soil laboratory testing, volume 2. Permeability, shear strength and compressibility tests. In *Manual of soil laboratory testing, volume 2. Permeability, shear strength and compressibility tests.* https://doi.org/10.1016/0016-7061(95)90001-2

Henkel, D. J., Gilbert, G. D. (1952). THE EFFECT MEASURED OF THE RUBBER MEMBRANE ON THE TRIAXIAL COMPRESSION STRENGTH OF CLAY SAMPLES.

Ho, D. Y. F., Fredlund, D. G. (1987). A multistage triaxial test for unsaturated soils. *Geotechnical Testing Journal*, *5*(1), 18–25. https://doi.org/10.1520/GTJ10795J

İspir, M. E. (2011). *A laboratory study of anisotropy in engineering properties of Ankara clay* (Master's thesis, Middle East Technical University).

Kayaturk, D., Bol, E., Sert, S., Özocak, A. (2021). Determination of Shear Strength Parameters by Multistage Triaxial Tests in the Long-Term Analysis of Slopes. *Academic Platform Journal of Natural Hazards and Disaster Management*, *2*(1), 29–36. https://doi.org/10.52114/apjhad.948154

Kenny, T. C. (1960). *Multiple-stage triaxial test for determining c' and o' of saturated soils*.

Khosravi, A., Alsherif, N., Lynch, C., McCartney, J. (2012). Multistage triaxial

testing to estimate effective stress relationships for unsaturated compacted soils. *Geotechnical Testing Journal*, *35*(1), 128–134.

Kim, M. M., Ko, H. Y. (1979). Multistage Triaxial Testing of Rocks. *Geotechnical Testing Journal*, *2*(2), 98–105. https://doi.org/10.1520/gtj10435j

Kondner. (1963). *o / Experiments in Army Besearch , Development*. 1962–1963.

Lambe, T. W., Whitman, R. V. (1991). *Soil mechanics* (Vol. 10). John Wiley & Sons

Mitchel. J. K., Soga, K. (2005). Fundamentals of Soil Behavior. In *Fundamentals of Soil Behavior*. https://doi.org/10.2136/sssaj1976.03615995004000040003

Nambiar, M. R. M., Venkatappa Rao, G., Gulhati, S. K. (1985). Multistage Triaxial Testing: a Rational Procedure. *ASTM Special Technical Publication*, 274–293. https://doi.org/10.1520/stp36340s

Saeedy, H., Mollah, M. (2009). Application of Multistage Triaxial Test to Kuwaiti Soils. *Advanced Triaxial Testing of Soil and Rock*, 363-363–13. https://doi.org/10.1520/stp29087s

Shahin, M. A., Cargeeg, A. (2011). Experimental investigation into multistage versus conventional triaxial compression tests for a c-phi soil. *Applied Mechanics and Materials*, *90–93*, 28–32. https://doi.org/10.4028/www.scientific.net/AMM.90-93.28

Skempton, A. W. (1984). the Pore-Pressure Coefficients a and B . *Selected Papers on Soil Mechanics*, 65–69. https://doi.org/10.1680/sposm.02050.0010

Soranzo, M. (1988). Results and Interpretation of Multistage Triaxial Compression Tests. *Advanced Triaxial Testing of Soil and Rock*, 353-353–10.

T.Willian Lambe., Robert V Whitman. (1969). Kupdf.Net_Lambe-Whitman-Soil-Mechanicspdf. In *T.William Lambe* .

Taheri, A., Sasaki, Y., Tatsuoka, F., Watanabe, K. (2012). Strength and deformation characteristics of cement-mixed gravelly soil in multiple-step triaxial compression. *Soils and Foundations*, *52*(1), 126–145.

Taylor, D. W. (1948). *Fundamentals of soil mechanics* (Vol. 66, No. 2, p. 161). LWW.

Toker, N. K. (2007). *Modeling the relation between suction, effective stress and shear strength in partially saturated granular media* (Doctoral dissertation, Massachusetts Institute of Technology).